National Technical University of Athens
School of Civil Engineering
Department of Geotechnical Engineering

Numerical Analysis of Piled-Raft Foundation For High-Rise Buildings

Postgraduate Thesis
By: Adel Kamel Ibrahim Mohammed

Under the supervision of:
Assoc. Prof: Gerolymos Nikos

Submitted in partial fulfillment of the requirements
For the degree of Master of Science in Structural Engineering

ATHENS - JUNE 2021

Examining Committee Members:

Professor. Bouckovalas George
Geotechnics Department, School of Civil Engineering, NTUA

Associate Professor. Papadimitriou Achileas
Geotechnics Department, School of Civil Engineering, NTUA

Associate Professor. Gerolymos Nikos
Geotechnics Department, School of Civil Engineering, NTUA

Abstract

Usually, the high-rise buildings exposed to excessive settlement and differential settlement, therefore the shallow foundation system was difficult to be used, so the direction went to the deep foundation's system. One of these systems was the piled raft foundation where both piles and raft carried the applied load. Also, the piles were not only used to carry the loads but also, they were used as settlement reducers because the settlements and differential settlement were the keys of that issue. The piled raft system was a complex system due to different kind of interactions, that's why the advanced numerical simulation was essential. This thesis was focused on 3D analysis by commercial software of PLAXIS 3D.

The purpose of that thesis was to check the validity of the embedded beam model to simulate the piles in PLAXIS 3D. At first, the thesis started with single pile behaviour under both vertical and lateral loads for nonlinear soil case, and measure the stiffness for a linear elastic case and then extended to pile groups and finally the piled raft for linear elastic cases and that compared with the analytical calculations for all cases and the volume pile model in some cases.

Finally, the piled raft system of The Kingdom Tower was studied via embedded beam model for linear elastic and nonlinear cases to estimate the load sharing factor between piles and raft, and determine the settlement and differential settlement in case of applying the gravity loads.

Acknowledgments

I would first like to thank my thesis supervisor *Assoc.Prof. Gerolymos Nikos* in the School of Civil Engineering at National Technical University of Athens, his door was always open whenever I had difficulties or questions about my research or writing.

I would also like to acknowledge *Prof. Koumousis Vlassis* in the School of Civil Engineering at National Technical University of Athens for his constant support and his great help in all the difficult situations I faced.

Finally, I must express my very profound gratitude to *Assoc.Prof. Mohamed M.A. Hussein* in the Faculty of Engineering at Sohag University for his unfailing support and continuous encouragement throughout this journey. This accomplishment would not have been possible without him.

Thank you all.

Author

Adel Kamel Ibrahim Mohammed

Table of contents

Chapter 1 Introduction 1

1.1 Background 1

1.2 Research Methodology 1

1.3 Outline of the thesis 2

Chapter 2 Behaviour of single pile 4

2.1 Introduction 4

2.2 Behaviour of single pile under vertical load 4

2.3 Methods of analysis 7

2.3.1 Analytical method 7

2.3.1.1 Ultimate vertical capacity of pile 7

2.3.1.2 Vertical stiffness 7

2.3.1.3 Ultimate Lateral capacity and lateral stiffness 8

2.3.2 Numerical method 9

2.4 Case of study 11

2.5 Comparing the results 14

2.5.1 Ultimate vertical capacity and vertical stiffness 14

2.5.2 Ultimate Lateral capacity and lateral stiffness 16

Chapter 3 Interaction factors between two piles under vertical loads 17

3.1 Introduction 17

3.2 literature overview 18

3.3 Parameters effect on the interaction factor 18

3.4 Methods of analysis 20

3.4.1 Analytical method 20

3.4.2 Numerical method 22

3.5 Case of study 23

3.6 Comparing the results of analytical and numerical methods 23

Chapter 4 Performance of pile groups under vertical loads 28
4.1 Introduction 28
4.2 Classifications of pile groups 28
4.2.1 Pile groups with perfectly rigid cap 29
4.2.2 Pile groups with perfectly flexible cap 30
4.3 Methods of analysis 31
4.3.1 Analytical method 31
4.3.2 Numerical method 32
4.4 Case of study 32
4.4.1 Uniform distribution of piles 32
4.4.2 Non-uniform distribution of piles 34
4.5 Comparing the results of analytical and numerical methods 35
4.5.1 Uniform distribution of piles 35
4.5.2 Non-uniform distribution of piles 42
Chapter 5 Piled raft foundations 44
5.1 Introduction 44
5.2 Pile raft Interaction factor and load sharing factor 45
5.3 Method of analysis 46
5.3.1 Analytical method 46
5.3.2 Numerical method 48
5.4 Case of study for single pile with raft 49
5.4.1 Comparing the results 49
5.5 Case of study for uniform piles distribution 50
5.5.1 Comparing the results for raft-pile interaction factor 50
5.5.2 Comparing the results for load sharing factor 52
5.6 Case of study for non-uniform pile distributions 55
5.6.1 Comparing the results 56

5.7 Application to real problem for "The Kingdom Tower" 58

5.7.1 General information 58

5.7.2 Modeling by PLAXIS 3D 60

5.7.2.1 Materials characteristics 60

5.7.2.2 Mesh generation and construction stages 62

5.7.3 Analysis results 63

5.7.3.1 Applying the uniform displacement for case 1 63

5.7.3.2 Applaying the gravity loads for case 2 64

Chapter 6 Conclusions and further work 68

6.1 Conclusions 68

6.2 Recommendations for further work..69

References...70

LIST OF TABLES

Table 2. 1 Soil input parameters for vertical capacity and vertical stiffness. 12
Table 2. 2 Soil input parameters for Lateral capacity and Lateral stiffness. 13
Table 2. 3 Pile input parameters for both vertical capacity, vertical and lateral stiffness. ...13
Table 2. 4 Pile input parameters for volume pile model for lateral capacity. 14
Table 2. 5 Pile input parameters for embedded beam model for lateral capacity................14
Table 2. 6 Comparison of the results for ultimate vertical capacity and vertical stiffness between analytical and numerical methods. 15
Table 2. 7 Comparison of the results for ultimate lateral capacity and lateral stiffness between analytical and numerical methods...16

Table 3. 1The input parameters for soil and pile material. 23

Table 4. 1The input parameters for soil and pile material. 33
Table 4. 2 Load distributions P/P_{av} for pile group 3x3. 36
Table 4. 3 Load distributions P/P_{av} for pile group 4x4. 36
Table 4. 4 Load distributions P/P_{av} for pile group 5x5. 37
Table 4. 5 Load distributions P/P_{av} for pile group 6x6. 38
Table 4. 6 Load distributions P/P_{av} for pile group 7x7. 39
Table 4. 7 Pile group efficiency factor for different pile groups with rigid cap. 41
Table 4. 8 Ratio of $\rho_d/\ \rho_{max}$ values for different pile groups without cap. 42

Table 5. 1 The raft-pile interaction and the ratio of raft load to total load for single raft with single pile. 50
Table 5. 2 Raft-pile interaction factors for different pile groups with different S/d and L/d. 51
Table 5. 3 Ratio of raft load to total load results. 53
Table 5. 4 Ratio of piles load to total load results. 54
Table 5. 5 Soil Properties for Jeddah tower. 61
Table 5. 6 pile base resistance for bored piles in rock according to DIN 1054:2005. 61
Table 5. 7 The input parameters for embedded beam model...62
Table 5. 8 The input parameters for raft. 62
Table 5. 9 The analysis results for raft-pile interaction and the ratio of raft load to total load linear and nonlinear cases. 64

LIST OF FIGURES

Figure 2. 1 A schematic overview of the vertical load and resistances acting on a pile. 5
Figure 2. 2 The load-settlement curve for vertically loaded pile. 6
Figure 2. 3 Visualization of volume pile in PLAXIS 3D. 10
Figure 2. 4 Schematic view for the embedded beam model. 10
Figure 2. 5 The dimensions and the boundaries of 3D model in PLAXIS. 12
Figure 2. 6 Load - settlement curves for three models for pile under vertical loads. 15
Figure 2. 7 Load-settlement curves for different coarseness factors. 15
Figure 2. 8 Lateral load - displacement curves for Vp and Eb modeles 16

Figure 3. 1 Representation of approaches I and II. 17
Figure 3. 2 The effect of the relative soil density to the interaction factor. 19
Figure 3. 3 The dimensions of 3D model in PLAXIS and the coarseness factor considerations for the interaction factor 22
Figure 3. 4 Comparison of the interaction factors for homogeneous soil layer between the analytical and numerical method for L/d =10, K =500 and ν_s =0.35...................................25
Figure 3. 5 Comparison of the interaction factors for homogeneous soil layer between the analytical and numerical method for L/d =25, K =500 and ν_s =0.35...................................25
Figure 3. 6 Comparison of the interaction factors for homogeneous soil layer between the analytical and numerical method for L/d =25, K =500 and ν_s =0..26
Figure 3. 7 The effect of soil Poisson's ratio (ν_s =0, 0.35) on the interaction factors between the analytical and numerical method. 26
Figure 3. 8 The effect of L/d ratio (L/d=10, 25) on the interaction factors between the analytical and numerical method. 27

Figure 4. 1 A schematic view for pile groups with perfectly rigid cap 29
Figure 4. 2 A schematic view for pile groups with equal loads (perfectly flexible cap). 30
Figure 4. 3 The dimensions of 3D model in PLAXIS and the coarseness factor considerations for pile group. 33
Figure 4. 4 Plan view for 228 pile distribution. 34
Figure 4. 5 Foundation cross-section and soil properties. 35
Figure 4. 6 Profiles and plans for pile groups. 35
Figure 4. 7 Group efficiency for case 1 for E_{s2} =E_{s1}. 43

Figure 4. 8 Group efficiency for case 1 for $E_{s2} \neq E_{s1}$. 43

Figure 5. 1 Interactions in piled raft foundation. 45
Figure 5. 2 Simplified load settlement curve for piled raft foundation. 46
Figure 5. 3 Three models for estimating the stiffnes for (1) unpiled raft, (2) pile group and (3) piled raft... 49
Figure 5. 4 Raft-pile interaction factor at L/d=10 and for groups 2x2 and 6x6. 52
Figure 5. 5 Ratio of raft load to total load for L/d=10. 55
Figure 5. 6 Ratio of raft load to total load for L/d=25. 55
Figure 5. 7 Raft-pile interaction factor for case 1 and 2. 56
Figure 5. 8 Ratio of raft load to total load for case 1. 57
Figure 5. 9 Ratio of raft load to total load for case 2. 57
Figure 5. 10 The structural system of Jeddah tower. 58
Figure 5. 11 Gravity load distribution of the superstructure... 59
Figure 5. 12 Three-dimensional view for piles. 59
Figure 5. 13 The assumed piled raft system. 60
Figure 5. 14 The 3D model in PLAXIS with very fine mesh discretization and refined around the piled raft. 62
Figure 5. 15 Load settlement case for linear and nonlinear cases. 63
Figure 5. 16 Settlement contours for raft syetem only. 64
Figure 5. 17 Settlement contours for piled raft syetem... 65
Figure 5. 18 Bearing pressure contours for raft syetem only.. 66
Figure 5. 19 Bearing pressure contours for piled raft syetem... 66
Figure 5. 20 Piles loads distribution within the piled raft system. 67

Chapter 1 Introduction

1.1 Background

The past two decades have seen a remarkable increase in the rate of construction of high-rise buildings or other civil structures which produce excessive loads, excessive settlements and differential settlements. The piled foundations have been developed and widely used to transmit the structural loads to stiff strata at depth in the ground. This system considered that the piles are designed to carry the entire load and neglect the raft participation. Therefore, the piled raft system was used to get the economical foundation type comparing with the conventional piled foundations where the raft used to carry a portion of loads and the piles used to carry loads, reduce both total and differential settlements of the foundation system.

In this thesis, the behaviour of piled raft foundation is investigated by comparing the analytical and numerical methods for the linear elastic case, where the piles have the same length.
The main purpose is to check the validity of the embedded beam model and see how it works for a single pile, piled foundation, and piled raft system. The study was depended on the comparison of the embedded beam model with the analytical methods and volume pile model.

1.2 Research Methodology

The used research methodology in this thesis relied on using PLAXIS 3D for numerical analysis and using analytical methods. The most common approaches that were used to simulate the pile in PLAXIS 3D were the embedded beam model and the volume element.
The embedded beam model was used mainly to reduce the complexity of such models because the volume pile model leads to very large models and thus long calculation times.

The search method was done through comparisons between the numerical method (embedded beam and volume pile models) and analytical method which starts with a single pile and ends with piled raft foundations by the following steps: -

- Estimating the single pile capacity and stiffness (vertical and lateral).
- Determining the interaction factor between piles and study the effect of different parameters on it.
- Calculating the load distribution within piles groups and the group efficiency for uniform and non-uniform pile groups and investigate the effect of the parameters on results.
- Calculating the raft-pile interaction factor and the load sharing between piles and raft.

All of the above were based on linear elastic analysis except the single pile capacity.

Finally, an application of a real piled raft system was studied by using the embedded beam model.

1.3 Outline of the thesis

The methodology was completed across four technical chapters, ranging from numerical to analytical research.

Chapter 2 gives an overview of the single pile behaviour, calculating the ultimate capacity of the pile by using one of the analytical methods and the numerical method by using PlAXIS 3D which contains these three models: (volume pile, embedded beam, and beam models), they are also used where the behaviour of a pile is related to measured soil properties and the applied load direction. Then comparing these results for the ultimate capacity and the stiffness under the vertical and the horizontal loads.

Chapter 3 demonstrates the interaction factor between two piles and gives a brief literature overview only for the analytical methods to calculate the interaction factors. Then, a study of the parameters is done to see the effect on the interaction factor values. Finally, some of the analytical expressions and numerical method by using PlAXIS 3D (volume pile, embedded beam models) are used to calculate the interaction factors. Based on the different methods, a study for parameters that affect the interaction factor and then comparing them to view the efficiency of embedded beam model for estimating the interaction factor.

Chapter 4 discusses the performance of pile groups under vertical load and their classification according to the cap rigidity to pile group with perfectly rigid cap and pile group with perfectly flexible cap. For piles group with perfectly rigid cap, all piles have the same settlement but the loads distribution on piles were different and for pile group with perfectly flexible cap was the opposite. Based on the analytical calculation of the interaction between two piles, the analysis was extended to piles group for estimating the load distribution between piles, the group efficiency, and differential settlement for different piles groups with different spacing and different ratios of pile length to pile diameter. For the numerical method based on PLAXIS 3D, a sensitivity analysis was done to determine the model dimensions in order to not affect the results. The analysis was done by using volume pile and embedded beam models for the same analytical cases. The analysis was done for different piles groups with uniform piles distribution (from 2x2 up to 7x7). Finally, a case of study for non-uniform piles distribution where the number of piles was 228. The analysis was used to measure the group efficiency by using the embedded beam model and different analytical methods.

The piled raft foundation is presented in chapter 5. As the raft and soil become connected, new types of interactions appeared as follows: raft-pile interaction, pile-raft interaction, and raft-soil interaction. The raft-pile interaction factor is calculated by one of the analytical methods for single pile with single raft and then extended to the pile groups with uniform and non-uniform piles distribution. Based on the analytical calculation for piled foundation stiffness from chapter 4, the raft stiffness, and the raft-pile interaction the load sharing factor is calculated for different piles groups with uniform pile distribution and the case of non-uniform piles distribution. For numerical method based on PLAXIS 3D, the analysis is done by using volume pile and embedded beam models for uniform piles distribution but for the non-uniform case where the piles number was 228, the analysis used the embedded beam model only. At the end of chapter 5, the discussed project is The Kingdom Tower in the Kingdom of Saudi Arabia. The analysis was done by using the embedded beam model only to simulate the piles which have different lengths and diameters. The soil is modeled with two constitutive models (Linear elastic and Mohr-Coulomb models) to estimate the raft-pile interaction and the load sharing factor between piles and raft in case of applying a uniform displacement. Also, the case of applying the actual gravity load is done to estimate the total and differential settlements.

Finally, the Conclusions were given in chapter 6.

Chapter 2 Behaviour of single pile

2.1 Introduction

Foundations are used to support structures and transfer their loads to soil layers and they are classified into shallow and deep foundations. Generally, shallow foundations are used when the structural loads are low relative to the bearing capacity of the surface soils, while deep foundations are used when the bearing capacity of the surface soils is insufficient to support the imposed loads, so they are transferred to deeper layers with a higher bearing capacity and also to control the settlement.

Pile foundations are one of the deep foundation types and used to transfer the load of the superstructure into the subsoil and stiff bearing layers, as well as controlling the settlement if the soil is not suitable to prevent excessive settlement. Also, they are used to carry the uplift loads when they support tall structures subjected to overturning forces from winds or waves.

Piles are classified by their basic design function into; end-bearing piles, friction piles, and friction/ end-bearing piles, or classified by their methods of installation into; displacement (driven) piles and replacement (bored) piles.

The behaviour of single pile depends on the soil properties, installation methods, and the applied load direction (horizontal or vertical).

This chapter gives a short brief about the single pile behaviour under vertical and horizontal loads and illustrates the load transfer mechanism for both cases. Then, it describes one of the analytical and numerical methods to calculate the ultimate capacity and stiffness and comparing these results for both methods.

2.2 Behaviour of single pile under vertical load

Piles are designed to ensure the structural safety of the pile body, sufficient for geotechnical capacity, acceptable settlement, and rarely used as single piles.
For the load transfer mechanism: vertical load is transferred to the surrounding soil through shear stress (skin friction) at the lateral pile-soil interface and by normal stress at the pile base. Figure 2. 1 shows a schematic overview of the vertical load and resistances acting on a pile.
The rate at which the vertical load is transferred to the soil along the pile and the overall deformations of the system is based on several factors. Among them: -

(a) Pile cross-section, material, length, and surface roughness.
(b) Soil type and its stress-strain characteristics.
(c) Groundwater absence or presence.
(d) Pile installation methods.
(e) The absence or presence of residual stresses due to pile installation [1].

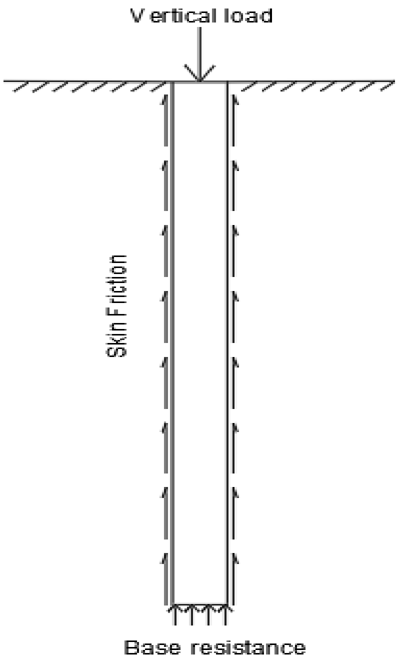

Figure 2. 1 A schematic overview of the vertical load and resistances acting on a pile.

The ultimate load capacity $\mathbf{Q_{ult}}$ of a single pile consists of two components, the ultimate shaft resistance $\mathbf{Q_{su}}$ and the ultimate base resistance $\mathbf{Q_{bu}}$. The sum of these two components minus the weight of the pile $\mathbf{W_p}$ gives the ultimate load capacity $\mathbf{Q_{ult}}$.

$$Q_{ult} = Q_{su} + Q_{bu} - W_p \qquad (2.\ 1)$$

Commonly $\mathbf{W_p}$ is small and could be neglected comparing to $\mathbf{Q_{ult}}$. However, in the case of piles in marine structures in deep water where a considerable length of shaft extends the seabed, and that should be taken into consideration.

$\mathbf{Q_{su}}$ and $\mathbf{Q_{bu}}$ from a static approach that were used, they are considered independent of each other but they are strictly speaking interdependent. Yang (2006) showed that the influence zone above the pile tip depends on the soil type with length up to 2.5d where **d** is the pile diameter [2]. Of course, when dealing with finite element analyses, the interaction of tip and shaft resistance are automatically taken into account.

Both the base and shaft resistances of a single pile develop as a function of pile displacements, but in general $\mathbf{Q_{su}}$ and $\mathbf{Q_{bu}}$ are not mobilized at the same displacement, so when the load is small yields to small relative displacements between pile and soil while most of the load is supported by shaft resistance. Due to increasing the load, the ultimate shaft resistance mobilizes and then the load is transferred to the pile base and the base resistance gets mobilized. In general terms, at relatively small settlement, $\mathbf{Q_{su}}$ is mobilized while large settlement is necessary to mobilize $\mathbf{Q_{bu}}$. According to Tomlinson & Woodward (2008), the settlement required to mobilize the maximum shaft friction is quite small and it ranges from 0.3% to 1% of the pile diameter and it ranges from 10% to 20% of the base diameter to mobilize the maximum base resistance [3]. Guo (2012) stated that the ultimate shaft resistance mobilized at settlement's range from 0.5% to 2% of the pile diameter and the ultimate base resistance mobilized at settlement up to 20% of the pile diameter and that also depends on pile-soil relative stiffness [4].

For the load settlement curve, initially the pile system behaves elastically until point **A** on the curve, if the load is increased until reaching point **B**, the maximum shaft resistance is mobilized and if the load is released, the residual settlement **OC** remaines. With increasing the load till point **D**, the ultimate base resistance is mobilized. At point **D**, any further increase in load produces significantly large settlements [3]. Figure 2. 2 shows the load-settlement curve for vertically loaded pile.

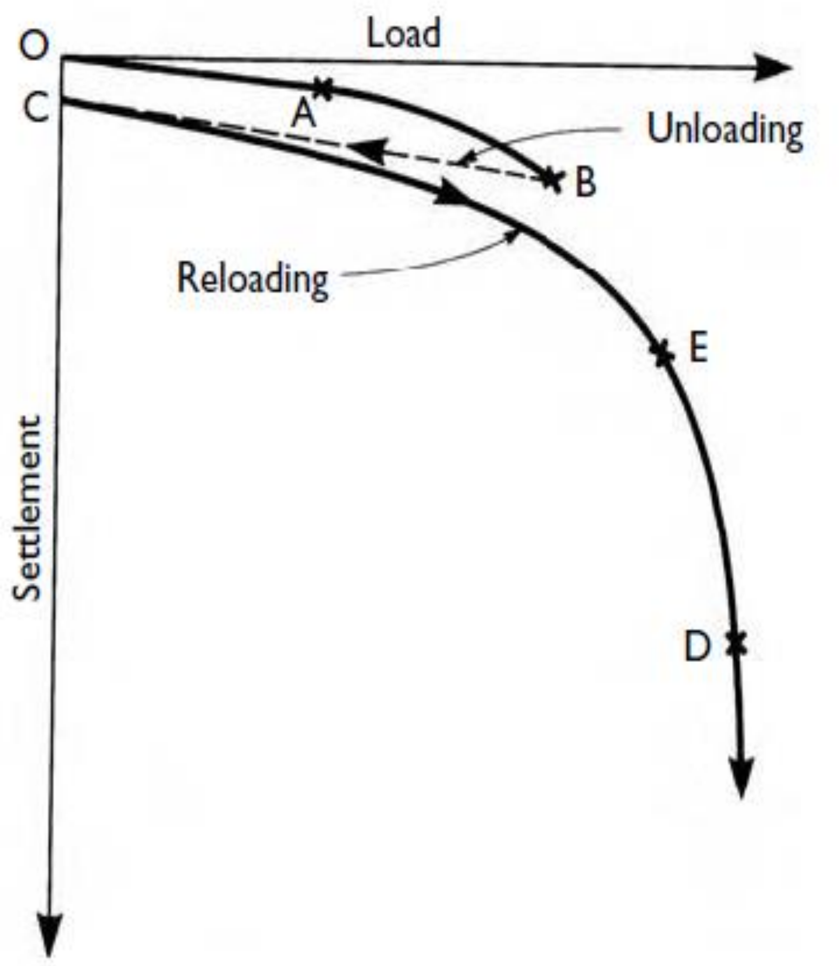

Figure 2. 2 The load-settlement curve for vertically loaded pile.

Usually, the pile ultimate load capacity is assumed to be the load causing the pile head settlement equal to 10% of the pile diameter and the allowable load might be determined either from considerations of shear failure or settlement, and it is determined from the lower of the following two values:

1. Allowable load obtained from dividing the ultimate failure load by a factor.
2. Load corresponding to an allowable settlement of the pile.

2.3 Methods of analysis

2.3.1 Analytical method

2.3.1.1 Ultimate vertical capacity of pile

Usually, "static" approaches are used to calculate the ultimate capacity of piles and there are many used methodologies which depend on the soil properties (coarse-grained soils or fine-grained soils), and the installation methods of the pile (driven or bored pile). The study focused on the clay soil case with bored pile.

For calculating $\mathbf{Q_{bu}}$, the following equation was used: -

$$Q_{bu} = N_c * S_b * A_p \qquad (2.\ 2)$$

where; $\mathbf{N_c}$ is the bearing capacity factor approximately equal to 9, $\mathbf{S_b}$ is the characteristic undisturbed undrained shear strength at the pile toe, and $\mathbf{A_p}$ is the pile cross-sectional area at the base.
For calculating $\mathbf{Q_{bu}}$, the following equation was used: -

$$Q_{us} = \alpha * S_u * A_s \qquad (2.\ 3)$$

where; $\boldsymbol{\alpha}$ is an adhesion factor and it ranges from 0.3 to 0.6 and its recommended value equal 0.45 for normal conditions, $\mathbf{S_u}$ is the average undisturbed undrained shear strength of the soil surrounding the pile shaft and $\mathbf{A_s}$ is the surface area of the pile shaft [3].

2.3.1.2 Vertical stiffness

In order to calculate the vertical stiffness $\mathbf{K_v}$ for a flexible single pile in a homogeneous soil with linear elastic conditions, this equation was used: -

$$K_v = E_p\, A_p\, \lambda\ \frac{\Omega + \tanh(L\lambda)}{1 + \Omega \tanh(L\lambda)} \qquad (2.\ 4)$$

where; $\mathbf{E_p}$ is the pile Young's modulus, $\boldsymbol{\Omega}$ is the base stiffness parameter, $\boldsymbol{\lambda}$ is the load transfer parameter, and **L** is the pile length.

$$\lambda = \sqrt{\frac{K_z}{A_p\, E_p}} \qquad (2.\ 4a)$$

where; Winkler spring $\mathbf{K_z}$ = (0.6 to 0.8) E_s, and $\mathbf{E_s}$ is the Young's modulus for soil.

$$\Omega = \frac{K_b}{A_p\ E_p\ \lambda} \tag{2. 4b}$$

The base stiffness $\mathbf{K_b} = \frac{d\ E_s}{1-\nu_s^2}$ where, ν_s is the soil Poisson's ratio [5].

2.3.1.3 **Ultimate Lateral capacity and lateral stiffness**

The main focus in the next chapters is related to vertical loads, nevertheless the performance of single pile under horizontal load was checked in this chapter. There is a big difference between the pile behaviour under horizontal and vertical loads. Under vertical load, the structural section of the pile subjected to normal compression stress and that stress always less than the pile material strength so the failure usually occurs in the interface between pile and soil. On the other hand, under the horizontal load, the pile subjected to bending and shear so the pile cross-section has a large influence on the pile for both response; the serviceability limit state and the ultimate limit state.

Furthermore, the behaviour of vertically loaded pile and in particular its bearing capacity, dependes on the characteristics of the soil immediately close to the shaft and below the base so the installation methods have a significant effect on the soil properties. In the case of laterally loaded pile, on the contrary, the installation techniques were usually considered not significantly effective to the pile behaviour and its capacity[6]. The evidence was found from the experiment for a small number of horizontal loading tests on piles at the same site, where the subsoil was mainly dense sand and the groundwater level was close to the ground surface, but the installation methods for partly jetting with driven method showed a small effect. The site tests showed that the different installation techniques didn't affect the settlement curves for that case. However, for other piles like displacement screw and driven pile at same soil, the installation methods affected slightly the pile behaviour[7].

For estimating the lateral capacity $\mathbf{H_{ult}}$ for free head pile in homogenous soil with constant undrained shear strength with depth $\mathbf{S_u}$, this equation was used:

$$H_{ult} = \sqrt{2\ M_y\ P_y} \tag{2. 5}$$

$$P_y = 9\ S_u\ d \tag{2. 5a}$$

where $\mathbf{M_y}$ is the bending moment capacity for pile[8].

For estimating the stiffness for laterally loaded pile in a homogeneous soil with linear elastic Young's modulus with free head $\mathbf{K_h^{free}}$.

$$K^{fixed} = \begin{bmatrix} K_h^{fixed} & K_{hr}^{fixed} \\ K_{rh}^{fixed} & K_r^{fixed} \end{bmatrix}$$

$$K^{fixed} = \begin{bmatrix} 4E_pI_pg^3 \frac{\sin(2gL)+\sinh(2gL)}{2+\cos(2gL)+\cosh(2gL)} & E_pI_pg^2 \frac{-\cos(2gL)+\cosh(2gL)}{2+\cos(2gh)+\cosh(2gL)} \\ 2E_pI_pg^2 \frac{-\cos(2gL)+\cosh(2gL)}{2+\cos(2gL)+\cosh(2gL)} & 2E_pI_pg \frac{-\sin(2gL)+\sinh(2gL)}{2+\cos(2gL)+\cosh(2gL)} \end{bmatrix} \quad (2.6)$$

where;

$$I_p = \frac{\pi d^4}{64} \quad (2.6a)$$

$$K_x = 1.2 E_s \quad (2.6b)$$

$$g = \left(\frac{K_x}{4E_p I_p}\right) \quad (2.6c).$$

$$K_h^{free} = K_h^{fixed} - \frac{\left(K_{rh}^{fixed}\right)^2}{K_r^{fixed}} \quad (2.7)$$

and $\mathbf{K^{fixed}}$ is the stiffness matrix for laterally loaded pile with fixed head[9].

2.3.2 Numerical method

Within the last decades, numerical modeling was used for deep foundation analyses. One of these numerical methods was the finite element method which is a very powerful tool that takes into account all different interactions between the soil and the structure and this needs high knowledge of soil mechanics and the behaviour of constitutive models. There are many finite element programs like PLAXIS 3D, FLAC 3D, and Abaqus. However, PLAXIS 3D is directed to analyze finite element geotechnical engineering problems, so it was used in the modeling of the study case.

To simulate the pile in PLAXIS 3D, there were three methods: -

1. **Volume element** in which the geometry of the volume pile was defined horizontally by choosing a cross-section and vertically by specifying two work planes between them the pile was drawn. The material properties were subsequently assigned to the pile. The pile-soil interaction was modeled with interface elements which placed around the pile periphery and that led to large models and as a result it gave long calculation time. Figure 2. 3 shows the volume pile visualization in PLAXIS 3D.

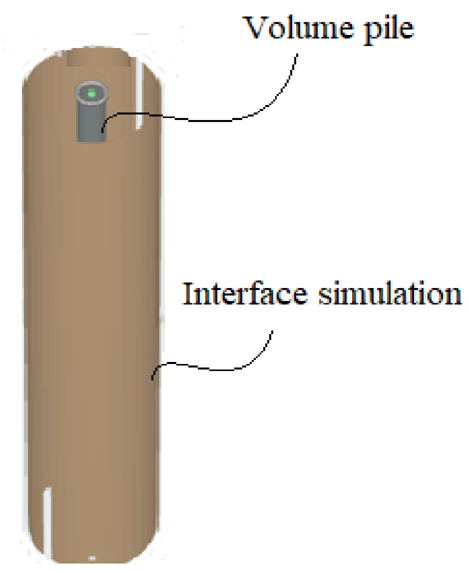

Figure 2. 3 Visualization of volume pile in PLAXIS 3D.

2. **Embedded beam** is an attractive method to reduce the model complexity and it takes into account the penetration of the pile for the finite element in any orientation thus it is convenient for analysis of inclined piles. The input parameters were; pile stiffness, unit weight, and the pile cross-section in addition, it allowed to define the interaction between the pile and the surrounding soil by defining the axial skin resistance and base resistance. Figure 2. 4 illustrates a schematic view for the embedded beam model.

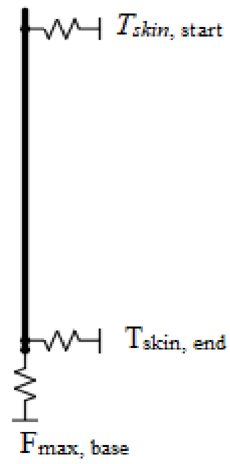

Figure 2. 4 Schematic view for the embedded beam model.

3. **Beam model** only allows to define the input parameters (pile stiffness, unit weight, and the pile cross-section) and does not take into consideration the penetration of the pile to the soil in all directions or the interaction between the pile and the surrounding soil.

PLAXIS 3D provides 14 different material models, suitable for different cases. In the present work, the used constitutive models were linear elastic model and linear elastic-perfectly plastic model or Mohr-Coulomb model (MC).

Under horizontal load, the pile material nonlinearity must be taken into account in modeling. The constitutive model for volume pile material was Mohr-Coulomb with some modifications in the cohesion **C** and friction angle **φ** parameters to simulate the macroscopic response of a reinforced concrete circular pile section by using the following equations: -

$$C_{\mathrm{M-C}} = 38.5 \; f_c^{0.34} \; f_s^{0.626} \; \rho_{tot}^{0.61} \; c^{-0.04} \tag{2. 8}$$

$$\varphi_{\mathrm{M-C}} = 187 \left[\frac{f_c}{\rho_{tot}} \right]^{0.41} \; f_s^{-0.437} \; c^{0.36} \tag{2. 9}$$

where $\boldsymbol{C_{\mathrm{M-C}}}$ and $\boldsymbol{\varphi_{\mathrm{M-C}}}$ are the modified strength parameters of the Mohr-Coulomb model, $\boldsymbol{f_c}$ is concrete strength in Mpa, $\boldsymbol{f_s}$ is the steel yield strength, **c** is the concrete cover for pile in meter, and $\boldsymbol{\rho_{tot}}$ is the longitudinal reinforcement ratio (1 to 3%) [10].

For the embedded beam model, the pile material was defined as elastoplastic by calculating bending moment capacity for the pile $\mathbf{M_y}$ which is related to the geometry and material properties of the pile. $\mathbf{M_y}$ was estimated by using USC-RC software for analyzing behavior of a single reinforced concrete member [11].

The finite element model geometry had the same length and width from **1.2L** to **1.5L** and depth equal to **L+10d** in order to take the effect of the boundaries on the response of the pile. The boundary conditions were automatically applied to prevent the out of plane deformations at vertical sides while the base was fixed in all three directions. Figure 2. 5 shows the dimensions and boundaries of 3D model in PLAXIS.

2.4 Case of study

To check the validity of the embedded beam model by using PLAXIS 3D software, a simple three-dimensional model was created. Where the model dimensions X*Y*Z are 30*30*18 m. A borehole was defined with 18 meters deep and with dry soil conditions. The borehole was assigned by the material properties.

The soil was described with two constitutive models for vertical capacity and vertical stiffness: a) Mohr-Coulomb model (MC) and, b) linear elastic model. Table 2. 1 illustrates the input parameters for both models.
And for lateral capacity and stiffness, the soil input parameters are shown in Table 2. 2.

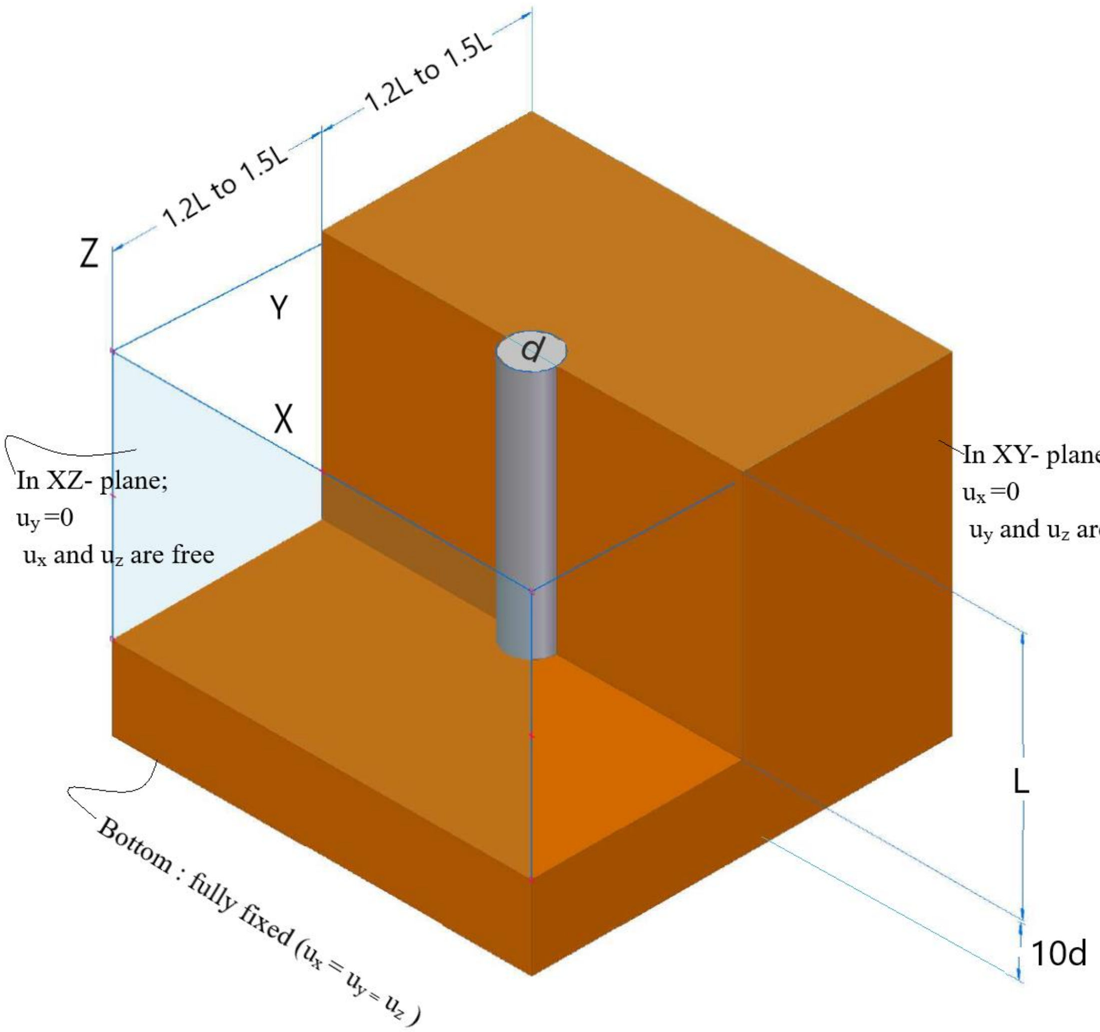

Figure 2. 5 The dimensions and the boundaries of 3D model in PLAXIS.

Case / Parameter	Vertical capacity	Vertical stiffness	Unit
Young's modulus (E)	10.9*10^3	50*10^3	KN/m^2
Poisson's ratio (ν)	0.3	0.3	-----
Density (γ)	≈ 0	≈ 0	KN/m^3
undrained shear strength (S_u)	60	-----	KN/m^2
Increase of stiffness with depth (E_{inc})	2600	-----	KN/m^2
Increase of undrained shear strength with depth ($S_{u, inc}$)	4	-----	KN/m^2
Interface strength (R_{inter})	0.45	1	-----

Table 2. 1 Soil input parameters for vertical capacity and vertical stiffness.

Case / Parameter	Lateral capacity	Lateral stiffness	Unit
Young 's modulus (E)	$10.9*10^3$	$50*10^3$	KN/m^2
Poisson's ratio (ν)	0.3	0.3	-----
Density (γ)	≈ 0	≈ 0	KN/m^3
undrained shear strength (S_u)	60	-----	KN/m^2
Increase of stiffness with depth (E_{inc})	2600	-----	KN/m^2
Increase of undrained shear strength with depth ($S_{u, inc}$)	4	-----	KN/m^2
Interface strength (R_{inter})	0.45	1	-----

Table 2. 2 Soil input parameters for Lateral capacity and Lateral stiffness.

The pile was assumed to be in contact with the surrounding soil over its entire length. The pile dimensions are; length **L**= 12.4 m and diameter **d**=0.5 m.

The pile material type was linear elastic and the parameters for vertical capacity, vertical and lateral stiffness are illustrated in Table 2. 3.

Case / Parameter		Vertical capacity	Vertical and lateral stiffness	Unit
Young 's modulus (E)		$300*10^6$	$30*10^6$	KN/m^2
Poisson's ratio (ν)		0.2	0.2	-----
Density (γ)		≈ 0	≈ 0	KN/m^3
Axial skin resistance (EP)	$T_{skin, start}$	42.5	$42.5*10^6$	KN/m
	$T_{skin, end}$	78	$78*10^6$	KN/m
Base resistance F_{max} (EP)		194	$194*10^6$	KN

Table 2. 3 Pile input parameters for both vertical capacity, vertical and lateral stiffness.

For lateral capacity, Table 2. 4 shows the pile input parameters for volume pile model material as Mohr-Coulomb model where, the parameters were used to calculate the modified cohesion and friction angle are; fc =30 Mpa, f_s = 500 Mpa, and ρ =2%. Table 2. 5 illustrates the pile input parameters for embedded beam model.

Parameter	Value	Unit
Young's modulus (E)	$10*10^6$	KN/m^2
Poisson's ratio (ν)	0.2	-----
Density (γ)	≈ 0	KN/m^3
Modified cohesion (C_{M-C})	10301	KN/m^2
Modified friction angle (φ_{M-C})	33.7	°
Interface strength (R_{inter})	1	-----

Table 2. 4 Pile input parameters for volume pile model for lateral capacity.

<table>
<tr><th colspan="2">Parameter</th><th>Value</th><th>Unit</th></tr>
<tr><td colspan="2">Young's modulus (E)</td><td>$30*10^6$</td><td>KN/m^2</td></tr>
<tr><td colspan="2">Density (γ)</td><td>≈ 0</td><td>KN/m^3</td></tr>
<tr><td colspan="2">Bending moment capacity (M_y)</td><td>340</td><td>KN.m</td></tr>
<tr><td rowspan="2">Axial skin resistance</td><td>$T_{skin, start}$</td><td>35.34</td><td>KN/m</td></tr>
<tr><td>$T_{skin, end}$</td><td>35.34</td><td>KN/m</td></tr>
<tr><td colspan="2">Base resistance (F_{max})</td><td>0</td><td>KN</td></tr>
</table>

Table 2. 5 Pile input parameters for embedded beam model for lateral capacity.

2.5 Comparing the results

The results from PLAXIS 3D analysis were presented in this part and compared with analytical expressions to check the validity of the embedded beam model under different loads for both capacity and stiffness.

2.5.1 Ultimate vertical capacity and vertical stiffness

The following results were based on sections 2.3.1.1 and 2.3.1.2 for the analytical method and the three pile models (volume pile, embedded beam, and beam models) for the finite element method **FEM**. Table 2. 6 Compares the ultimate vertical capacity and vertical stiffness for both numerical and analytical methods, in addition to the error percentage with respect to the analytical method. The comparison showed clear agreement between the embedded beam model and both volume pile model and analytical method.
Figure 2. 6 shows the load-settlement curves for three different pile models. The load-settlement curves are almost identical between the volume pile model and embedded beam model, but different from the beam model.
Also, Figure 2. 7 presents the influence of coarseness factors for the embedded beam on the load-settlement curve.

Method	PLAXIS 3D models for pile			Analytical method
	Volume pile	Embeddd beam	Beam	
Ultimate vertical capacity (KN)	973	986	1859	939.4
Error %	3.45	4.96	49.47	………
Vertical stiffness (KN/m)	328262	313995	250468	310670
Error %	5.36	1.06	24.04	………

Table 2. 6 Comparison of the results for ultimate vertical capacity and vertical stiffness between analytical and numerical methods.

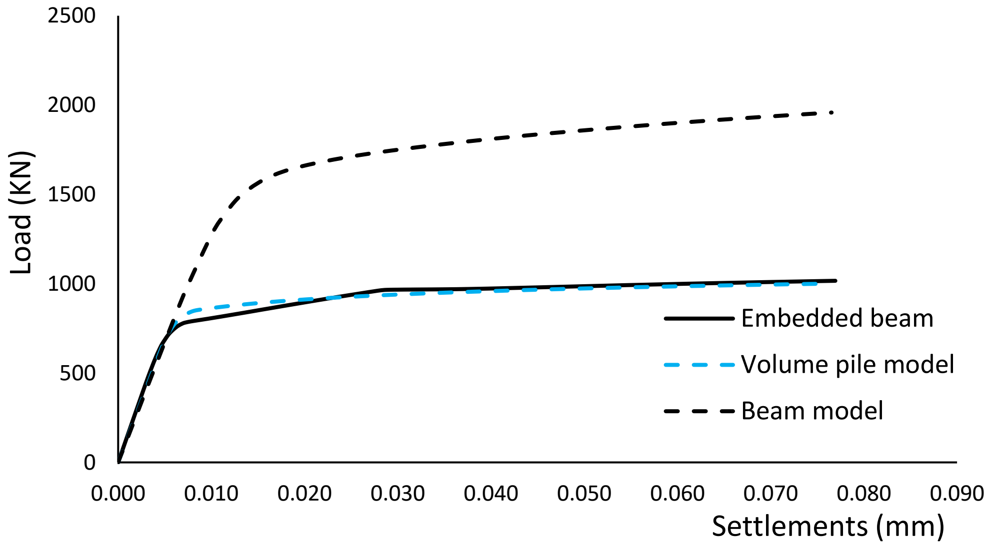

Figure 2. 6 Load - settlement curves for three models for pile under vertical loads.

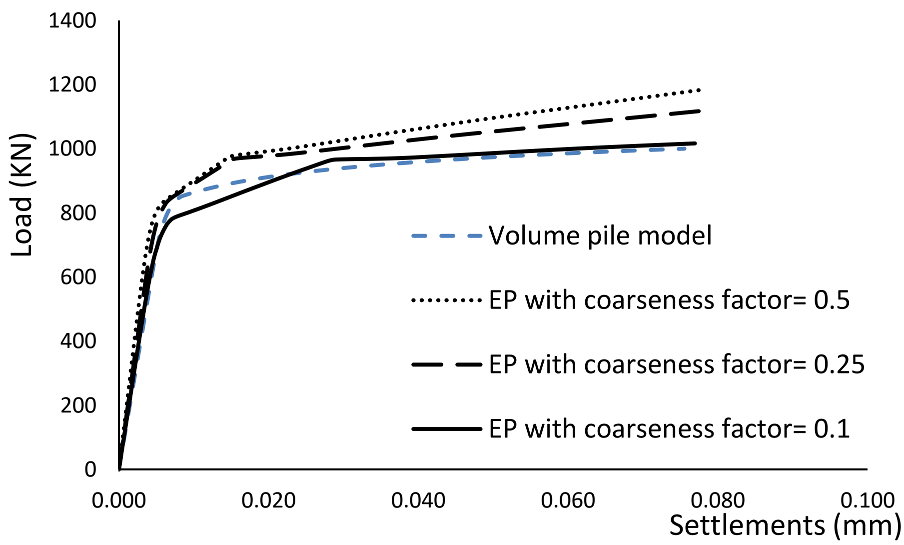

Figure 2. 7 Load-settlement curves for different coarseness factors.

2.5.2 **Ultimate Lateral capacity and lateral stiffness**

The following results were established according to section 2.3.1.3 for analytical method and the two models for piles (volume pile and embedded beam models) for FEM.
Table 2. 7 presents a comparison for the ultimate lateral capacity and lateral stiffness for both FEM and analytical method, in addition to the error percentage with respect to analytical method. This also agreed with the earlier observations, which showed that a good agreement between the embedded beam model and both analytical method and volume pile model.

Method	PLAXIS 3D models for pile		Analytical method
	Volume pile	Embeddd beam	
Ultimate lateral capacity (KN)	328	330	391
Error %	16.1	15.6	……...
Lateral stiffness (KN/m)	52000	502099	47216
Error %	9.2	9.38	……...

Table 2. 7 Comparison of the results for ultimate lateral capacity and lateral stiffness between analytical and numerical methods.

Also, Figure 2. 8 provides the lateral load - displacement curves for different two pile models under lateral load and both of them were modelled without interface.

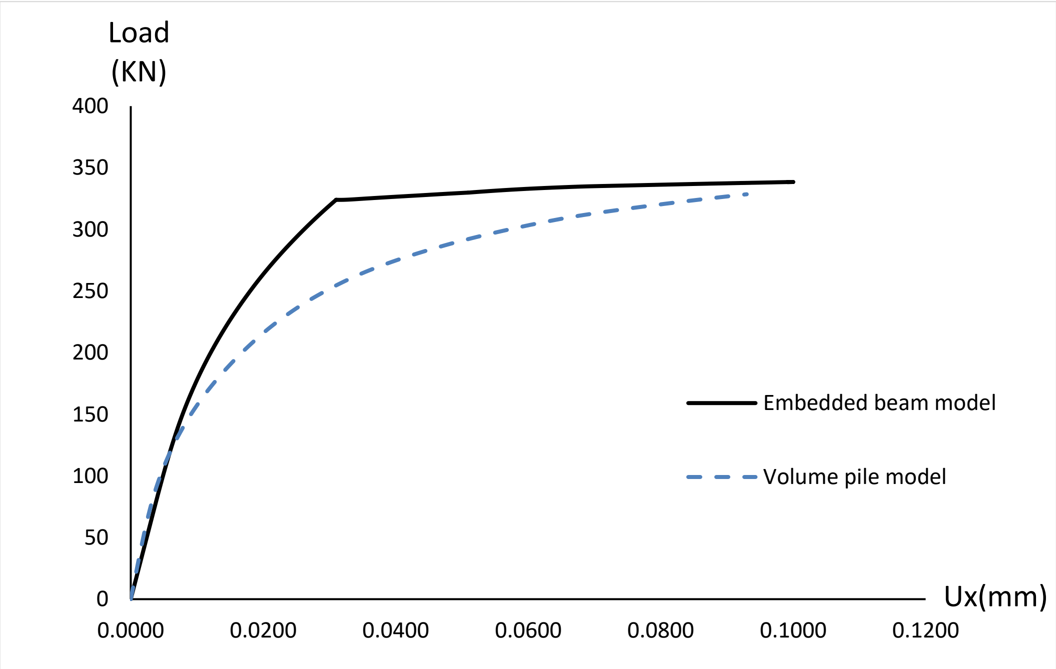

Figure 2. 8 Lateral load - displacement curves for Vp and Eb modeles

Chapter 3 Interaction factors between two piles under vertical loads

3.1 Introduction

Usually, the single pile study is focused on the assessment of the stiffness and the load-settlement behaviour, but in the case of the pile groups, the focus also should be on the increased settlements due to the neighbouring piles, especially that the recent trend in design gives great attention to the total and differential settlements because of its significant impact on the structural behavior of the building.

The additional settlement of pile due to the effect of neighbouring pile is expressed in term of an interaction factor **α**. For a group of two piles (loaded pile is called the source or active pile and the unloaded pile is called the receiver or passive pile), there are two approaches to calculate the interaction factor: -

- Approach I: both of source and receiver pile are loaded.
- Approach II: the source pile is loaded and the receiver pile is free.

For both approaches, **α** is defined as the ratio of additional vertical displacement of the receiver pile due to the presence of source pile over the vertical displacement of the source pile, when it is subjected to its own load. Figure 3. 1 shows the representation of approaches I and II.

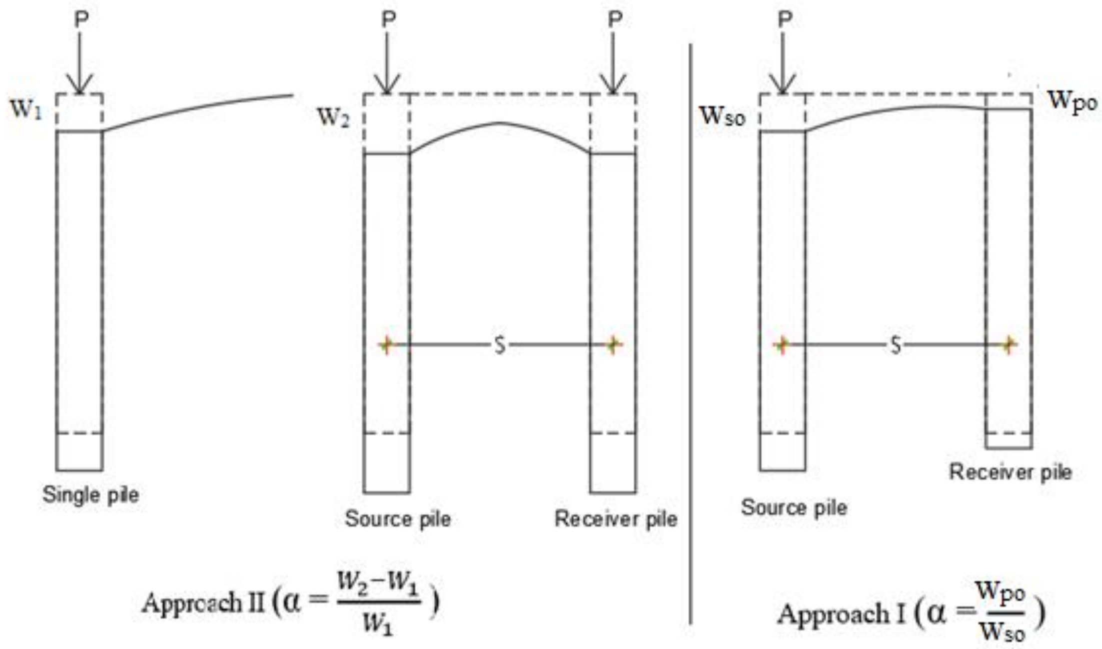

Figure 3. 1 Representation of approaches I and II.

3.2 literature overview

Several methods to analyze the interaction factor between two piles under vertical static loads and number of studies published over the past few decades. Poulos (1968) studied the settlement interaction between two identical incompressible piles with equal load (Approach II) in an elastic soil with constant Young's modulus $\mathbf{E_s}$ and Poisson's ratio $\boldsymbol{\nu_s}$ for both cases; floating piles and end-bearing piles to find the interaction factor. The influence of pile spacing to pile diameter ratio **S/d**, pile length to diameter **L/d**, and Poisson's ratio have been studied in the interaction factor calculations [12]. Also, Poulos and Mattes (1971) have continued the study and took the effect of pile stiffness factor **K** which is equal to the ratio of soil elastic modulus to the pile elastic modulus $\mathbf{E_p/E_s}$ [13]. Poulos and Davis (1980) extended the study of parameters that affect the interaction factors value for floating piles and provided correlation factors for enlarged pile base, Poisson's ratio, and nonuniform soil modulus (linearly increasing with depth) [14].

For a group of two rigid piles with the same length as in approach I, Randolph and Wroth (1979) used an attenuation function $\boldsymbol{\psi_{(s)}}$ to calculate the displacement field around the source pile. They assumed that the receiver pile follows exactly the free-field soil displacement and consequently $\boldsymbol{\psi_{(s)}}$ approximately equal the interaction factor. Also, they studied the effect of soil homogeneity on the interaction factor values [15].

Under vertical dynamic loads, Dobry and Gazetas (1988) suggested another expression to calculate $\boldsymbol{\psi_{(s)}}$ to find the displacement field around the source pile [16]. Also, Makris and Gazetas (1991) used another rigorous expression for estimating $\boldsymbol{\psi_{(s)}}$ [17], and then Mylonakis and Gazetas (1998) presented a straightforward expression for $\boldsymbol{\psi_{(s)}}$ [18]. The main assumption for the attenuation function depended on the centerline approach where the distance **S** was measured from the centerline of the source pile to the centerline of the receiver pile. Recently, Luan (2020) presented a new attenuation function $\boldsymbol{\psi_{(s)}}$ that allowed to consider the effect of the actual pile geometry on the contribution of pile-soil-pile interaction [19].

Actuality, the receiver pile did not follow the free-field displacement generated by the source pile, Mylonakis and Gazetas (1998) used a new model for pile -to- pile interaction to take into account the effect of pile axial rigidity and the interaction between the pile and surrounding soil by using a new expression $\boldsymbol{\zeta}$ **function** [5].

3.3 Parameters effect on the interaction factor

As mentioned in the literature review, Poulos and Davis (1980) used the second approach to calculate $\boldsymbol{\alpha}$ for two floating piles in homogenous semi-infinite mass with ν_s =0.5 and constant $\mathbf{E_s}$ with depth. The parameters that affect the interaction factor can be listed as follows:

- By increasing **S/d** ratio, the value of $\boldsymbol{\alpha}$ decreases.
- By increasing the stiffness factor **K**, the value of $\boldsymbol{\alpha}$ increases.

- By increasing the **L/d** ratio, the value of **α** increases.
- In case of present a finite layer, the value of **α** decreases.
- By decreasing $\mathbf{v_s}$, the value of **α** increases.
- For increasing $\mathbf{E_s}$ with depth linearly, the value of **α** decreases with percentage ranges from 20 to 25%.

For end-bearing piles on a rigid stratum, as **S/d** increases, the value of **α** decreases with high rate. on the other hand, by increasing **K**, the value of **α** decreases [14].

Nguyen (2013) studied the effect of soil relative density $\mathbf{D_r}$ for dense and loose sand by using the FEM and he found that the interaction factor **α** was reduced when the relative density of soil decreased [20].
Also, Modarresi and Rasouli (2016) studied profusely the effect of relative soil density on **α** for sandy soil by using series of centrifuge model tests and FEM and found that the soil relative density had a significant effect and it must be taken into account in the interaction factor calculations. They did a comparison between experimental and numerical analysis as provided in Figure 3. 2. The interaction factor increased with increasing the soil relative density but after D_r = 56% a slight increase was observed. Also, the effect of the relative soil density was very small at **S/d** =3 and has a large effect on **S/d** ≥ 5 [21].

McCabe and Sheil (2014) showed the influence of soil nonlinearity on the interaction factor by using the hardening soil model (HS) and linear elastic soil model (LE) and found the load-displacement curve for both the source pile and the receiver pile with S/d =3. The analysis found that, the receiver pile vertical displacement was almost identical for the HS model and the LE soil model and that supported the theory that pile-to-pile interaction is essentially a linear phenomenon. Also, they presented the difference between approach I and II for calculating the interaction factor and they found that approach I gave the most accurate predictions [22].

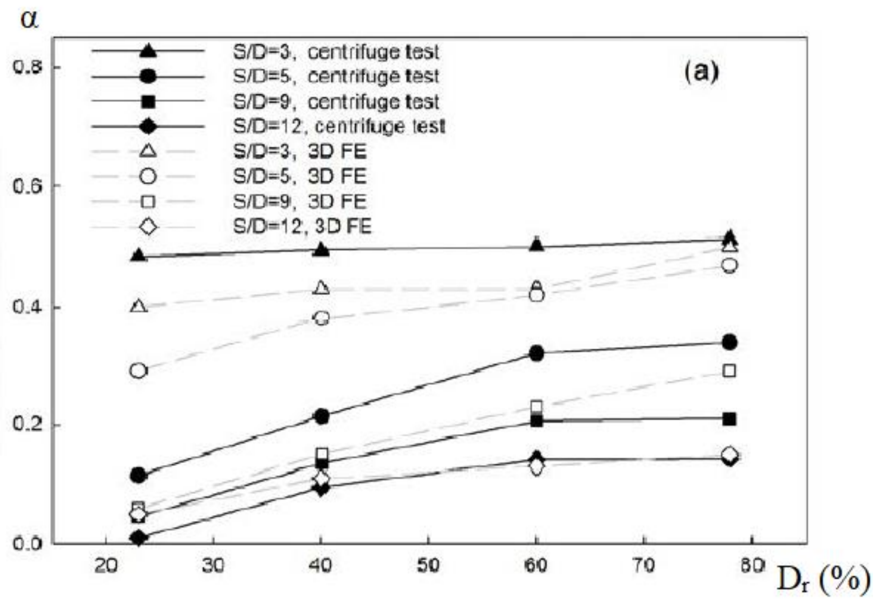

Figure 3. 2 The effect of the relative soil density to the interaction factor.

3.4 Methods of analysis

3.4.1 Analytical method

To calculate the interaction factor **α** between two piles having central distance **S** in an elastic homogeneous soil with constant $\mathbf{E_s}$, the start came from calculating the vertical displacement for the source pile $\mathbf{w_s}$ which can be calculated by using the flowing differential equation for vertically loaded pile: -

$$E_p\, A_p \frac{d^2 w_{so}}{d\, z^2} - k_z\, w_{so} = o \qquad (3.\ 1)$$

This vertical displacement $\mathbf{w_{so}}$ get reduced as the radial distance **S** from the source pile increases. At the receiver pile, the vertical displacement was found by this equation: -

$$W_{po} = \psi_{(s)}\, w_{so} \qquad (3.\ 2)$$

Several methods are used to calculate the attenuation function $\boldsymbol{\psi_{(s)}}$.
Randolph and Wroth (1979) assumed the following expression: -

$$\psi(s) = \begin{cases} \dfrac{\mathrm{Ln}\ r_m - \mathrm{Ln}\ S}{\mathrm{Ln}\ 2r_m - \mathrm{Ln}\ d} & \dfrac{d}{2} < S < r_m \\ 0 & S \geq r_m \end{cases} \qquad (3.\ 3)$$

$$r_m = \chi_1 \chi_2\, L\, (1-\nu_s) \qquad (3.3a)$$

where; $\boldsymbol{\chi_1\chi_2}$ ≈ 2.5 for homogeneous half-space conditions and $\boldsymbol{\chi_1\chi_2}$ ≈ 1 for gibson soil on bedrock conditions. In this relation, the two piles must have the same length [15].

Makris and Gazetas (1991) used a rigorous formula to express the attenuation function in case of harmonic vertical load: -

$$\psi_{(s)} = \frac{H_0^2\left(\frac{S}{d}\, \frac{a_0}{\sqrt{1+2\, i\, \beta_S}}\right)}{H_0^2\left(\frac{1}{2}\, \frac{a_0}{\sqrt{1+2\, i\, \beta_S}}\right)} \qquad (3.\ 4)$$

This formula could be applicable at static conditions at very low frequencies for static condition where; Dimensionless frequency $\mathbf{a_0} = \frac{wd}{Vs}$ = 0.0001, $\mathbf{H_0^2(\quad)}$ is the Hankel function of zero-order and second kind and $\boldsymbol{\beta_s}$ is the hysteretic damping ratio of soil (β_s = 5%) [17].

Mylonakis and Gazetas (1998) proposed the following approximate expression for the attenuation function: -

$$\psi_{(s)} = \left(\frac{2S}{d}\right)^{-0.5} \exp\left[-(\beta_s + i)\left(\frac{S}{d} - \frac{1}{2}\right) a_0\right] \approx \sqrt{\frac{d}{2\,S}} \qquad (3.\ 5)$$

this expression is approximately the same as Dobry and Gazetas (1988) [18].

The main assumption for all previous relations depends on the centerline approach **S** and applicable for **S/d** > 2. However, in the case of **S/d** ≤ 2 the centerline approach couldn't be applicable because the influence of the geometry of the receiver pile must be taken into account because of the vertical displacement would be different around the receiver pile. Luan (2020) presented a 3D attenuation function $\boldsymbol{\psi_{(s)}}$ which took the effect of pile geometry into consideration: -

$$\psi_{(s)} = \frac{\sum_{n=1}^{\infty} R_n(S)\ Z_n(z)\ A_n}{\sum_{n=1}^{\infty} R_n(\frac{d}{2})\ Z_n(z)\ A_n} \qquad (3.\ 6)$$

where; $\mathbf{A_n}$ is an undetermined coefficient, $\mathbf{R_n(\ )}$ is the soil reaction factor, $\mathbf{Z_n(z)}$ is the soil mode and subscript **n** denotes the nth mode (n = 1,2,3...) [19].

Actually, the receiver pile does not follow the free field displacement generated by the source pile. The axial pile rigidity and its interaction with the soil at the pile tip lead to reduce the vertical displacement which is calculated in equation (3.2). Mylonakis and Gazetas (1998) proposed the following attenuation function **ζ** to take the effect of pile axial rigidity: -

$$\zeta = \frac{2\,L\lambda + \sinh(2\,L\lambda) + \Omega^2[\sinh(2\,L\lambda) - 2\,L\lambda\,] + 2\,\Omega\,[\cosh(2\,L\lambda) - 1]}{2\sinh(2\,L\lambda) + 2\,\Omega^2\sinh(2\,L\lambda) + 4\,\Omega\cosh(2\,L\lambda)} \qquad (3.\ 7)$$

where; **Ω** and **λ** are calculated from equations (2.4a) and (2.4b).

So, the interaction factor for two piles in a single soil layer is calculated from the following equations: -

$$\alpha_s = \psi_{(s)}\ \zeta \qquad (3.\ 8)$$

All the previous calculations for the interaction factor $\boldsymbol{\alpha_s}$ represented the interaction between pile shafts. With the same steps, the interaction factor between pile bases is represented by the following equations: -

$$\psi_{b(s)} \approx \frac{d}{\pi S} \qquad (3.\ 9)$$

$$\zeta_b = \frac{2\Omega}{2\Omega\cosh(2L\lambda) + \sinh(2L\lambda)(\Omega^2+1)} \qquad (3.\ 10)$$

$$\alpha_b = \psi_{b(s)}\ \zeta_b \tag{3. 11}$$

The total interaction factor **α** is the sum of the shaft-to-shaft and the base-to-base components but the base-to-base interaction is very small, so it can be neglected [5].

3.4.2 Numerical method

The analysis was done by using PLAXIS 3D for calculating the interaction factor between two piles. The material type was linear elastic (LE) for both soil and pile material. The finite element model geometry had dimensions (X= S+2* max (1.5L+5S), Y= 2* max (1.5L+5S), and Z= L+max (1.5L+5S)) in order to take the effect of the boundaries to be compatible with the analytical method. Figure 3. 3 shows the dimensions of 3D model in PLAXIS and the coarseness factor considerations. The analysis method depended on applying a unit vertical displacement (w_{so}=1m) on the source pile and then running the analysis to measure the vertical displacement on the receiver pile $\mathbf{w_{po}}$. For a given pile spacing, the interaction factor $\left(\alpha = \frac{w_{po}}{w_{po}}\right)$ was calculated.

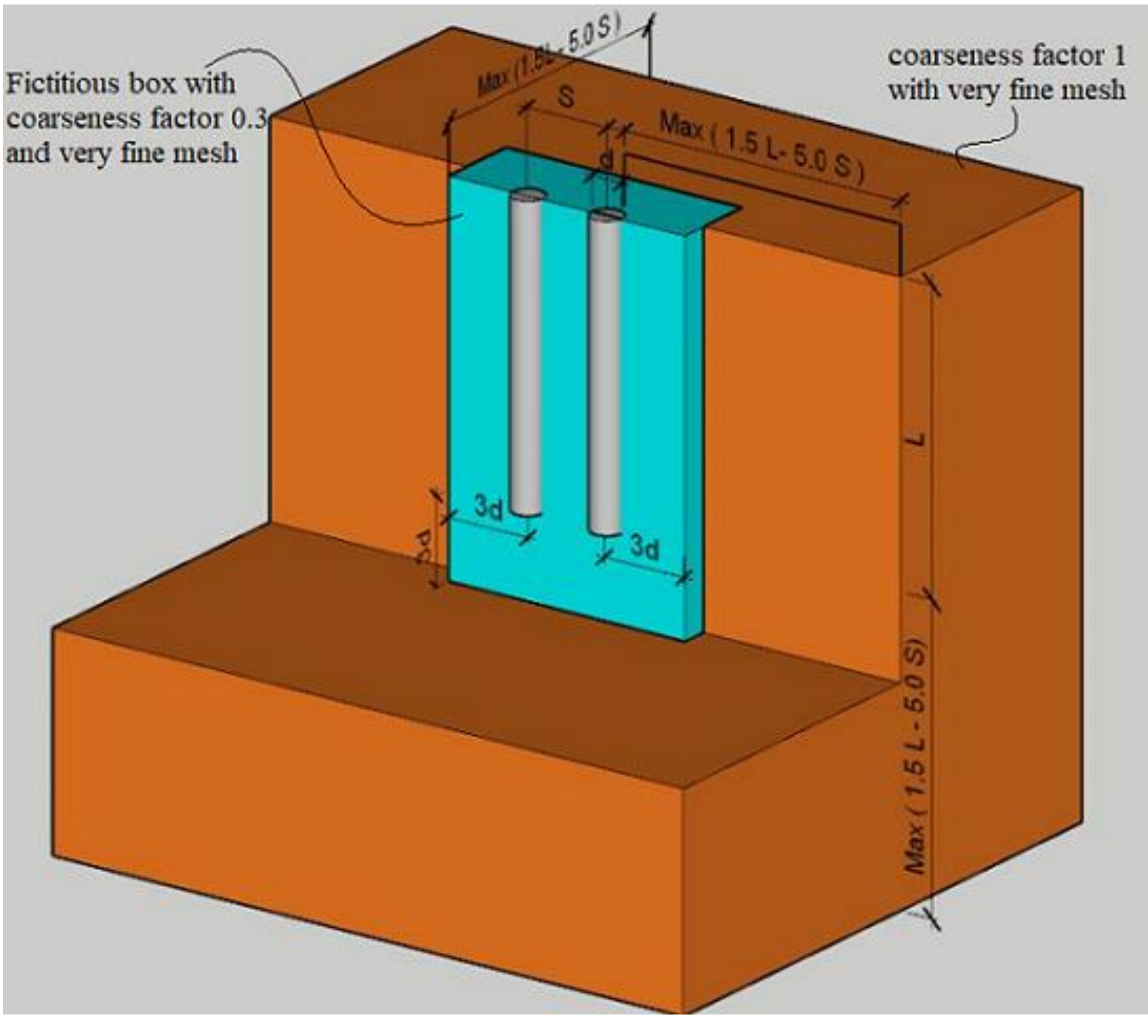

Figure 3. 3 The dimensions of 3D model in PLAXIS and the coarseness factor considerations for the interaction factor

3.5 Case of study

To determine the pile-to-pile interaction factor and measure the effectiveness of embedded beam model, a simple three-dimensional model was used. The model dimensions depended on the spacing between piles **S** and pile geometry **L** and **d**. A borehole was defined with dry soil conditions.

Both soil and pile were described by linear elastic model. Table 3. 1 shows the input parameters for soil and pile material.

Material type	Soil material	Pile material	Unit
Parameter	Input value	Input value	
Young's modulus (E)	$60*10^3$	$30*10^6$	KN/m^2
Poisson's ratio (ν)	0.35	0.2	-----
Density (γ)	≈ 0	≈ 0	KN/m^3
Interface strength (R_{inter})	1	1	-----

Table 3. 1The input parameters for soil and pile material.

The pile-to-pile interactions were discussed for pile spacing (S/d = 3, 5, 8, 10, 12,15) for both FEM by using the volume pile and embedded beam models, and analytical methods. Also, a study for the effect of Poisson's ratio for soil (ν_s = 0.35, 0) and the effect of L/d ratio (L/d = 10, 25) was displayed.

3.6 Comparing the results of analytical and numerical methods

The following results were depended on section 3.4.1 for the analytical method and the two pile models (volume pile and embedded beam models) for the FEM.

Figure 3. 4 and Figure 3. 5 show a comparison of the interaction factors for homogeneous soil layer between the analytical and numerical method for L/d =10 & L/d=25. Generally, the interaction factor values decrease with increasing the pile spacing for the analytical and numerical methods. This means that when the distance **S** between the two piles is small, this leads to large additional settlement on the receiver pile caused by the neighbouring pile. But when the distance **S** is large, this leads to small additional settlement on the receiver pile caused by the neighbouring pile and makes the receiver pile behaviour more closely to the behaviour of single pile.

The followings were observed: -

- Randolph and Wroth (1979) expression for L/d =10 gave very good results till S =6d and after that, it gave lower results for the interaction factor in comparison with the numerical method. But for L/d =25, it gave higher values for the interaction factor values for all pile spacing.

- For Poulos and Davis (1980), the interaction curve for L/d =10 showed a very good agreement with the numerical analysis till S= 8d and after that, it gave a little bit lower values for the interaction factor values. On contrary, for L/d =25, it gave slightly higher values till S= 10d and very accurate values for S more than 10d.
- The expression that was given by Makris and Gazetas (1991) gave a high estimation for the interaction factor in comparison with the other methods for L/d=10 and L/d=25.
- Mylonakis and Gazetas (1998) expression for L/d=10 gave a very good agreement till S= 5d and after that, it gave slightly higher values in comparison with the numerical analysis. But for L/d= 25, it gave slightly lower values in comparison with the numerical analysis.
- Both volume pile model and embedded model gave good agreement for L/d= 10 and L/d =25.

Figure 3. 6 shows a comparison of the interaction factors for homogeneous soil layer between the analytical and numerical methods for L/d= 25, K= 500, and ν_s= 0. For Poulos and Davis (1980), volume pile, and embedded beam models, a very clear agreement was observed but Randolph and Wroth (1979) gave higher values and Mylonakis and Gazetas (1998) gave lower values for the interaction factors.

Figure 3. 7 illustrates the effect of soil Poisson's ratio (νs = 0, 0.35) on the interaction factors between the analytical and numerical methods. For both embedded beam and volume pile models, the interaction factor **α** increased by decreasing the Poisson's ratio for soil and that gave a good agreement with Poulos and Davis (1980). But for Mylonakis and Gazetas (1998), it didn't give a difference that could be mentioned.

Figure 3. 8 shows the effect of L/d ratio (L/d=10, 25) on the interaction factors between the analytical and numerical methods. Poulos and Davis (1980), embedded beam and volume pile models explained that the interaction factor increased by increasing the L/d ratio. That meant, when the pile length increased, the pile settlement decreased and thus led to increasing in the interaction factor. But for Mylonakis and Gazetas (1998), it gave the opposite.

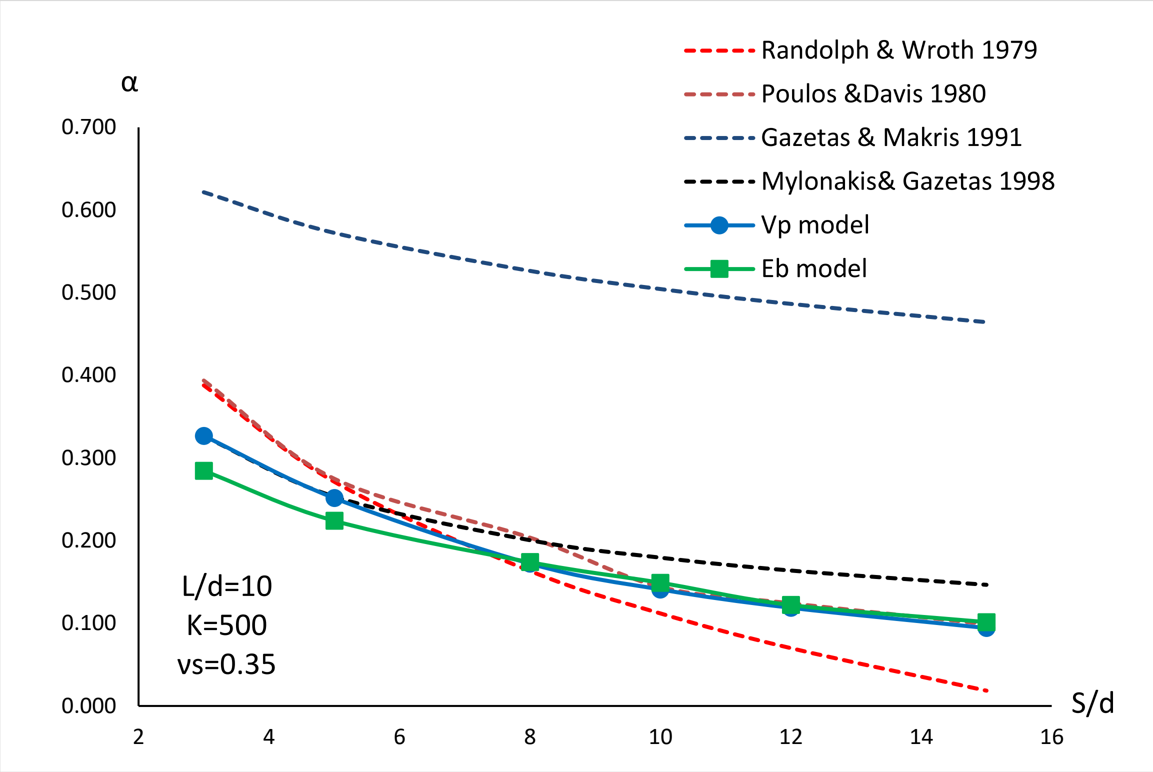

Figure 3. 4 Comparison of the interaction factors for homogeneous soil layer between the analytical and numerical method for L/d =10, K =500 and ν_s =0.35.

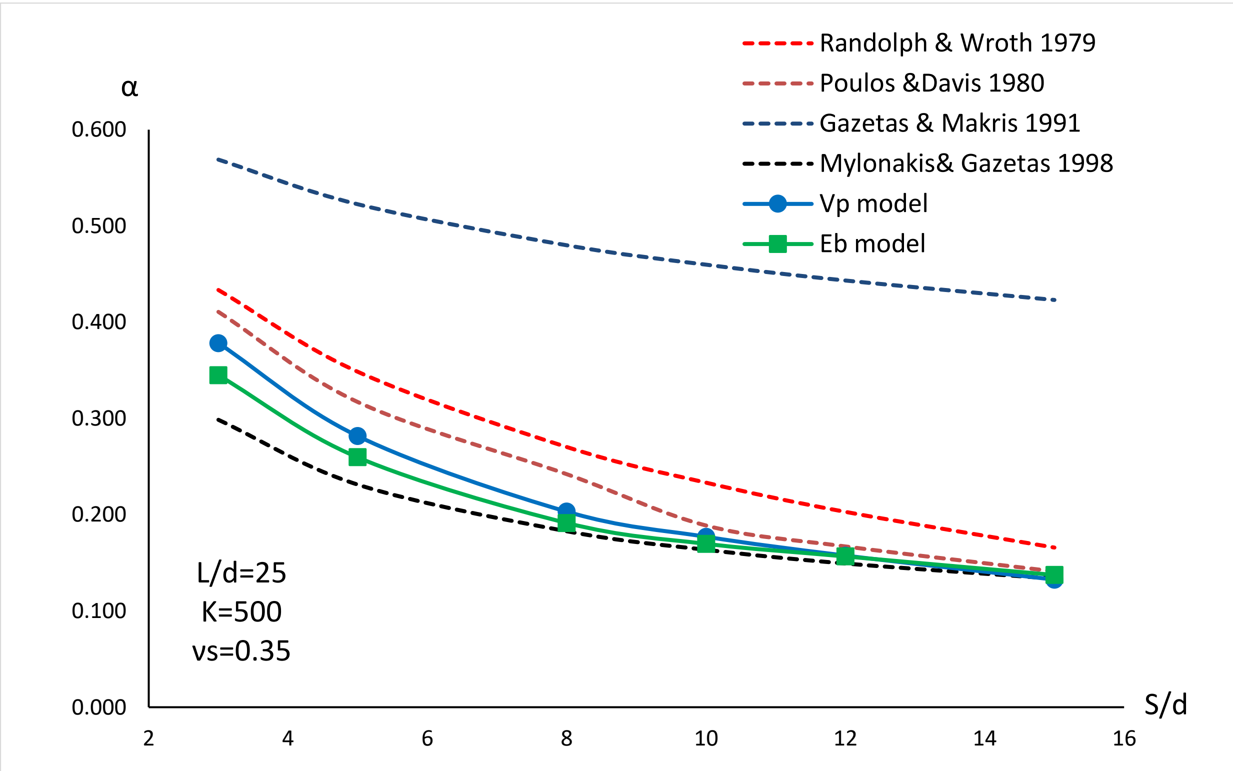

Figure 3. 5 Comparison of the interaction factors for homogeneous soil layer between the analytical and numerical method for L/d =25, K =500 and ν_s =0.35.

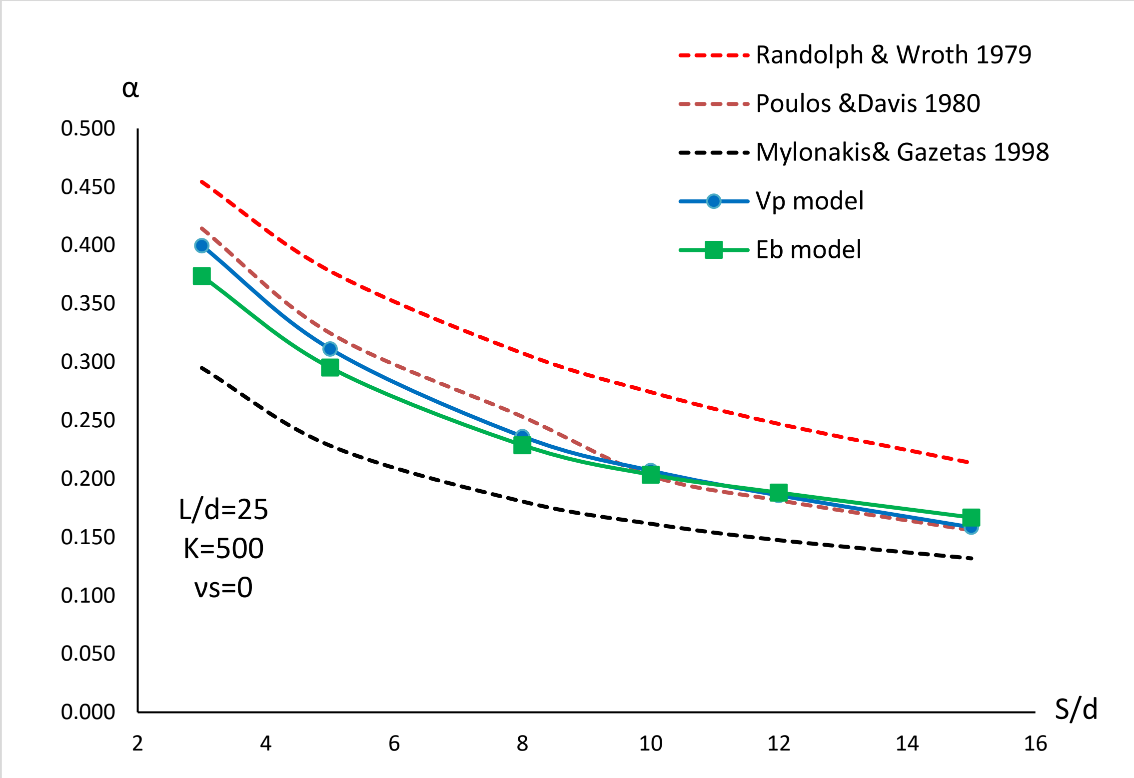

Figure 3. 6 Comparison of the interaction factors for homogeneous soil layer between the analytical and numerical method for L/d =25, K =500 and ν_s =0.

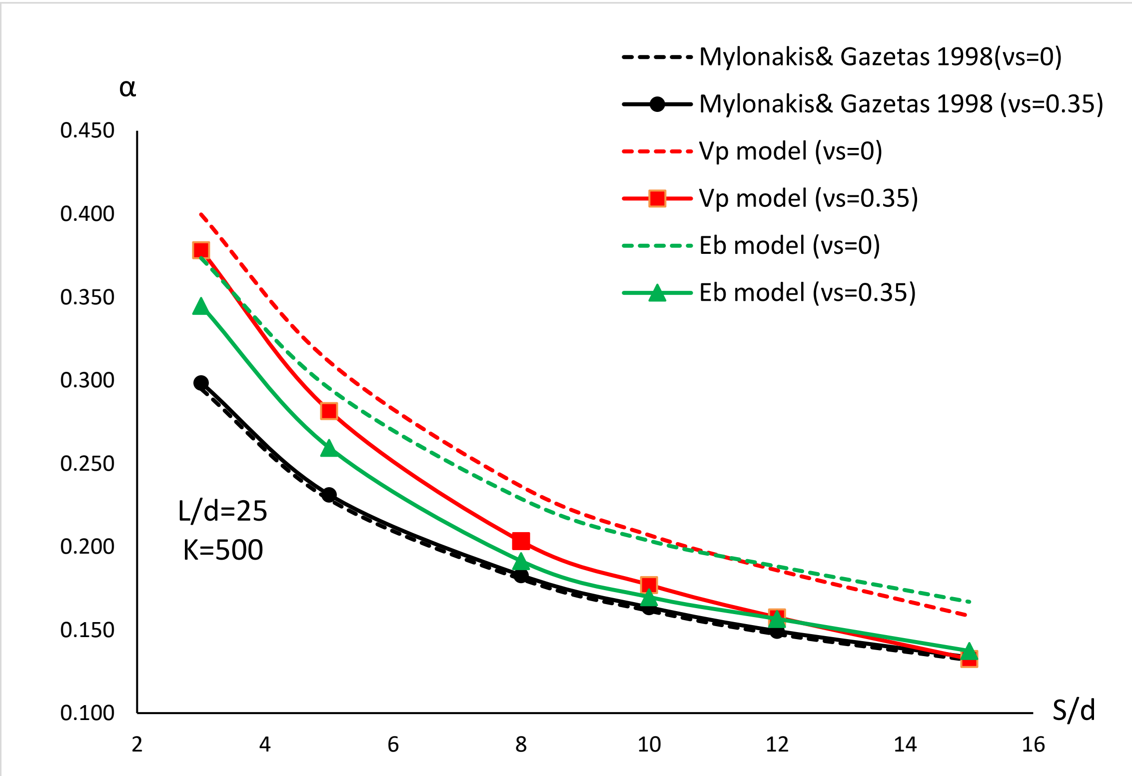

Figure 3. 7 The effect of soil Poisson's ratio (ν_s =0, 0.35) on the interaction factors between the analytical and numerical method.

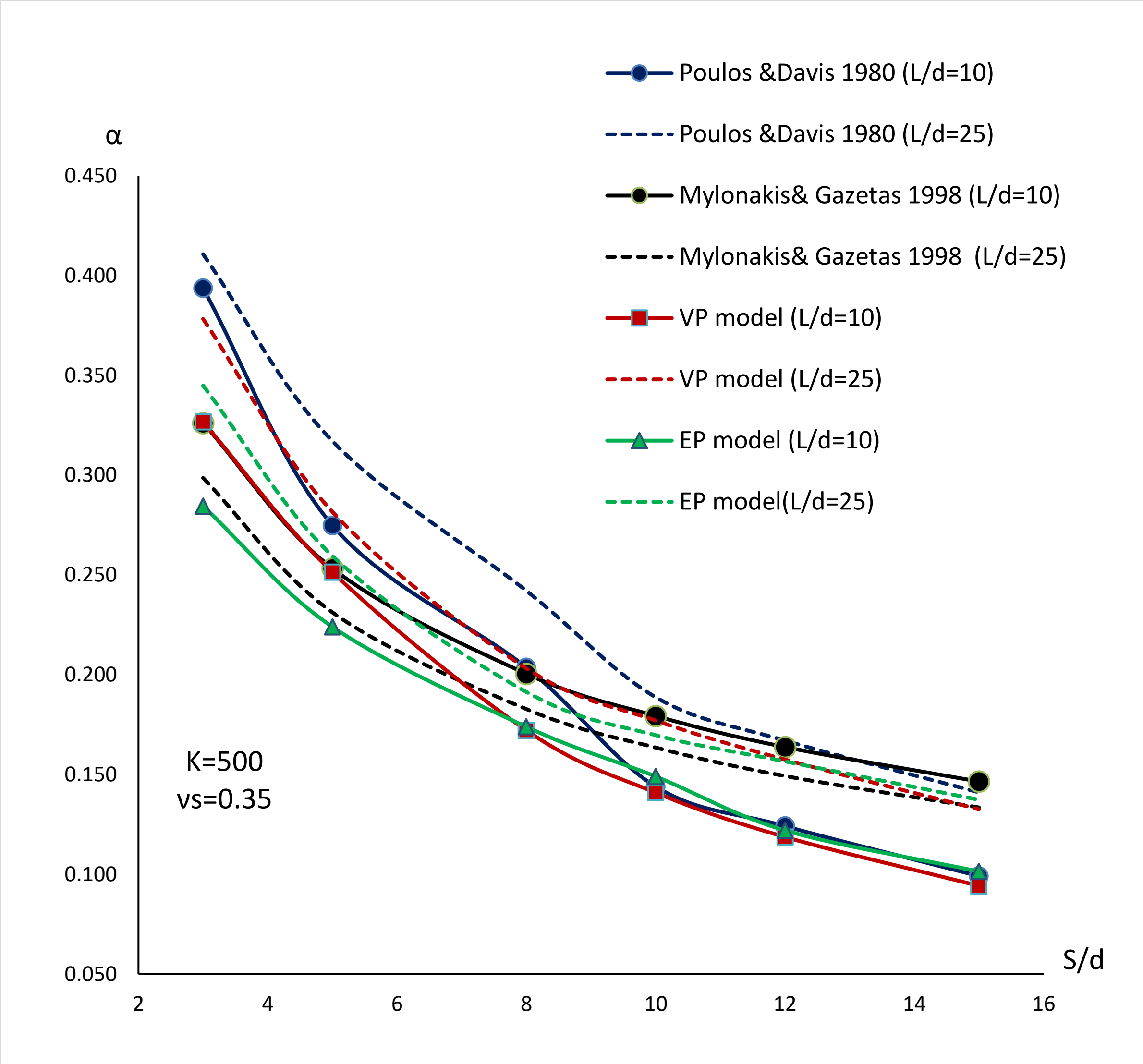

Figure 3. 8 The effect of L/d ratio (L/d=10, 25) on the interaction factors between the analytical and numerical method.

Chapter 4 Performance of pile groups under vertical loads

4.1 Introduction

Piles are commonly used in groups arranged in square or rectangular grids (uniform distribution) where the pile spacing determines the size of the foundation but in some cases, the piles are arranged with nonuniform distribution. A pile group may be subjected to vertical, lateral, moment, and possibly torsional loads or combinations of loads. This chapter deals with pile groups under vertical loads only. There are several factors that affect the pile group behaviour such as the soil properties, pile length, distance between piles, number of piles, and shapes and sizes of the pile group. In the case of single pile, the installation methods have a very significant effect on the selection of design parameters for shaft friction and end bearing, but for the pile groups behaviour, the installation methods have less effect, that is because of the disturbance zone of the soil occurs only within a radius of a few pile diameters around and beneath the individual pile, whereas the soil is significantly stressed to a depth or greater than the width of the group [3].

This chapter gives a brief about the classifications of pile groups and then describes the methods of analysis to calculate the group efficiency, loads distribution, and the total or the differential settlement. This chapter also examines the validity of embedded beam model to be used in the piled foundation for linear cases.

4.2 Classifications of pile groups

In general, the primary function of the pile cap is to transfer the superstructure forces to the piles. Pile cap is the main component in controlling the pile group behaviour so from that point of view, the pile groups are classified according to the flexibility of pile cap which is determined from the following equation: -

$$S_r = \frac{E_c \; t^3}{G_s \; B^3} \tag{4. 1}$$

where; $\mathbf{E_c}$ is the cap Young's modulus, **t** is the cap thickness, $\mathbf{G_s}$ is the soil shear modulus and **B** is the cap equivalent diameter.

From that, the pile groups are classified into: -

1. pile groups with perfectly rigid cap.
2. Pile groups with perfectly flexible cap (without cap).
3. pile groups with flexible cap or semi rigid cap.

the focus in this study was on the first and the second classification whereas the soil is linear elastic.

4.2.1 Pile groups with perfectly rigid cap

In that case, all piles have the same settlement but the loads distribution on piles are different. The corner piles attract the biggest loads and the center piles take the least loads, that is due to the effect of the interaction factors phenomenon. Figure 4. 1 illustrates a pile group with a rigid pile cap (not connected with soil), whereas all piles have the same displacement **w** but the forces in piles are different (P_1 or $P_3 > P_2$).

For floating pile group, the loads distribution become more uniform when the spacing between piles increase. On the other hand, when the number of piles, **L/d**, and the stiffness factor **K** increase, this makes the loads distribution less uniform within the pile group.

For pile groups bearing on rigid stratum, they are similar to floating pile group but it differs only when the stiffness factor **K** increases, the distribution of loads become more uniform [14].

The pile group efficiency **η** is defined as the ratio of the group stiffness to the sum of the stiffnesses of the individual piles. The group efficiency increases with increasing the pile spacing but it decreases as the number of piles increase. Also, for soil consists of two layers when the bottom layer stiffness is increased, the group efficiency is increased a little [5].

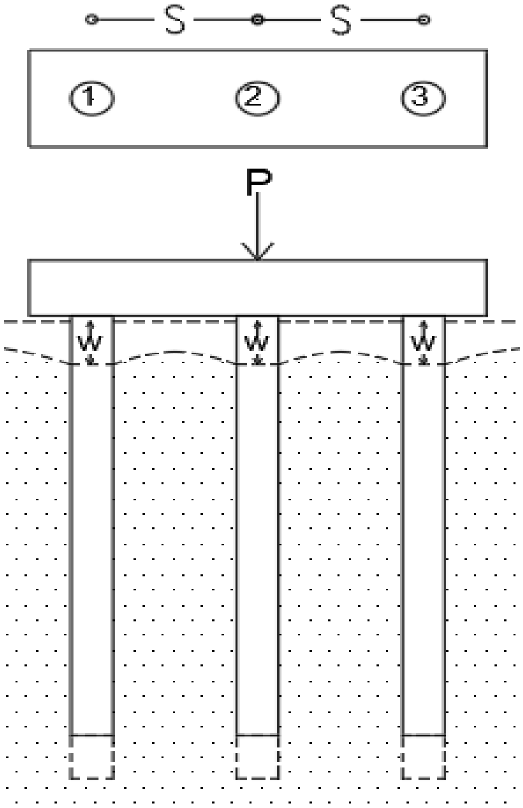

Figure 4. 1 A schematic view for pile groups with perfectly rigid cap

4.2.2 Pile groups with perfectly flexible cap

In that case, all piles have the same load but they have different settlement. The maximum settlement takes place at the central piles while the minimum settlement occurs at the corner piles, and this due to the effect of the interaction factors phenomenon. Figure 4. 2 shows a pile group with equal loads but with different settlement ($w_2 > w_1$).

For floating pile group, the ratio of maximum differential settlement to the maximum settlement **ρd /ρmax** increases when the spacing between the piles increases up to **15d** and then it decreases for larger spacing. Also, this ratio increases as the number of piles increases. But it decreases when the ratio of **L/d** increases, and **K** does not have much influence on that ratio.

For pile groups bearing on rigid stratum, the relative differential settlement depends on **K** and it is decreased rapidly with increasing **K** [14].

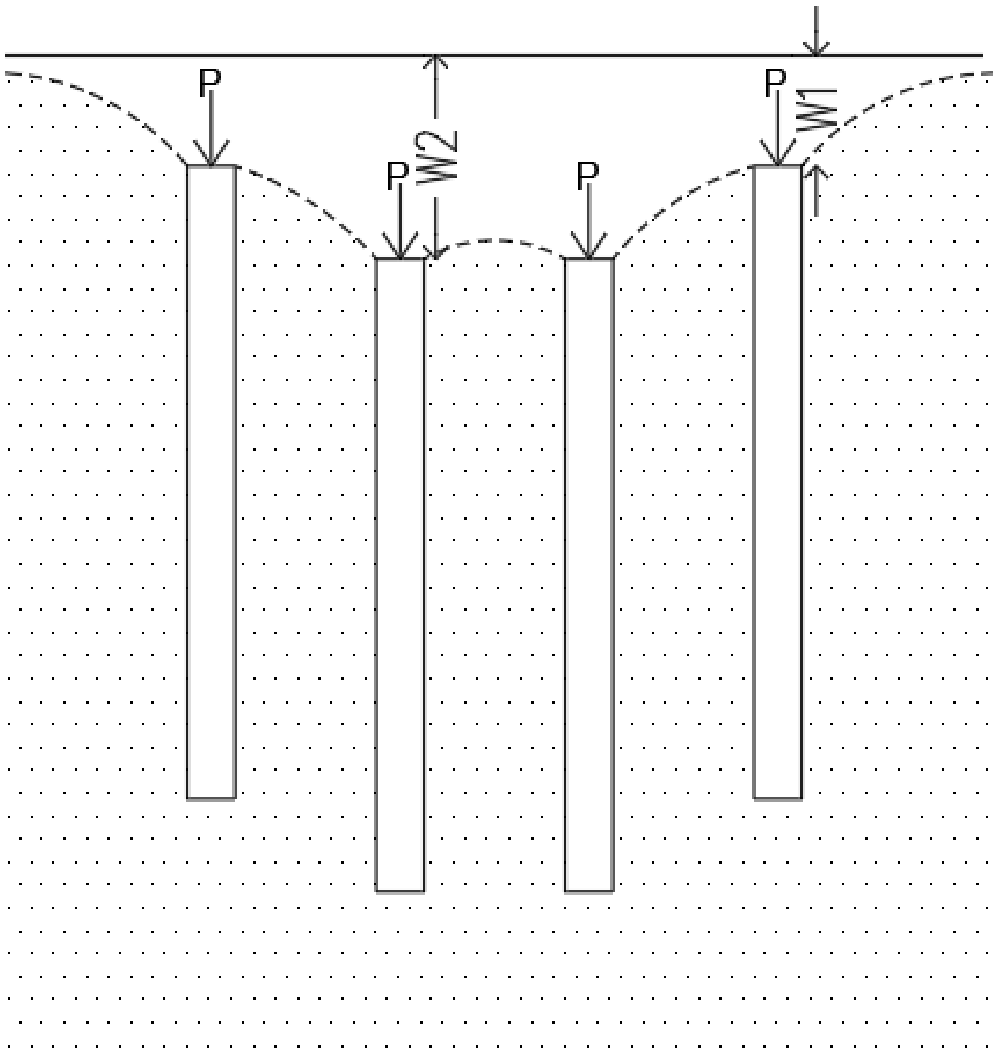

Figure 4. 2 A schematic view for pile groups with equal loads (perfectly flexible cap).

4.3 Methods of analysis

The group analysis is classified into three categories: -

1. **Simplified empirical methods such as the equivalent raft method** in which the pile groups are replaced with an equivalent raft located at a depth aimed to reflect the imposed loads but the raft has equivalent dimensions that reflect the geometry of the pile group. This method is used to calculate the ultimate bearing capacity and the settlement for the pile groups [3].
2. **Analytical method** in which the interaction factor between two piles can be extended to pile groups.
3. **Numerical method** is the most rigorous means of modeling and capable of modeling soil stiffness non-linearity, large group sizes, and various non-standard geometries.

This chapter focused on the second and the third categories.

4.3.1 Analytical method

The behaviour of pile groups mainly depends on the accurate prediction of the behaviour of a single pile in addition to the interaction effects of neighbouring loaded piles within the group. As the interaction factor approach is valid for any two neighbouring piles, so this approach could be extended to group of piles by taking into consideration the total number of piles and their position. The interaction factor approach is applied at the pile head, this makes the pile head constraints in the group important.

To facilitate the calculations, the two extreme cases for pile cap were considered: -

- Pile group with perfectly rigid cap (equal settlement).
- Pile group with perfectly flexible cap (equal force).

For group consisted of numbers of piles equal to **N** and had the same length and diameter, the matrix form between the applied force, vertical stiffness of single pile, interaction factors, and the settlement was written as follow: -

$$\begin{bmatrix} w_1 \\ w_2 \\ w_3 \\ \vdots \\ w_n \end{bmatrix} = \frac{1}{K_v} \begin{bmatrix} 1 & \alpha_{12} & \alpha_{13} & \cdots & \alpha_{1n} \\ \alpha_{21} & 1 & \alpha_{23} & \cdots & \alpha_{2n} \\ \alpha_{31} & \alpha_{32} & 1 & \cdots & \alpha_{3n} \\ \vdots & \vdots & \vdots & \cdots & \vdots \\ \alpha_{n1} & \alpha_{n2} & \alpha_{n3} & \cdots & 1 \end{bmatrix} \begin{bmatrix} p_1 \\ p_2 \\ p_3 \\ \vdots \\ p_n \end{bmatrix} \qquad (4.\ 2)$$

$$K_c = K_v\ [\{1\}^T \quad [A]^{-1} \quad \{1\}] = K_v \left[\{1\}^T \quad \begin{bmatrix} 1 & \alpha_{12} & \alpha_{13} & \cdots & \alpha_{1n} \\ \alpha_{21} & 1 & \alpha_{23} & \cdots & \alpha_{2n} \\ \alpha_{31} & \alpha_{32} & 1 & \cdots & \alpha_{3n} \\ \vdots & \vdots & \vdots & \cdots & \vdots \\ \alpha_{n1} & \alpha_{n2} & \alpha_{n3} & \cdots & 1 \end{bmatrix}^{-1} \quad \{1\} \right] \tag{4. 3}$$

where; $\mathbf{K_c}$ is the pile group stiffness with rigid cap,{1} is a unit vector (n ×1).
Equation (4.3) applied for both cases: perfectly rigid cap to calculate the stiffness and the force distribution within the group, and for perfectly flexible cap to calculate the ratio of $\boldsymbol{\rho_d / \rho_{max}}$.

The interaction factors inside the matrix were based on equation (3.8) but the formula for the attenuation function $\boldsymbol{\psi_s}$ came from: -

- Randolph and Wroth (1979) as mentioned in equations (3.3) and (3.3a).
- Mylonakis and Gazetas (1998) as mentioned in equation (3.5).

4.3.2 Numerical method

The analysis was done by using PLAXIS 3D and the material type was linear elastic for both soil and pile material. The finite element model geometry dimensions were (X= S+2* max(1.5L+5S), Y= 2* max(1.5L+5S), and Z= L+max(1.5L+5S)) in order to take the effect of the boundaries to be compatible with the analytical method. Figure 4. 3 shows the dimensions of 3D model in PLAXIS and the coarseness factor considerations. For perfectly rigid pile cap, the analysis method depended on applying a uniform distributed vertical displacement (w=1m) on the rigid cap (not connected with soil) which was defined as plate element with high Young's modulus and big thickness and then running the analysis to estimate the group stiffness $\mathbf{K_G}$ and the force distribution within the group. For perfectly flexible pile cap (without cap), the analysis method depended on applying the same force on each pile and measure the settlement of each pile to calculate the ratio of $\boldsymbol{\rho_d / \rho_{max}}$.

4.4 Case of study

To measure the effectiveness of embedded beam model, a simple three-dimensional model was used for both cases. The model dimensions depended on the spacing between piles **S** and the pile geometry **L** and **d**. A borehole was defined with dry soil conditions.

4.4.1 Uniform distribution of piles

The discussed floating pile groups were 2x2, 3x3, 4x4, 5x5, 6x6, and 7x7 where the pile spacing (S/d = 2, 5, 8, 10) for both FEM by using the volume pile and embedded beam models, and analytical methods. Also, a study for the effect of L/d ratio (L/d = 10, 25) was displayed. Both soil and pile are described by linear elastic model. Table 4. 1 shows the input parameters for soil and pile material.

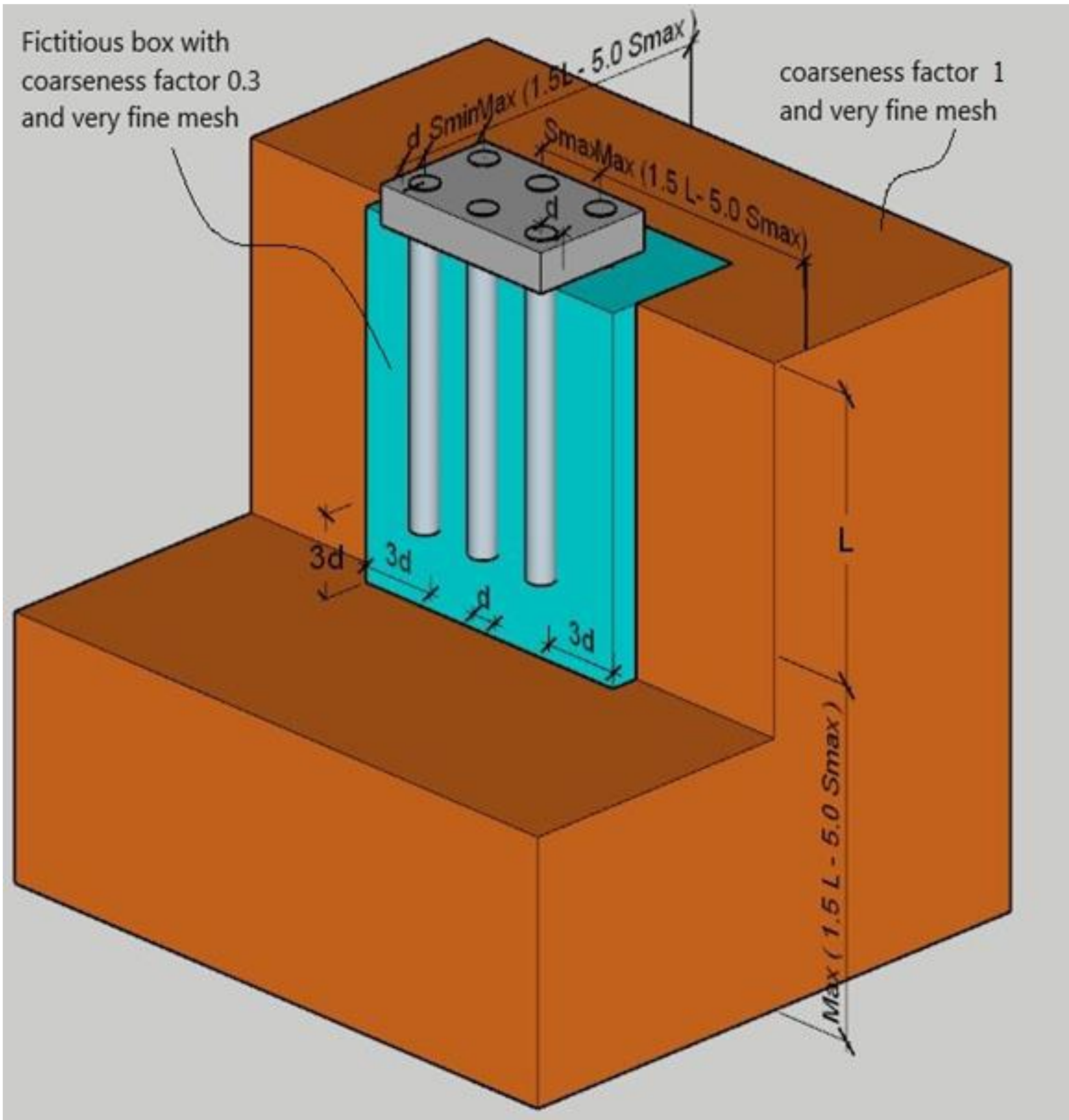

Figure 4. 3 The dimensions of 3D model in PLAXIS and the coarseness factor considerations for pile group.

Material type	Soil material	Pile material	Unit
Parameter	Input value	Input value	
Young's modulus (E)	$60*10^3$	$60*10^6$	KN/m^2
Poisson's ratio (ν)	0.35	0.2	-----
Density (γ)	≈ 0	≈ 0	KN/m^3
Interface strength (R_{inter})	1	1	-----

Table 4. 1The input parameters for soil and pile material.

4.4.2 **Non-uniform distribution of piles**

This case returns to a realistic example for non-uniform pile distribution but the pile cap was assumed to be perfectly rigid [23]. The pile group distribution is sketched in Figure 4. 4 where the number of piles was 228. The foundation cross-section and the soil properties are shown in Figure 4. 5 where, the pile had a length = 12 m, diameter =1.3 m, and Young's modulus E_p = 30 Gpa. The Young's modulus for each soil layer was calculated from this equation: -

$$E_s = 2\,\rho\, V_s^{\,2}\,(1+\nu_s) \qquad (4.\,4)$$

where: **ρ** is the soil density and $\mathbf{V_s}$ is the shear wave velocity.

The analysis was done for two cases: -

1. Both soil layers have the properties of soil layer 1($E_{s2} = E_{s1}$).
2. The soil consists of two layers ($E_{s1} \neq E_{s2}$).

Both soil and pile were described by linear elastic model.

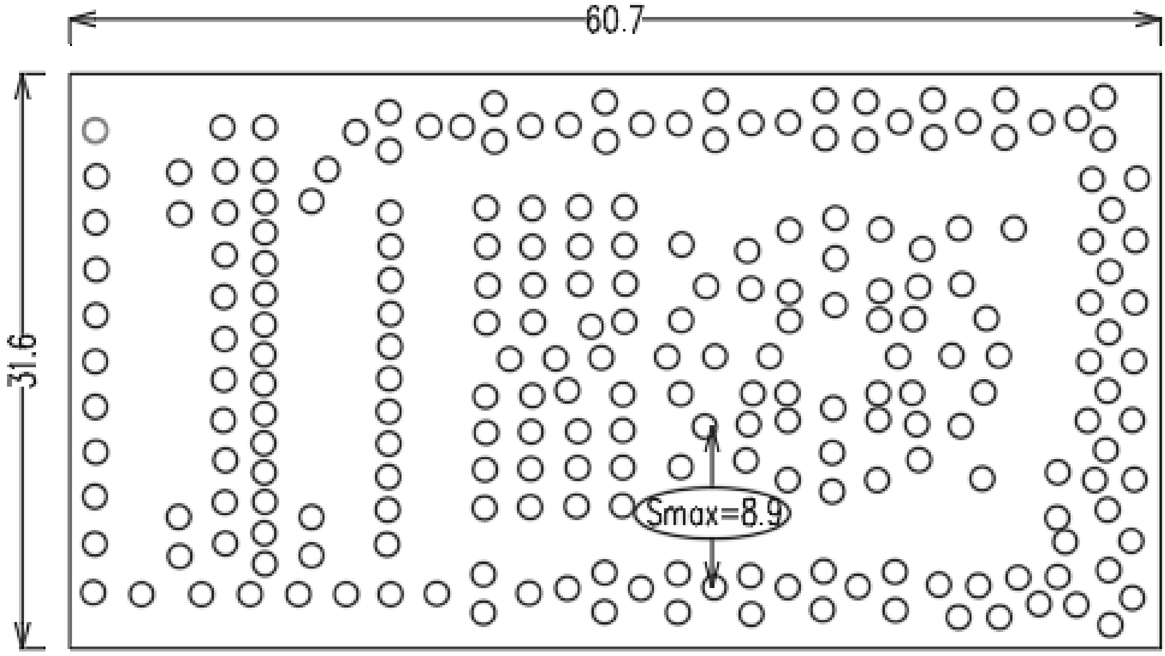

Figure 4. 4 Plan view for 228 pile distribution.

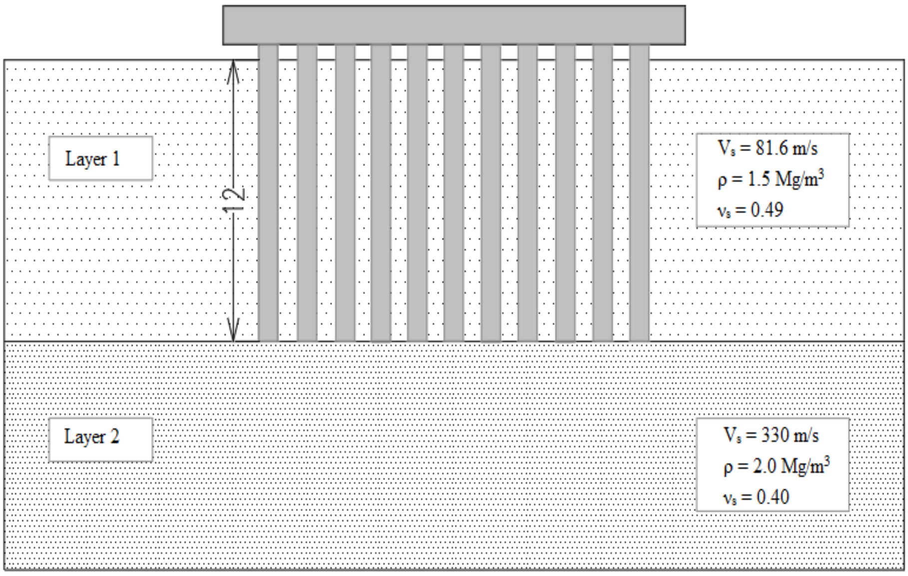

Figure 4. 5 Foundation cross-section and soil properties.

4.5 Comparing the results of analytical and numerical methods

4.5.1 Uniform distribution of piles

For floating pile groups with rigid cap that are showed in Figure 4. 6, the load distributions for different pile groups with different **S/d** and **L/d** are given from Table 4. 2 to Table 4. 6. the pile load was given as a fraction of the average load. (R&W → Randolph and Wroth, M&G →Mylonakis and Gazetas).

For all groups, there was a clear agreement between volume pile and embedded beam models in the load distributions but for the analytical methods there was a small difference in case of group 3x3 and 4x4 and this difference increased as the number of piles increased within the group especially for corner and central piles.

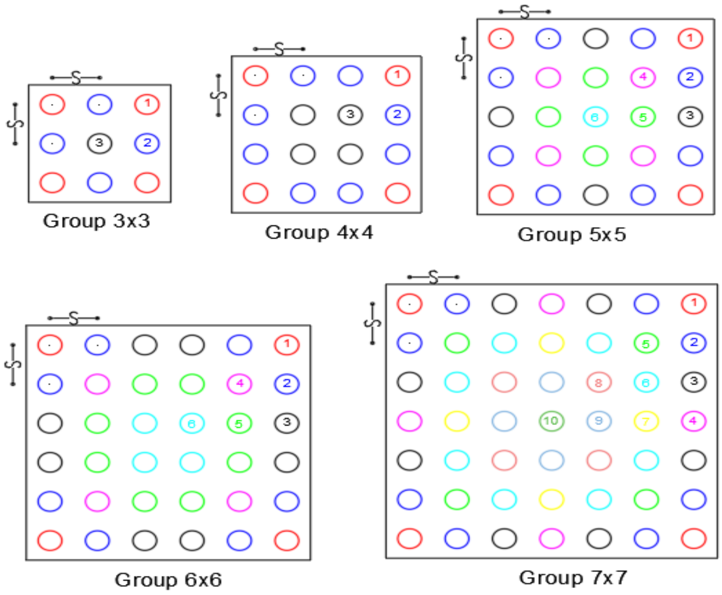

Figure 4. 6 Profiles and plans for pile groups.

L/d		10				25			
S/d		2	5	8	10	2	5	8	10
Pile 1	R&W	1.43	1.31	1.20	1.11	1.38	1.28	1.24	1.23
	M&G	1.25	1.13	1.10	1.08	1.24	1.12	1.09	1.08
	Vp model	1.38	1.24	1.16	1.13	1.31	1.24	1.19	1.18
	Eb model	1.26	1.14	1.13	1.09	1.27	1.24	1.18	1.15
Pile 2	R&W	0.78	0.85	0.91	0.95	0.81	0.87	0.88	0.89
	M&G	0.88	0.94	0.96	0.96	0.88	0.94	0.96	0.96
	Vp model	0.80	0.87	0.92	0.94	0.84	0.88	0.91	0.92
	Eb model	0.87	0.95	0.93	0.96	0.87	0.89	0.91	0.93
Pile 3	R&W	0.13	0.37	0.54	0.77	0.22	0.42	0.49	0.52
	M&G	0.48	0.73	0.80	0.82	0.50	0.73	0.80	0.83
	Vp model	0.29	0.54	0.67	0.72	0.41	0.52	0.59	0.63
	Eb model	0.48	0.67	0.73	0.78	0.41	0.51	0.64	0.68

Table 4. 2 Load distributions P/P_{av} for pile group 3x3.

L/d		10				25			
S/d		2	5	8	10	2	5	8	10
Pile 1	R&W	1.96	1.61	1.26	1.15	1.87	1.67	1.60	1.56
	M&G	1.54	1.30	1.23	1.20	1.52	1.29	1.22	1.20
	Vp model	1.78	1.43	1.32	1.26	1.71	1.53	1.43	1.37
	Eb model	1.53	1.36	1.25	1.25	1.62	1.47	1.41	1.30
Pile 2	R&W	0.98	1.03	1.01	1.00	0.99	1.00	1.00	1.01
	M&G	1.00	1.01	1.01	1.01	1.00	1.01	1.01	1.01
	Vp model	0.96	1.01	1.00	1.01	0.96	1.00	1.00	1.01
	Eb model	0.99	0.99	1.01	0.99	1.00	1.00	0.99	1.03
Pile 3	R&W	0.09	0.33	0.73	0.85	0.16	0.33	0.39	0.42
	M&G	0.46	0.68	0.76	0.78	0.47	0.69	0.76	0.79
	Vp model	0.30	0.54	0.67	0.72	0.36	0.48	0.57	0.62
	Eb model	0.49	0.65	0.73	0.77	0.37	0.53	0.61	0.64

Table 4. 3 Load distributions P/P_{av} for pile group 4x4.

L/d		10				25			
S/d		2	5	8	10	2	5	8	10
Pile 1	R&W	2.53	1.71	1.31	1.18	2.40	2.12	1.98	1.81
	M&G	1.83	1.49	1.38	1.34	1.81	1.48	1.37	1.33
	Vp model	2.16	1.66	1.45	1.38	2.11	1.83	1.64	1.57
	Eb model	1.81	1.51	1.40	1.31	1.98	1.75	1.56	1.51
Pile 2	R&W	1.23	1.17	1.03	1.02	1.23	1.22	1.22	1.20
	M&G	1.16	1.12	1.10	1.09	1.16	1.12	1.09	1.09
	Vp model	1.15	1.12	1.10	1.08	1.17	1.16	1.13	1.11
	Eb model	1.17	1.12	1.08	1.10	1.21	1.13	1.11	1.13
Pile 3	R&W	1.11	1.04	1.11	1.05	1.09	1.07	1.07	1.08
	M&G	1.08	1.04	1.03	1.03	1.07	1.04	1.03	1.03
	Vp model	1.06	1.07	1.05	1.05	1.04	1.05	1.06	1.05
	Eb model	1.03	1.03	1.05	1.02	1.06	1.05	1.06	1.04
Pile 4	R&W	0.10	0.61	0.72	0.86	0.18	0.36	0.42	0.52
	M&G	0.50	0.71	0.78	0.80	0.51	0.72	0.78	0.81
	Vp model	0.35	0.60	0.71	0.77	0.40	0.53	0.63	0.67
	Eb model	0.52	0.70	0.77	0.78	0.42	0.58	0.68	0.70
Pile 5	R&W	0.05	0.47	0.82	0.89	0.10	0.23	0.29	0.38
	M&G	0.43	0.63	0.71	0.74	0.44	0.64	0.71	0.74
	Vp model	0.31	0.55	0.68	0.72	0.31	0.44	0.55	0.60
	Eb model	0.46	0.62	0.71	0.77	0.32	0.49	0.59	0.60
Pile 6	R&W	0.01	0.33	0.91	0.92	0.03	0.12	0.16	0.22
	M&G	0.37	0.55	0.63	0.67	0.38	0.56	0.64	0.68
	Vp model	0.28	0.50	0.63	0.68	0.22	0.37	0.48	0.53
	Eb model	0.36	0.56	0.69	0.71	0.23	0.42	0.52	0.56

Table 4. 4 Load distributions P/P_{av} for pile group 5x5.

L/d		10				25			
S/d		2	5	8	10	2	5	8	10
Pile 1	R&W	3.15	1.82	1.34	1.20	2.98	2.61	2.22	1.89
	M&G	2.14	1.69	1.55	1.49	2.11	1.68	1.53	1.48
	Vp model	2.54	1.85	1.58	1.48	2.55	2.11	1.83	1.70
	Eb model	2.12	1.69	1.53	1.40	2.41	1.94	1.69	1.70
Pile 2	R&W	1.50	1.22	1.06	1.04	1.50	1.47	1.42	1.32
	M&G	1.33	1.25	1.20	1.19	1.32	1.24	1.20	1.18
	Vp model	1.33	1.25	1.19	1.16	1.38	1.31	1.25	1.22
	Eb model	1.33	1.23	1.17	1.07	1.39	1.31	1.26	1.21
Pile 3	R&W	1.30	1.19	1.12	1.06	1.28	1.23	1.23	1.14
	M&G	1.19	1.12	1.10	1.09	1.19	1.12	1.09	1.08
	Vp model	1.18	1.15	1.11	1.10	1.16	1.17	1.14	1.14
	Eb model	1.15	1.10	1.10	1.04	1.19	1.16	1.14	1.13
Pile 4	R&W	0.12	0.58	0.75	0.88	0.22	0.42	0.57	0.73
	M&G	0.55	0.77	0.83	0.85	0.57	0.77	0.83	0.85
	Vp model	0.41	0.65	0.77	0.81	0.47	0.59	0.69	0.73
	Eb model	0.59	0.74	0.78	0.78	0.47	0.67	0.73	0.73
Pile 5	R&W	0.06	0.58	0.82	0.90	0.11	0.24	0.38	0.55
	M&G	0.46	0.64	0.71	0.74	0.47	0.65	0.72	0.75
	Vp model	0.36	0.59	0.70	0.75	0.34	0.48	0.60	0.65
	Eb model	0.47	0.66	0.74	0.73	0.35	0.52	0.63	0.66
Pile 6	R&W	0.01	0.64	0.90	0.92	0.02	0.08	0.15	0.36
	M&G	0.36	0.52	0.60	0.63	0.37	0.53	0.61	0.64
	Vp model	0.31	0.53	0.64	0.68	0.22	0.38	0.51	0.55
	Eb model	0.39	0.59	0.67	0.66	0.25	0.41	0.51	0.57

Table 4. 5 Load distributions P/P_{av} for pile group 6x6.

L/d		10				25			
S/d		2	5	8	10	2	5	8	10
Pile 1	R&W	3.74	1.91	1.37	1.21	3.58	3.10	2.31	1.99
	M&G	2.44	1.90	1.72	1.65	2.41	1.88	1.70	1.63
	Vp model	2.85	2.01	1.69	1.57	2.95	2.35	2.00	1.86
	Eb model	2.35	1.85	1.60	1.43	2.80	2.25	1.93	1.82
Pile 2	R&W	1.81	1.27	1.08	1.05	1.79	1.76	1.54	1.37
	M&G	1.50	1.38	1.32	1.29	1.50	1.38	1.32	1.29
	Vp model	1.50	1.34	1.26	1.22	1.60	1.47	1.37	1.33
	Eb model	1.47	1.29	1.23	1.20	1.63	1.43	1.35	1.31
Pile 3	R&W	1.53	1.23	1.14	1.07	1.49	1.43	1.29	1.27
	M&G	1.32	1.22	1.18	1.16	1.32	1.21	1.18	1.16
	Vp model	1.35	1.23	1.18	1.15	1.33	1.27	1.23	1.21
	Eb model	1.30	1.18	1.20	1.14	1.35	1.29	1.24	1.22
Pile 4	R&W	1.47	1.35	1.13	1.07	1.43	1.35	1.24	1.22
	M&G	1.28	1.18	1.14	1.13	1.28	1.17	1.14	1.12
	Vp model	1.30	1.22	1.16	1.14	1.27	1.25	1.19	1.20
	Eb model	1.25	1.18	1.08	1.12	1.32	1.22	1.19	1.21
Pile 5	R&W	0.15	0.58	0.76	0.89	0.27	0.50	0.78	0.71
	M&G	0.62	0.84	0.89	0.91	0.63	0.84	0.90	0.91
	Vp model	0.46	0.71	0.81	0.86	0.54	0.66	0.75	0.79
	Eb model	0.66	0.80	0.81	0.84	0.52	0.71	0.77	0.79
Pile 6	R&W	0.07	0.56	0.84	0.91	0.13	0.28	0.55	0.63
	M&G	0.49	0.68	0.75	0.77	0.50	0.69	0.75	0.78
	Vp model	0.40	0.64	0.74	0.79	0.38	0.54	0.65	0.68
	Eb model	0.51	0.72	0.78	0.75	0.37	0.58	0.67	0.69
Pile 7	R&W	0.06	0.73	0.82	0.91	0.12	0.24	0.51	0.57
	M&G	0.47	0.64	0.71	0.74	0.48	0.65	0.72	0.74
	Vp model	0.39	0.62	0.73	0.78	0.36	0.52	0.62	0.66
	Eb model	0.50	0.67	0.76	1.09	0.35	0.54	0.65	0.66
Pile 8	R&W	0.01	0.56	0.92	0.94	0.02	0.08	0.32	0.57
	M&G	0.37	0.53	0.60	0.63	0.38	0.53	0.61	0.64
	Vp model	0.34	0.57	0.67	0.72	0.24	0.42	0.54	0.59
	Eb model	0.43	0.61	0.72	0.74	0.25	0.44	0.55	0.59
Pile 9	R&W	0.00	0.75	0.90	0.93	0.01	0.05	0.28	0.54
	M&G	0.35	0.49	0.56	0.60	0.35	0.50	0.57	0.60
	Vp model	0.33	0.56	0.66	0.70	0.22	0.40	0.53	0.57
	Eb model	0.39	0.61	0.70	0.68	0.24	0.41	0.53	0.58
Pile 10	R&W	0.00	0.93	0.87	0.93	0.00	0.03	0.16	0.55
	M&G	0.32	0.45	0.52	0.56	0.33	0.46	0.53	0.57
	Vp model	0.33	0.55	0.65	0.69	0.21	0.38	0.51	0.56
	Eb model	0.38	0.61	0.64	0.69	0.22	0.38	0.53	0.58

Table 4. 6 Load distributions P/P_{av} for pile group 7x7.

The pile group efficiency **η** is shown in Table 4. 7. The analysis showed that: -

- Eb model gave a slightly higher estimation for the pile group efficiency **η** more than Vp model for all cases.
- Randolph and Wroth equation showed that: -

a) For L/d =10 when (S/d =2 and 5) it gave a good agreement with Vp model but for (S/d=8 and 10) it gave a higher estimation for the pile group efficiency **η**.
b) For L/d=25, for all values of (S/d) it gave a slightly lower estimation for the pile group efficiency **η** in comparison with Vp model.

- Mylonakis and Gazetas equation revealed that: -

a) For L/d =10 when (S/d =2) it gave a good agreement with Vp model but for (S/d=5,8 and 10) the calculations gave a lower estimation for the pile group efficiency **η**.
b) For L/d=25, at pile groups up to 4x4 for all values of S/d the analysis gave a good agreement with Vp model but for the other group it gave a lower estimation for the pile group efficiency **η** in comparison with Vp model.

For floating pile groups without cap, the ratio of ρ_d / ρ_{max} values for different pile groups are illustrated in Table 4. 8. The results showed a very good agreement between Randolph and Wroth, Vp and Eb models for all cases but Mylonakis and Gazetas gave a lower value for this ratio.

L/d		10				25			
S/d		2	5	8	10	2	5	8	10
2x2	R&W	0.42	0.57	0.70	0.79	0.39	0.48	0.55	0.59
	M&G	0.46	0.57	0.63	0.66	0.47	0.58	0.64	0.66
	Vp model	0.44	0.58	0.67	0.71	0.41	0.52	0.60	0.64
	Eb model	0.55	0.67	0.74	0.75	0.45	0.57	0.63	0.66
3x3	R&W	0.25	0.43	0.64	0.74	0.21	0.29	0.37	0.42
	M&G	0.27	0.37	0.43	0.45	0.28	0.38	0.43	0.46
	Vp model	0.27	0.43	0.53	0.58	0.24	0.35	0.44	0.48
	Eb model	0.33	0.52	0.59	0.64	0.27	0.39	0.47	0.51
4x4	R&W	0.17	0.38	0.60	0.71	0.14	0.21	0.29	0.35
	M&G	0.19	0.26	0.31	0.33	0.19	0.27	0.31	0.34
	Vp model	0.21	0.36	0.45	0.51	0.16	0.27	0.36	0.40
	Eb model	0.27	0.43	0.52	0.54	0.18	0.29	0.39	0.42
5x5	R&W	0.14	0.35	0.58	0.69	0.10	0.17	0.25	0.32
	M&G	0.14	0.20	0.24	0.26	0.14	0.20	0.24	0.26
	Vp model	0.17	0.31	0.41	0.47	0.12	0.22	0.31	0.35
	Eb model	0.23	0.37	0.47	0.53	0.14	0.24	0.33	0.37
6x6	R&W	0.12	0.33	0.56	0.68	0.08	0.14	0.23	0.30
	M&G	0.10	0.15	0.19	0.20	0.11	0.16	0.19	0.21
	Vp model	0.14	0.29	0.38	0.44	0.10	0.19	0.28	0.32
	Eb model	0.19	0.35	0.42	0.47	0.11	0.21	0.30	0.33
7x7	R&W	0.10	0.31	0.55	0.67	0.06	0.13	0.22	0.28
	M&G	0.08	0.13	0.15	0.17	0.09	0.13	0.16	0.17
	Vp model	0.13	0.27	0.36	0.42	0.08	0.17	0.26	0.30
	Eb model	0.17	0.32	0.41	0.45	0.09	0.18	0.28	0.31

Table 4. 7 Pile group efficiency factor for different pile groups with rigid cap.

L/d		10				25			
S/d		2	5	8	10	2	5	8	10
3x3	R&W	0.15	0.24	0.29	0.21	0.11	0.14	0.18	0.20
	M&G	0.12	0.11	0.10	0.09	0.12	0.10	0.10	0.09
	Vp model	0.13	0.21	0.21	0.19	0.09	0.16	0.19	0.19
	Eb model	0.16	0.19	0.17	0.17	0.12	0.17	0.19	0.19
4x4	R&W	0.20	0.36	0.29	0.21	0.13	0.20	0.26	0.30
	M&G	0.14	0.13	0.12	0.12	0.14	0.13	0.12	0.12
	Vp model	0.19	0.28	0.27	0.25	0.12	0.21	0.25	0.26
	Eb model	0.22	0.26	0.25	0.25	0.15	0.22	0.24	0.24
5x5	R&W	0.29	0.47	0.30	0.21	0.19	0.29	0.39	0.44
	M&G	0.18	0.17	0.16	0.16	0.18	0.17	0.16	0.16
	Vp model	0.27	0.38	0.36	0.34	0.17	0.30	0.36	0.36
	Eb model	0.31	0.36	0.33	0.31	0.21	0.30	0.35	0.35
6x6	R&W	0.35	0.47	0.30	0.21	0.21	0.34	0.47	0.48
	M&G	0.19	0.18	0.17	0.17	0.19	0.18	0.17	0.17
	Eb model	0.36	0.41	0.39	0.38	0.24	0.35	0.40	0.40
7x7	R&W	0.43	0.48	0.30	0.21	0.25	0.42	0.54	0.52
	M&G	0.21	0.20	0.20	0.19	0.21	0.20	0.20	0.19
	Eb model	0.41	0.47	0.44	0.41	0.28	0.41	0.47	0.46

Table 4. 8 Ratio of ρ_d/ ρ_{max} values for different pile groups without cap.

4.5.2 Non-uniform distribution of piles

The pile group efficiency results obtained from the analysis for non-uniform pile distribution are illustrated in Figure 4. 7 and Figure 4. 8. The analysis showed that: -

- For case 1 when both soil layers had the same properties of soil layer 1, there was a very good agreement between the numerical method (Eb model) and the analytical method by using Mylonakis and Gazetas equation when r_m= 10d while Randolph and Wroth equation gave a little higher result than Eb model.
- For case 2 when the soil consists of two layers, there was a very good agreement between the numerical method (Eb model) and the analytical method by using Randolph and Wroth equation Mylonakis and Gazetas equation gave a little lower result than Eb model.

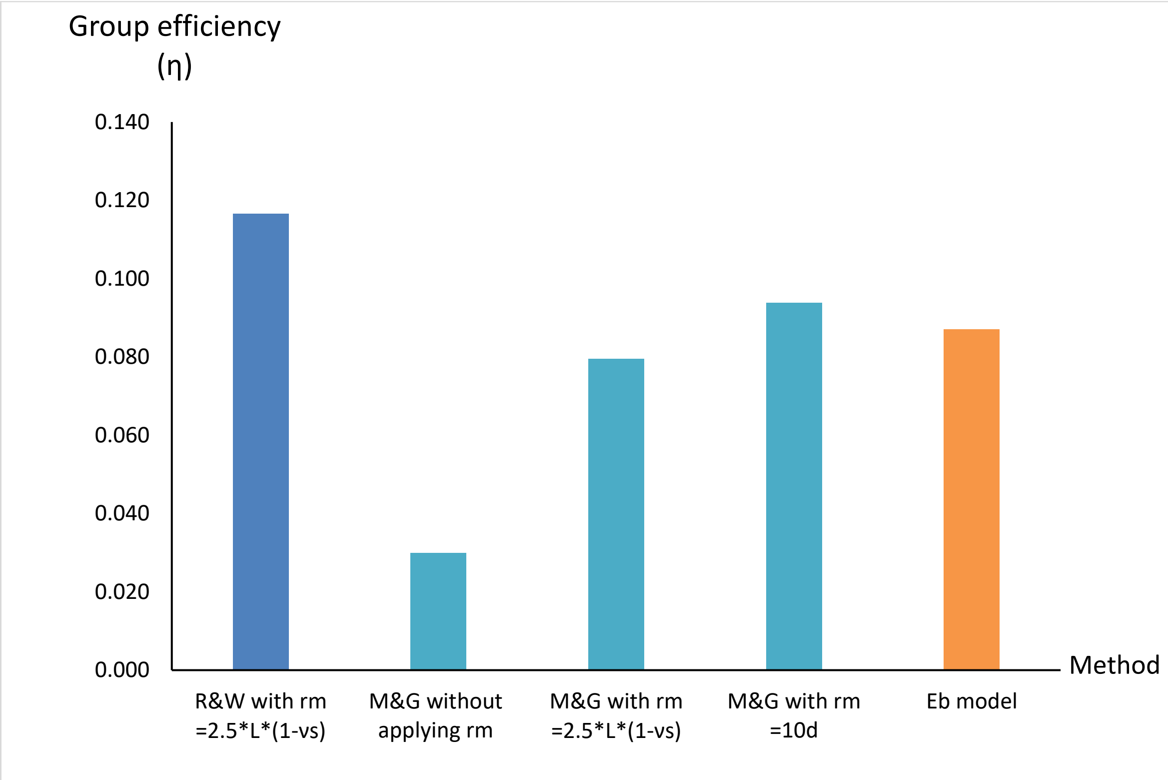

Figure 4. 7 Group efficiency for case 1 for $E_{s2} = E_{s1}$.

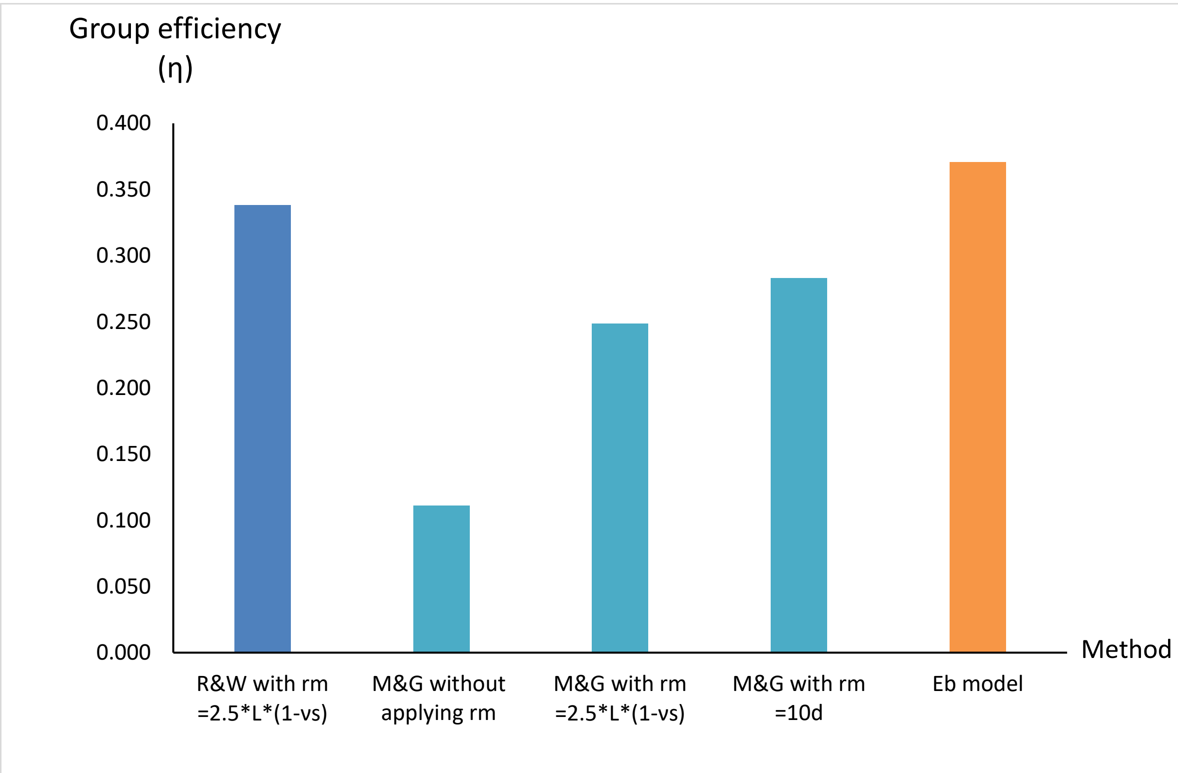

Figure 4. 8 Group efficiency for case 1 for $E_{s2} \neq E_{s1}$.

Chapter 5 Piled raft foundations

5.1 Introduction

Usually, the piled raft foundation term refers to a composite system consisting of piles, raft, and soil. For piled foundations, the entire load is carried by piles only but the piled raft foundations allow the load sharing between piles and raft and this affects the load-settlement behaviour of such foundations.

Lately, the number of high-rise buildings was increased and the structure designer faces a problem related to excessive settlement and differential settlement, so most types of these buildings were founded on piled raft foundation to reduce the vertical and differential settlements, and allowed the load sharing to get economic design. The term "settlement reducing piles" was mentioned by Broms in 1977 [24].

Piled raft foundation has five types of interactions: -

1. Pile- pile interaction.
2. Pile- soil interaction.
3. Pile- raft interaction.
4. Raft- pile interaction.
5. Raft- soil interaction.

Figure 5. 1 illustrates a schematic view for piled raft interactions where the pile-pile interaction is required in the analysis of both piled foundations and piled raft foundations and the pile-raft interaction is important in piled raft foundations analysis.

This chapter discusses the pile-raft interaction factor and how it could be calculated by using the analytical and numerical methods for single pile with single raft and then calculating the load sharing factor between piles and raft in piled raft foundation. Also, the method of single pile with single raft was extended to study piled raft with uniform pile distributions for different pile groups and non-uniform pile distributions case for linear elastic case.

Finally, an application to a real problem for "The Kingdom Tower" was discussed by using the Eb model. The analysis was done for two cases: -

- The first case for linear elastic and Mohr-Coulomb soil models to estimate the value of raft-pile interaction and the ratio of raft load to total load by applying uniform displacement for both models.
- The second case for Mohr-Coulomb soil model to see the settlement and differential settlement of piled raft system by applying the actual gravity load.

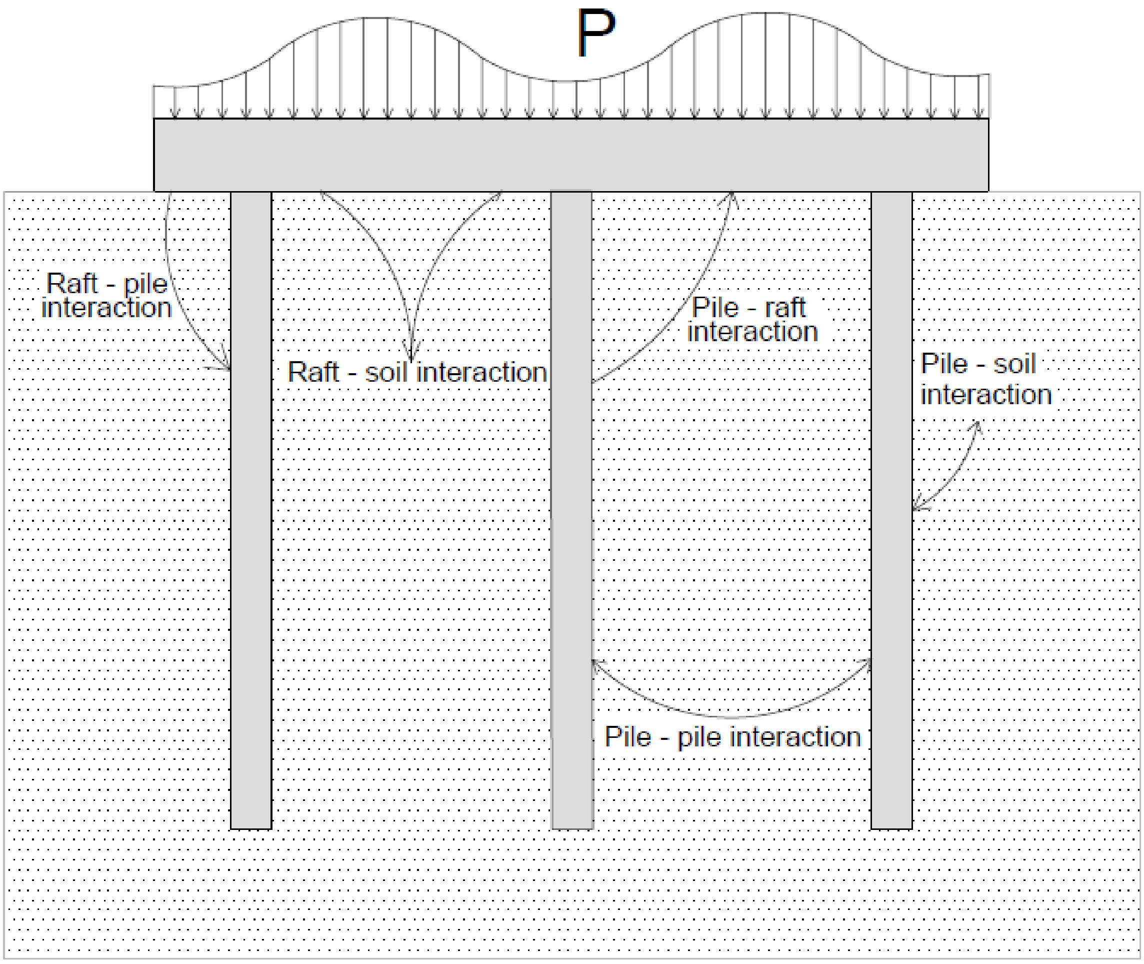

Figure 5. 1 Interactions in piled raft foundation.

5.2 Pile raft Interaction factor and load sharing factor

Compared to behaviour of piled foundations where the pile-pile interactions affect the group efficiency, the piled raft foundations include two additional interactions are named pile-raft interaction $\boldsymbol{\alpha_{pc}}$ and raft-pile interaction $\boldsymbol{\alpha_{cp}}$. The raft-pile interaction is defined as the additional displacement that occurs in the raft due to the unit displacement of the pile, this definition was given by Clancy and Randolph [25].

Poulos and Davis studied the pile-raft interaction for linear elastic soil with constant Young's modulus and Poisson's ratio for piled raft with rigid cap. They gave charts to estimate the pile-raft interaction factor as function of **S/d** for different values of **L/d**, and d_c/d where $\mathbf{d_c}$ is the effective pile diameter. They found that: -

- The pile-raft interaction factor decreased by increasing the value of **S/d**.
- The pile-raft interaction factor increased by increasing the value of d_c/d but the effect of $\mathbf{d_c/d}$ was smaller for lager value of **L/d**.
- The pile-raft interaction factor increased by increasing the value of **L/d**.
- The pile-raft interaction factor increased by decreasing the value of Poisson's ratio[14].

The main concept in piled raft foundation is the load sharing between the piles and the raft. The sharing of the external load depends on the load level that is related to the foundation settlement. Figure 5. 2 shows the simplified load settlement curve for piled raft foundations which illustrates the mechanism of load sharing between pile and raft. At low values of settlement, the applied load is taken by the pile then the load is increased until the pile ultimate load is mobilized at point **A**. By increasing the load, the raft starts to participate in the load carrying and the settlement increases until the piled raft ultimate load is mobilized at point **B** [26].

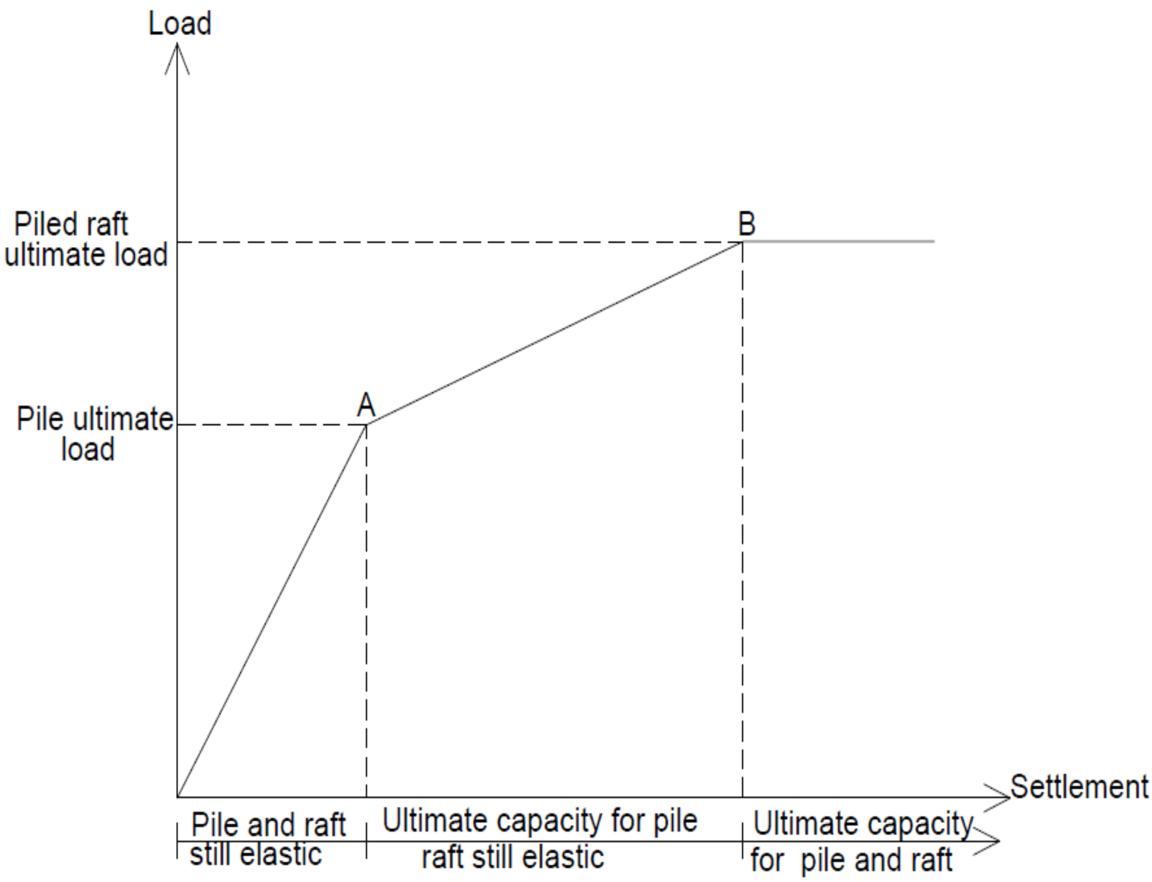

Figure 5. 2 Simplified load settlement curve for piled raft foundation.

5.3 Method of analysis

5.3.1 Analytical method

The behaviour of piled raft foundation depends on the interactions between piles, raft, and soil. To calculate the interaction between pile and raft in an elastic homogeneous soil with constant $\mathbf{E_s}$, Randolph and Clancy proposed a method to calculate both interaction factors $\boldsymbol{\alpha_{cp}}$ and $\boldsymbol{\alpha_{pc}}$ depending on the size of the rigid raft and pile. The raft-pile interaction factor was approximated by Randolph for single piles, which can be used for the large groups.

The raft-pile interaction factor is determined as follow: -

$$\alpha_{cp} = 1 - \frac{\ln\left(\frac{r_c}{r_o}\right)}{\ln\left(\frac{r_m}{r_o}\right)} \tag{5. 1}$$

where; $\mathbf{r_c}$ is the effective cap radius (corresponding to the area of the raft area divided by number of piles) and $\mathbf{r_o}$ is the pile radius.
$r_m = 2.5\ \rho L(1-\nu_s)$ for same soil stiffness along and below the pile where $\boldsymbol{\rho}$ is the soil degree of homogeneity [25].
For Considering different soil stiffness along and below the pile: -

$r_m = 0.25 + L\varsigma\ \{2.5\rho(1 - \nu_s) - 0.25\}$

$\varsigma = E_{s1}/E_{sb}$

$\rho = E_{av}/E_{s1}$

where; $\mathbf{E_{sl}}$ is the soil stiffness at level of pile tip, $\mathbf{E_{sb}}$ is the soil stiffness of bearing stratum below pile tip and $\mathbf{E_{av}}$ equals to the average soil stiffness along pile shaft [27].

The pile-raft interaction factor is estimated as follow: -

$$\alpha_{pc} = \alpha_{cp}\,\frac{K_c}{K_p} \tag{5. 2}$$

where; $\mathbf{K_p}$ is the pile group stiffness with rigid cap and $\mathbf{K_c}$ is the rigid cap stiffness [25].

The rigid cap stiffness for homogeneous soil is calculated as follow: -

$$K_c = \frac{4G_sR}{1-\nu_s} \tag{5. 2a}$$

where; $\mathbf{G_s}$ is the soil shear modulus and **R** is the equivalent raft radius.
For rigid cap based on two soil layers, the rigid cap stiffness is determined as follow: -

$$K_C = K_c\ \frac{1+m\left(\frac{R}{h}\right)}{1+m\left(\frac{R}{h}\right)\left(\frac{G_s}{G_r}\right)} \tag{5.2b}$$

where; **h** is the upper layer thickness, $\mathbf{G_s}$ and $\mathbf{G_r}$ are the upper- and lower-layers shear modulus for soil respectively, and m=1.3 for circular shape. This expression is valid for $G_s \leq G_r$ [28].

For piled raft system consists of one pile and rigid cap, the matrix form between the applied force and settlement is written as follow: -

$$\begin{bmatrix} w_p \\ w_c \end{bmatrix} = \begin{bmatrix} \frac{1}{K_p} & \frac{\alpha_{cp}}{K_c} \\ \frac{\alpha_{pc}}{K_p} & \frac{1}{K_c} \end{bmatrix} \begin{bmatrix} P_p \\ p_c \end{bmatrix} \tag{5. 3}$$

where; $\mathbf{w_p}$, $\mathbf{w_c}$, $\mathbf{P_p}$ and $\mathbf{P_c}$ are the pile settlement, cap settlement, pile load, and cap load, respectively.

The piled raft stiffness $\mathbf{K_{pc}}$ is calculated as follow: -

$$K_{pc} = \begin{bmatrix} 1 & 1 \end{bmatrix} \begin{bmatrix} \frac{1}{K_p} & \frac{\alpha_{cp}}{K_c} \\ \frac{\alpha_{pc}}{K_p} & \frac{1}{K_c} \end{bmatrix}^{-1} \begin{bmatrix} 1 \\ 1 \end{bmatrix} \tag{5. 4}$$

$$K_{pc} = \frac{K_p + K_c\,(1-2\alpha_{cp})}{1-\alpha_{cp}^2\,\frac{K_c}{K_p}} \tag{5. 5}$$

Where; $\mathbf{K_{pc}}$ is the piled raft stiffness and that method used for piled raft system with any number of piles being considered and this stiffness remained effective until the pile reached the ultimate capacity which happened at point **A** in Figure 5. 2 [25].

The load sharing factor $\mathbf{X_{pr}}$ between piles and raft is defined as the ratio of the load carried by the piles to the total applied load and estimated as follow: -

$$X_{pr} = \frac{P_p}{P_{tot}} = \frac{P_p}{P_p + P_c} = \frac{K_c\,(1-\alpha_{cp})}{K_p + K_c(1-2\alpha_{cp})} \tag{5. 6}$$

$$\frac{P_c}{P_{tot}} = 1 - X_{pr} \tag{5.6a}$$

where; $\mathbf{P_{tot}}$ is the total applied load on the piled raft [26].

5.3.2 Numerical method

The analysis was done by using PLAXIS 3D and the material type was linear elastic for both soil and pile material. The finite element model geometry was the same as in Figure 4. 3 in section 4.3.2. To estimate the raft-pile interaction and the load sharing factor by using PLAXIS 3D for perfectly rigid pile cap, the analysis method depended on applying a uniform distributed vertical displacement (w=1m) on the three models as shown in Figure 5. 3, and that used to estimate the stiffness for each system (unpiled raft, pile group and piled raft). By using equation (5.5), the raft-pile interaction determined by solving this equation: -

$$\left(\frac{K_{pc}\,K_c}{K_p}\right)\alpha_{cp}^2 - 2K_c\,\alpha_{cp} + \left(K_p + K_c - K_{pc}\right) = 0 \tag{5. 7}$$

After determining the raft-pile interaction factor value, equation (5.6) was used to estimate the load sharing factor.

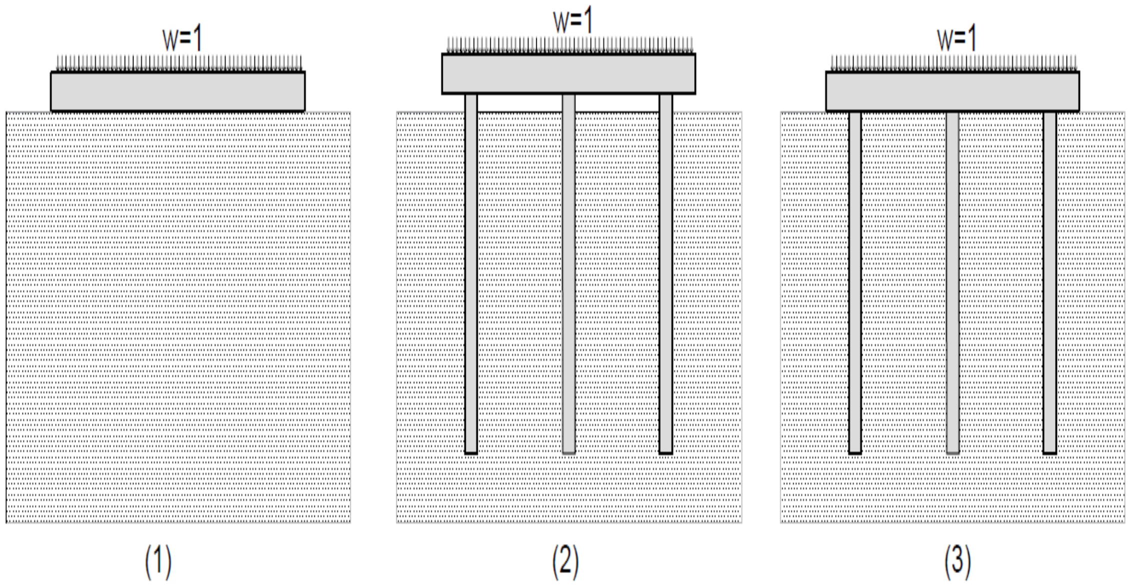

Figure 5. 3 Three models for estimating the stiffnes for (1) unpiled raft, (2) pile group and (3) piled raft

5.4 Case of study for single pile with raft

The main objective of studying the single pile-raft unit was to estimate the raft-pile interaction factor and the load sharing factor for the embedded beam model and compared with volume pile model and analytical method. The analysis was done for floating pile with two different values of L/d =10 and 25 for different cases of rigid raft with dimensions (2x2, 3x3, and 5x5). Both soil and pile are described by linear elastic model as in Table 4. 1 in section 4.4.1.

5.4.1 Comparing the results

The analysis results for $\boldsymbol{\alpha_{cp}}$ and the ratio of raft load to total load are provided in Table 5. 1 where R&C referred to Randolph and Clancy formula.

The results for the three methods showed similarity in the general behaviour where: -

- The value of $\boldsymbol{\alpha_{cp}}$ decreased by increasing the raft area.
- The value of $\boldsymbol{\alpha_{cp}}$ increased by increasing the value of **L/d**.
- The ratio of $\boldsymbol{P_c/P_{tot}}$ increased by increasing the raft area.
- The ratio of $\boldsymbol{P_c/P_{tot}}$ decreased by increasing the value of **L/d**.

The analytical method gave slightly higher values for $\boldsymbol{\alpha_{cp}}$ and lower values for $\boldsymbol{P_c/P_{tot}}$ in comparison with the Vp model while the Eb model presented low values for $\boldsymbol{\alpha_{cp}}$ and higher values for $\boldsymbol{P_c/P_{tot}}$ and especially for L/d=10 but for L/d=25, the Eb model gave slightly lower values but still acceptable results.

Raft dimensions	L/d \ Method	α_{cp}		P_c/P_{tot}	
		10	25	10	25
2x2	R & C	0.77	0.81	0.10	0.04
	Vp model	0.63	0.68	0.15	0.08
	Eb model	0.45	0.58	0.31	0.12
3x3	R & C	0.65	0.72	0.21	0.10
	Vp model	0.53	0.59	0.26	0.14
	Eb model	0.36	0.50	0.47	0.21
5x5	R & C	0.50	0.61	0.42	0.23
	Vp model	0.28	0.40	0.48	0.28
	Eb model	0.41	0.48	0.67	0.36

Table 5. 1 The raft-pile interaction and the ratio of raft load to total load for single raft with single pile.

5.5 Case of study for uniform piles distribution

To see the behaviour of the Eb model and see how it works with piled raft system and compare it with the Vp model, a simple three-dimensional model was used for both cases. The model dimensions depended on the spacing between piles **S**, and the pile geometry **L** and **d**. A borehole was defined with dry soil conditions.
The discussed floating pile groups were 2x2, 3x3, 4x4, 5x5, and 6x6 where the pile spacings were (S/d = 2, 5, 8, 10) with both FEM by using the Vp model and Eb model, and analytical methods. Also, a study for the effect of L/d ratio (L/d = 10, 25) displayed. Both soil and pile were described by linear elastic model as shown in Table 4. 1 in section 4.4.1.

5.5.1 Comparing the results for raft-pile interaction factor

For floating pile groups with rigid cap that were shown in Figure 4. 6 in section 4.5.1, the $\boldsymbol{\alpha_{cp}}$ values for different pile groups, **S/d**, and **L/d** are given in Table 5. 2.

For all different pile groups, there was a very good agreement between Vp and Eb models in the values of the raft-pile interaction factor.
The results for the three methods shared a number of similarities with Poulos and Davis (1980) findings where: -

- The value of $\boldsymbol{\alpha_{cp}}$ decreased by increasing the value of **S/d**.
- The value of $\boldsymbol{\alpha_{cp}}$ increased by increasing the value of **L/d**.

When the pile groups increased for the same **S/d** (the effective radius r_c still the same for S/d= 2 and increased for all other values of S/d) for example (group 2x2 and 6x6), both Vp and Eb models showed an increase in $\boldsymbol{\alpha_{cp}}$ and that gave a good agreement with what Poulos and Davis (1980) predicted. On the contrary, Randolph and Clancy's formula found decreasing in the values of $\boldsymbol{\alpha_{cp}}$ and that is illustrated in Figure 5. 4 which compares the results for both groups (2x2 and 6x6) for the different three methods.

L/d		10				25			
S/d		2	5	8	10	2	5	8	10
2x2	R & C	0.77	0.61	0.50	0.45	0.81	0.69	0.61	0.57
	Vp model	0.76	0.75	0.71	0.66	0.79	0.77	0.73	0.70
	Eb model	0.60	0.62	0.60	0.59	0.70	0.70	0.66	0.64
3x3	R & C	0.77	0.57	0.45	0.39	0.81	0.66	0.57	0.52
	Vp model	0.78	0.80	0.75	0.70	0.83	0.81	0.77	0.75
	Eb model	0.70	0.69	0.67	0.64	0.75	0.75	0.72	0.71
4x4	R & C	0.77	0.55	0.43	0.37	0.81	0.64	0.55	0.50
	Vp model	0.82	0.82	0.77	0.73	0.85	0.83	0.80	0.78
	Eb model	0.71	0.73	0.70	0.67	0.79	0.80	0.76	0.75
5x5	R & C	0.77	0.54	0.41	0.35	0.81	0.64	0.54	0.49
	Vp model	0.84	0.84	0.79	0.75	0.87	0.84	0.81	0.80
	Eb model	0.75	0.76	0.72	0.70	0.81	0.81	0.78	0.77
6x6	R & C	0.77	0.53	0.41	0.34	0.81	0.63	0.53	0.48
	Vp model	0.85	0.85	0.80	0.76	0.88	0.86	0.83	0.81
	Eb model	0.77	0.78	0.75	0.72	0.82	0.82	0.80	0.80

Table 5. 2 Raft-pile interaction factors for different pile groups
with different S/d and L/d.

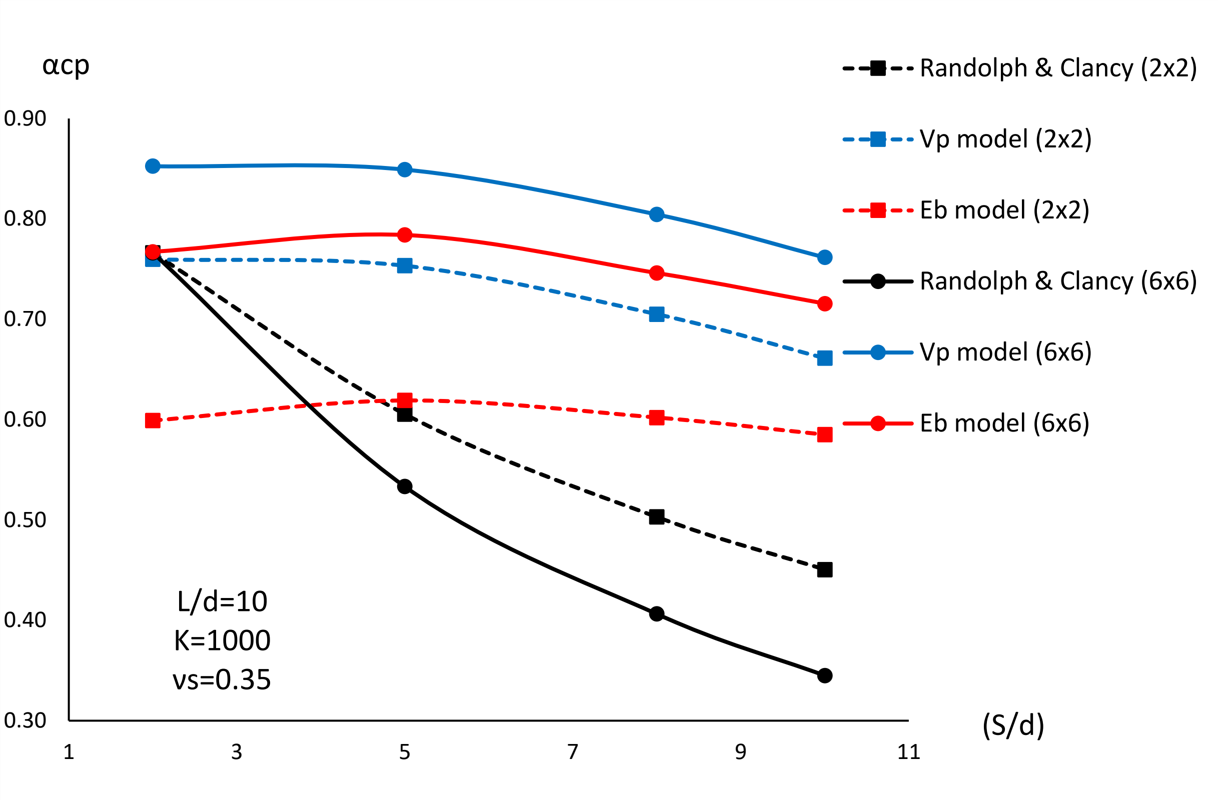

Figure 5. 4 Raft-pile interaction factor at L/d=10 and
for groups 2x2 and 6x6.

5.5.2 **Comparing the results for load sharing factor**

The evaluation of the load sharing behaviour between the piles and the raft depended on the system load settlement curve. This study case was focused on the linear load sharing behaviour of piled raft system. Table 5. 3 and Table 5. 4 illustrate the ratio of load that was taken by the raft and the load taken by piles respectively.

The results for both analytical and numerical methods had some similarities as follow: -

- The raft load increased by increasing the ratio of **S/d**.
- The raft load decreased by increasing the ratio of **L/d**.

The results in the below tables demonstrated the following: -

- For both Vp and Eb models, there were differences in the results for the raft load for L/d=10 and that differences about 40% at (S/d=2) and decreased to 15% at (S/d=10) where the Eb gave higher results than Vp model. But for L/d=25, there was a very good agreement between both models.
- For both Vp and Eb models as the pile groups increased from 2x2 to 6x6 for the same **S/d**, the raft load almost still the same because the pile group efficiency reduced but the raft-pile interaction also increased, and that created a balance between them.

- For Randolph and Wroth method revealed that: -

  a) For L/d =10 when S/d =2 and 5, it gave a good agreement with Vp model but for S/d=8 and 10, it gave a higher estimation for the raft load.

  b) For L/d=25 when S/d=2,5, and 8, it gave slightly higher values for the raft load than volume pile model.

- For Mylonakis and Gazetas method showed that: -

  a) For group 2x2, it gave very good agreement with the Vp model for both values of L/d.

  b) For the rest of groups, the raft load started to increase with increasing the pile groups (3x3 to 6x6) for same **S/d** and that because this method gave lower values for group efficiency **η** and that made larger load was taken by the raft.

L/d		10				25			
S/d		2	5	8	10	2	5	8	10
2x2	R&W	0.12	0.23	0.30	0.33	0.06	0.14	0.21	0.25
	M&G	0.11	0.23	0.34	0.40	0.05	0.11	0.18	0.22
	Vp model	0.13	0.21	0.33	0.41	0.07	0.11	0.16	0.21
	Eb model	0.26	0.36	0.45	0.51	0.10	0.15	0.22	0.26
3x3	R&W	0.14	0.25	0.28	0.31	0.08	0.19	0.26	0.30
	M&G	0.12	0.29	0.41	0.47	0.05	0.14	0.22	0.27
	Vp model	0.15	0.23	0.37	0.46	0.07	0.12	0.18	0.24
	Eb model	0.24	0.37	0.48	0.55	0.10	0.16	0.23	0.28
4x4	R&W	0.15	0.22	0.25	0.27	0.09	0.22	0.28	0.30
	M&G	0.14	0.33	0.45	0.51	0.06	0.17	0.26	0.31
	Vp model	0.13	0.23	0.39	0.49	0.07	0.12	0.19	0.25
	Eb model	0.24	0.36	0.50	0.57	0.10	0.15	0.24	0.29
5x5	R&W	0.16	0.20	0.22	0.24	0.10	0.23	0.27	0.27
	M&G	0.16	0.37	0.49	0.55	0.07	0.19	0.29	0.34
	Vp model	0.13	0.23	0.39	0.50	0.07	0.12	0.19	0.25
	Eb model	0.23	0.36	0.50	0.58	0.10	0.16	0.24	0.29
6x6	R&W	0.15	0.19	0.20	0.21	0.11	0.24	0.25	0.26
	M&G	0.18	0.41	0.53	0.58	0.08	0.21	0.31	0.36
	Vp model	0.12	0.23	0.40	0.51	0.07	0.12	0.19	0.25
	Eb model	0.22	0.35	0.50	0.58	0.10	0.16	0.23	0.28

Table 5. 3 Ratio of raft load to total load results.

L/d		10				25			
S/d		2	5	8	10	2	5	8	10
2x2	R&W	0.88	0.77	0.70	0.67	0.94	0.86	0.79	0.75
	M&G	0.89	0.77	0.66	0.60	0.95	0.89	0.82	0.78
	Vp model	0.87	0.79	0.67	0.59	0.93	0.89	0.84	0.79
	Eb model	0.74	0.64	0.55	0.49	0.90	0.85	0.78	0.74
3x3	R&W	0.86	0.75	0.72	0.69	0.92	0.81	0.74	0.70
	M&G	0.88	0.71	0.59	0.53	0.95	0.86	0.78	0.73
	Vp model	0.85	0.77	0.63	0.54	0.93	0.88	0.82	0.76
	Eb model	0.76	0.63	0.52	0.45	0.90	0.84	0.77	0.72
4x4	R&W	0.85	0.78	0.75	0.73	0.91	0.78	0.72	0.70
	M&G	0.86	0.67	0.55	0.49	0.94	0.83	0.74	0.69
	Vb model	0.87	0.77	0.61	0.51	0.93	0.88	0.81	0.75
	Eb model	0.76	0.64	0.50	0.43	0.90	0.85	0.76	0.71
5x5	R&W	0.84	0.80	0.78	0.76	0.90	0.77	0.73	0.73
	M&G	0.84	0.63	0.51	0.45	0.93	0.81	0.71	0.66
	Vp model	0.87	0.77	0.61	0.50	0.93	0.88	0.81	0.75
	Eb model	0.77	0.64	0.50	0.42	0.90	0.84	0.76	0.71
6x6	R&W	0.85	0.81	0.80	0.79	0.89	0.76	0.75	0.74
	M&G	0.82	0.59	0.47	0.42	0.92	0.79	0.69	0.64
	Vp model	0.88	0.77	0.60	0.49	0.93	0.88	0.81	0.75
	Eb model	0.78	0.65	0.50	0.42	0.90	0.84	0.77	0.72

Table 5. 4 Ratio of piles load to total load results.

The ratio of load that was taken by the raft for the same raft area (12x12) when the number of piles increased from 4 piles to 9 piles, the raft load decreased for both cases of L/d=10 or 25 are seen in Figure 5. 5 and Figure 5. 6.

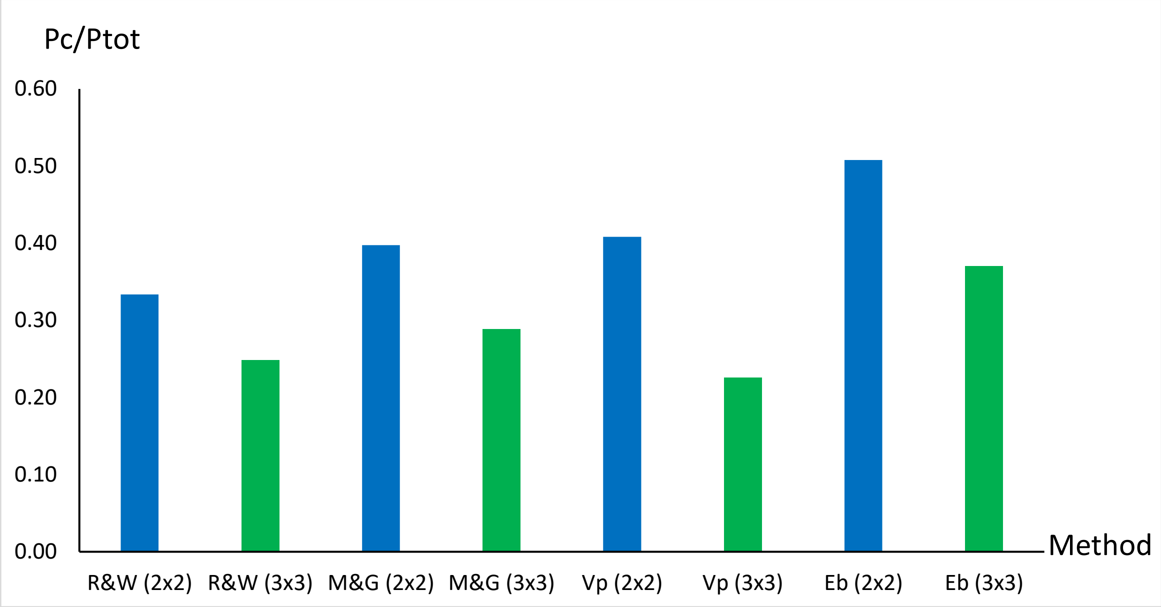

Figure 5. 5 Ratio of raft load to total load for L/d=10.

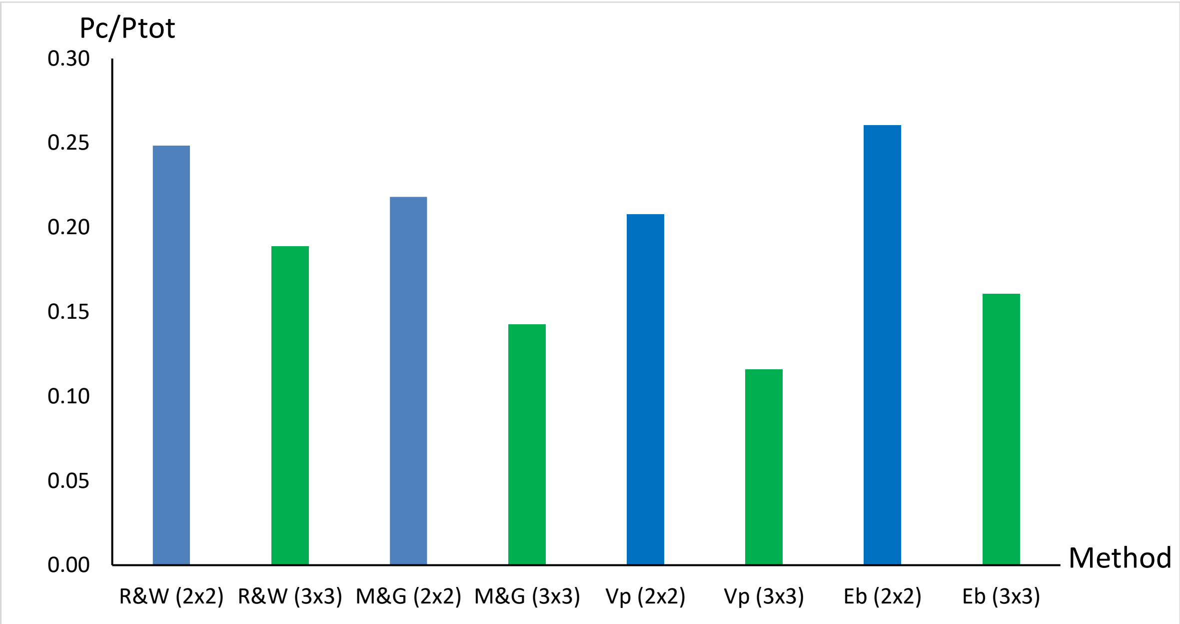

Figure 5. 6 Ratio of raft load to total load for L/d=25.

5.6 Case of study for non-uniform pile distributions

For the same study case in section 4.4.2 where the pile distribution was non-uniform, the soil foundation cross-section, and the soil properties were illustrated in Figure 4. 4 and Figure 4. 5 respectively. Both soil and pile were described by linear elastic model.
The analysis was done for two cases: -

1. Both soil layers have the properties of soil layer 1($E_{s2} = E_{s1}$).
2. The soil consists of two layers ($E_{s1} \neq E_{s2}$).

5.6.1 **Comparing the results**

The raft-pile interaction α_{cp} results are presented in Figure 5. 7 for both cases by using the Eb model and Randolph & Clancy's formula.
The analysis gave the following: -

- For case 1 when both soil layers had the properties of soil layer 1, there was a significant difference between the Eb model and the analytical method by Randolph & Clancy.
- For case 2 when the soil consisted of two layers, there was a very good agreement between the Eb model and the analytical method by Randolph & Clancy.

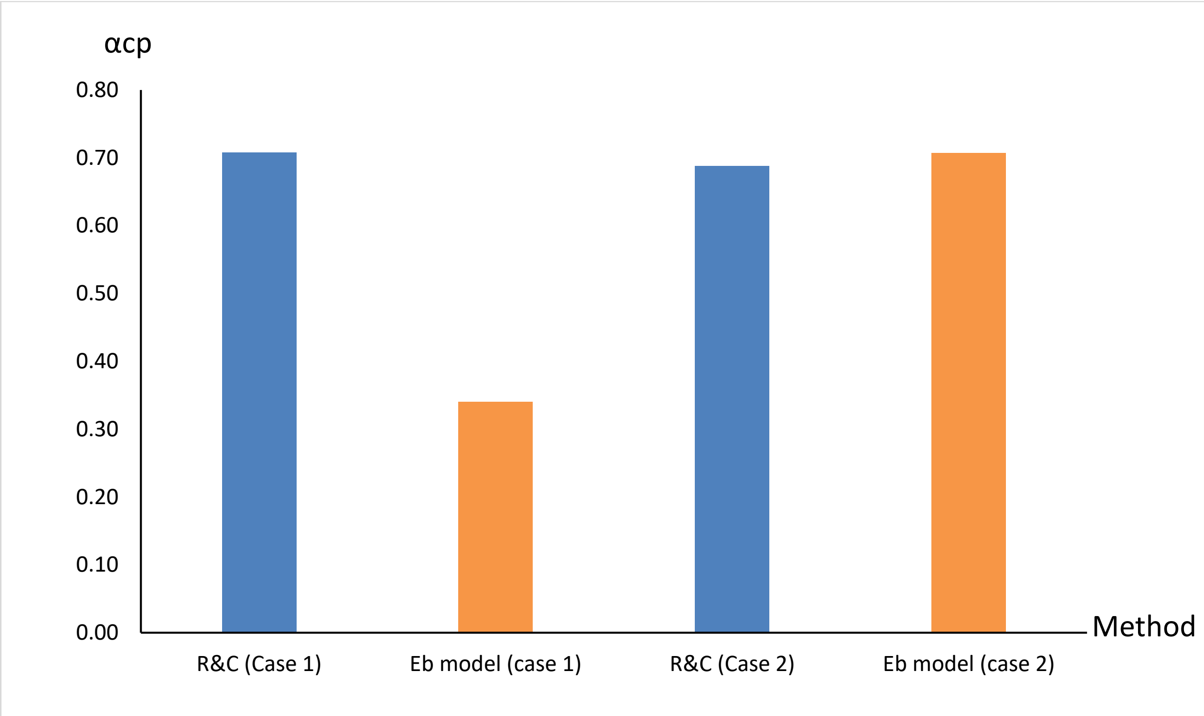

Figure 5. 7 Raft-pile interaction factor for case 1 and 2.

The ratio of the raft load to total load results are shown in Figure 5. 8 and Figure 5. 9 for case 1 and 2 respectively by using the Eb model and compared with the analytical methods.
The analysis gave the following: -

- For case 1, there was a difference between the Eb model and the analytical methods. The Eb model gave higher results than the analytical methods in the case of applying r_m limits but for Mylonakis and Gazetas without applying r_m, it gave the highest ratio of raft load to total load result.
- For case 2, as the soil layer below the pile tip was stiff, the ratio of raft load to total load results for all cases was small. the results of Eb model and Gazetas without applying r_m had very a good agreement.

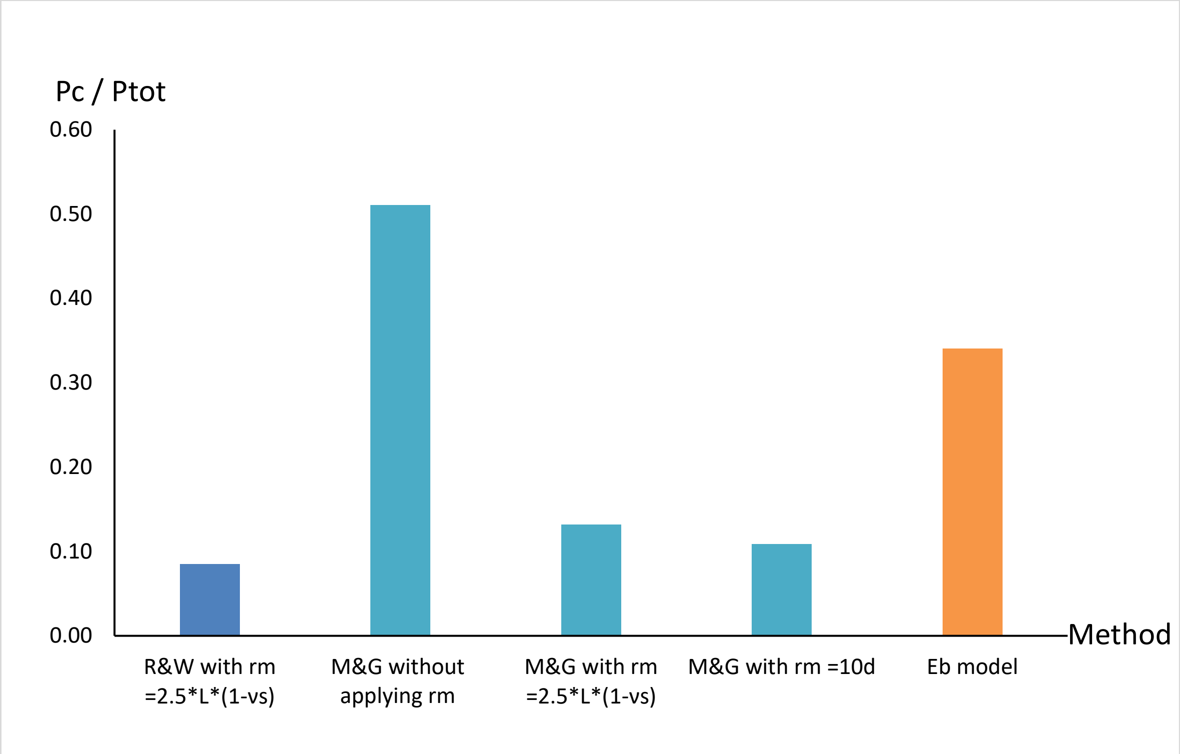

Figure 5. 8 Ratio of raft load to total load for case 1.

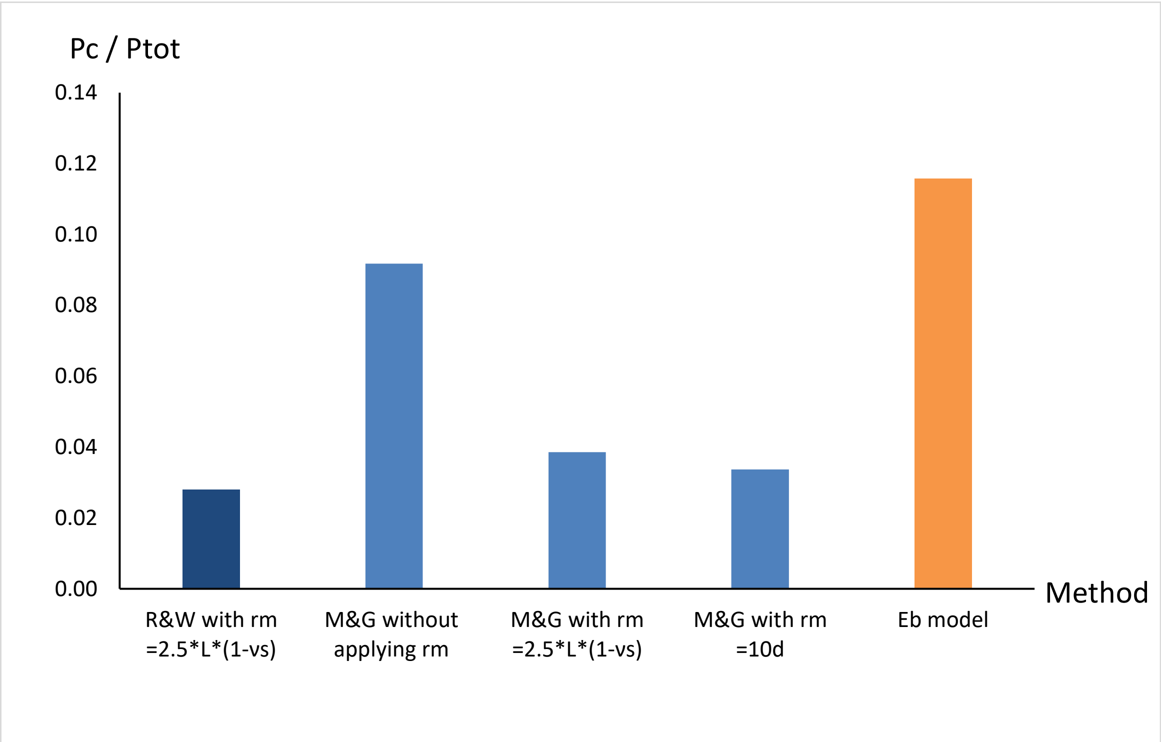

Figure 5. 9 Ratio of raft load to total load for case 2.

5.7 Application to real problem for "The Kingdom Tower"

5.7.1 General information

The tower site located in the Obhur district of Jeddah close to the Red Sea, in the Kingdom of Saudi Arabia. The building was designed to reach a height of one kilometer so it will be the tallest building or structure in the world as it will be taller than Burj Khalifa in Dubai, United Arab Emirates by 180 meters.

The structural system of the tower is a reinforced concrete shear wall and it is developed to maximize concrete material efficiency to resist the vertical and lateral load demands as the overall slenderness of the tower is 12:1 (height: width) demands this level of correlation. Figure 5. 10 illustrates the structural system of Jeddah tower.

The total gravity load (dead load+live load) of the superstructure is about 8600 MN and is distributed according to Figure 5. 11. The raft area is approximately 3720 m^2 and it can be divided into four zones of roughly equal sizes: the three wings and the center core area. The applied gravity loads give a uniform loading on the raft for the four zones where the average pressure below the raft is approximately 2.37 MPa by taking into consideration the raft weight. The foundation system of the Kingdom Tower is a piled raft system consists of 270 piles (with different lengths and different diameters), and raft with different thicknesses and levels.

The pile numbers and geometries are: -

- 226 cast-in-place piles with diameter equal to1.5 m.
- 44 cast-in-place piles with diameter equal to1.8 m.

The piles depth ranges from 45 m at the wings to 105 m at the center of the tower where the piles connected to a continuous concrete raft covering the entire pile field. The entire raft at the same level except the 6 m deep depression for the elevator core also, it has a thickness of 4.5 m at the center area and increases to 5 m at the end of the wings [29].

The Three-dimensional view for piles is shown in Figure 5. 12.

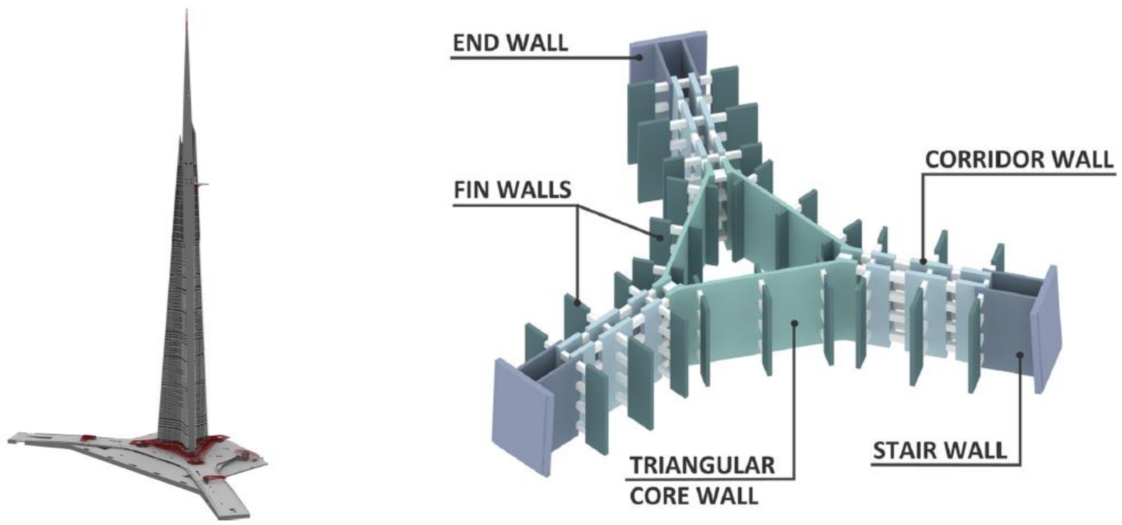

Figure 5. 10 The structural system of Jeddah tower.

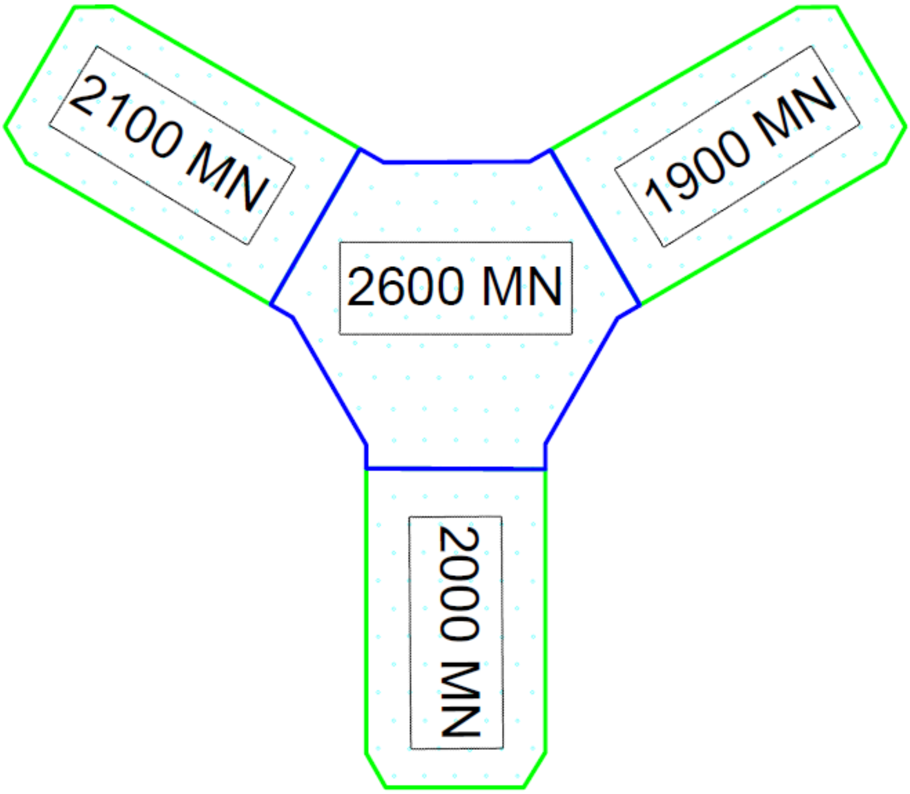

Figure 5. 11 Gravity load distribution of the superstructure.

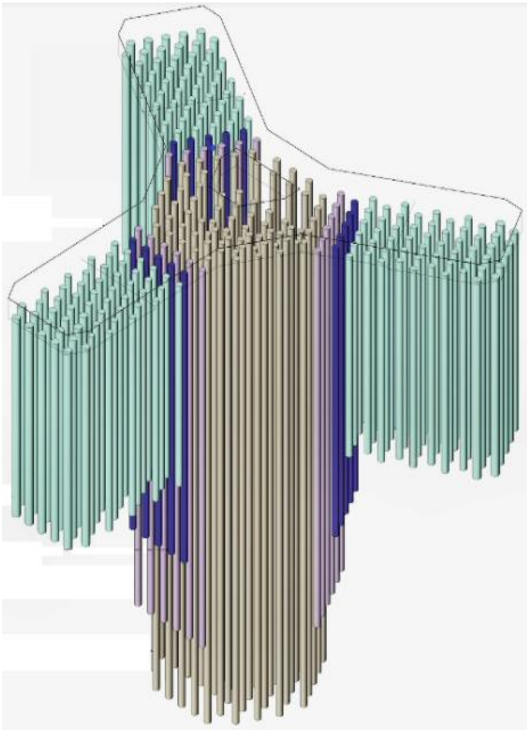

Figure 5. 12 Three-dimensional view for piles.

5.7.2 **Modeling by PLAXIS 3D**

The analysis was based on the Eb model by using PLAXIS 3D software where a three-dimensional model was used. The model boundaries were restrained in all three directions where the model dimensions X*Y*Z were 300*300*204. The used boundary conditions did not influence the results under the raft.
The analysis was done for two cases: -

- Case 1; by applying uniform displacement to estimate the value of raft-pile interaction and the ratio of raft load to total load.
- Case 2; by applying the gravity loads to see the settlement, differential settlement, and the ratio of raft load to total load.

In this study, the raft was considered at the same level and had the same thickness and the wing piles have the same diameters as shown in Figure 5. 13 . Also, the applied load was a uniform distributed load on each zone according to the load distribution in Figure 5. 11.

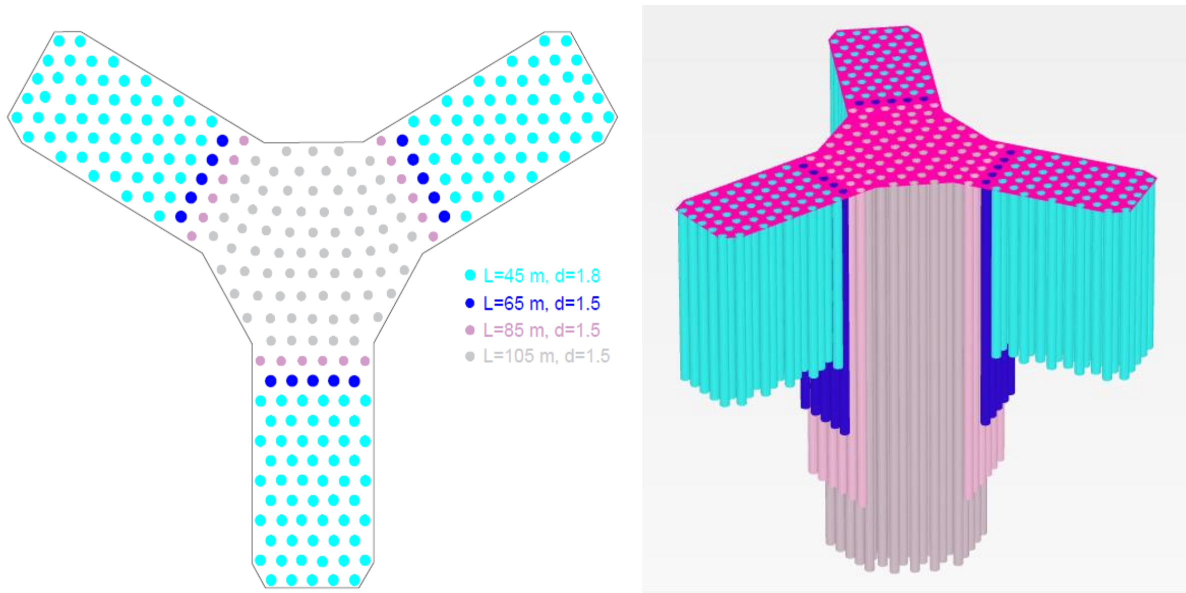

Figure 5. 13 The assumed piled raft system.

5.7.2.1 **Materials characteristics**

The ground conditions comprised from various horizontal layers which were complex and highly variable. The final soil parameters are listed in Table 5. 5. These parameters were assigned to the soil material data set and transferred to the model by a single borehole, which showed the information on the position of soil layers.
The soil was modeled with two constitutive models: -

- Linear elastic model and Mohr-Coulomb model for case 1 where the groundwater level was assumed at zero level.
- Mohr-Coulomb model (MC) for case 2 where the groundwater level was assumed at zero level.

Soil description	Level (m)		Soil parameters					
	From	To	E (MPa)	ν	γ (KN/m^3)	φ (degree)	C (KPa)	UCS (MPa)
Limestone	4	-10	500	0.35	18	24	170	2
Limestone	-10	-40	500	0.35	18	24	170	2
Limestone	-40	-47	440	0.35	18	24	170	3
Limestone	-47	-54	325	0.35	18	24	170	3
Gravel	-54	-60	200	0.35	17	38	0	3
Sandstone	-60	-90	150	0.35	20	24	300	1.5
Sandstone	-90	-110	150 to 500(1)	0.35	20	24	300 to 1000(1)	3.2
Sandstone	-110	-125	900 to 1200(1)	0.3	20	24	1800 to 2400(1)	2
Sandstone	-125	-200	1200	0.3	20	24	2400	2

(1) Linear decrease in stiffness values

Table 5. 5 Soil Properties for Jeddah tower.

The piles were modeled by using the Eb model where the piles have different lengths and different diameters as illustrated in Figure 5. 13.

The axial skin resistance for Eb model was calculated based on the soil uniaxial compressive strength (UCS) depending on the following equation: -

$$\tau_{si} = 0.45\sqrt{q_{ui}} \quad (5.\ 8)$$

$$T_{av} = \frac{1}{L} * \sum_{i=1}^{n} \tau_{si} h_i \quad (5.8a)$$

where; $\mathbf{q_{ui}}$ is the uniaxial compressive strength for each soil layer and $\mathbf{h_i}$ is the pile length at each soil layer [30].

The base resistance was estimated according to DIN 1054:2005 based on the uniaxial compressive strength from Table 5. 6 [31].

UCS (MPa)	0.5	5.00	20.00
q_b (MPa)	1.50	5.00	10.00

Table 5. 6 pile base resistance for bored piles in rock according to DIN 1054:2005.

Based on the previous calculation, the input parameters for embedded beam model are shown in Table 5. 7.

The raft was modeled using solid tetrahedral volume elements with an equivalent elastic modulus to take superstructure stiffness into account which was captured in the structural ETABS model. The input parameters for raft are presented in Table 5. 8.

Pile model	dimenssions		Properties		Axial skin resistance	Base resistance
	L (m)	d (m)	E (GPa)	γ (KN/m^3)	T_{ave} (KN/m)	F_{max} (KN)
1	45	1.8	36	25	3688.6	8765.04
2	65	1.5	36	25	3175.42	4025.17
3	85	1.5	36	25	3039.36	4025.17
4	105	1.5	36	25	3126.02	6361.73

Table 5. 7 The input parameters for embedded beam model.

Raft model	Material type	Properties		
		E (GPa)	t(m)	γ (KN/m^3)
volume element	Elastic	36.7	4.5	25

Table 5. 8 The input parameters for raft.

5.7.2.2 **Mesh generation and construction stages**

The mesh was defined as very fine and refined in the cluster surrounding the piled raft by using coarseness factor equal to 0.3. Figure 5. 14 shows the 3D model in PLAXIS with very fine mesh discretization.

The construction stage process consisted of three stages: -

- Stage 1, the model of soil block was allowed to settle due to its own weight and then the settlements were reset to zero.
- Stage 2, the piled raft system was installed and also, the settlements were reset to zero.
- Stage 3, the uniform displacement was applied for cases 1 and 2, or the uniform gravity load was applied for case 2.

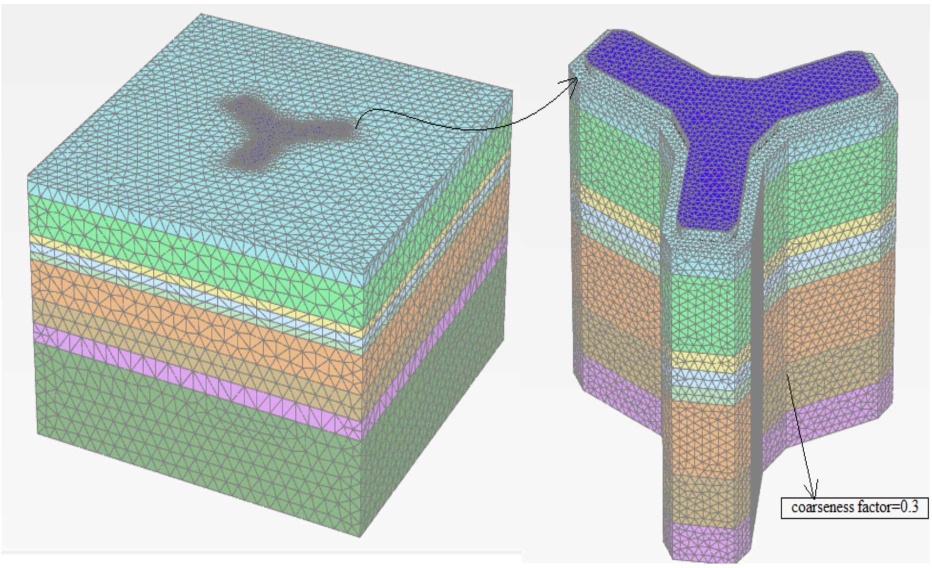

Figure 5. 14 The 3D model in PLAXIS with very fine mesh discretization and refined around the piled raft.

5.7.3 **Analysis results**

The results from PLAXIS 3D analysis were presented in this part where the first case aimed to compare the ratio of raft load to total load and the raft-pile interaction for linear and nonlinear cases. The second case showed the settlement, differential settlement, and the ratio of raft load to total load.

5.7.3.1 **Applying the uniform displacement for case 1**

The method depended on determining the load settlement curve for each system (piled raft, pile group, and raft) from PLAXIS 3D to calculate the stiffness. Figure 5. 15 provides the load settlement case for linear and nonlinear cases.

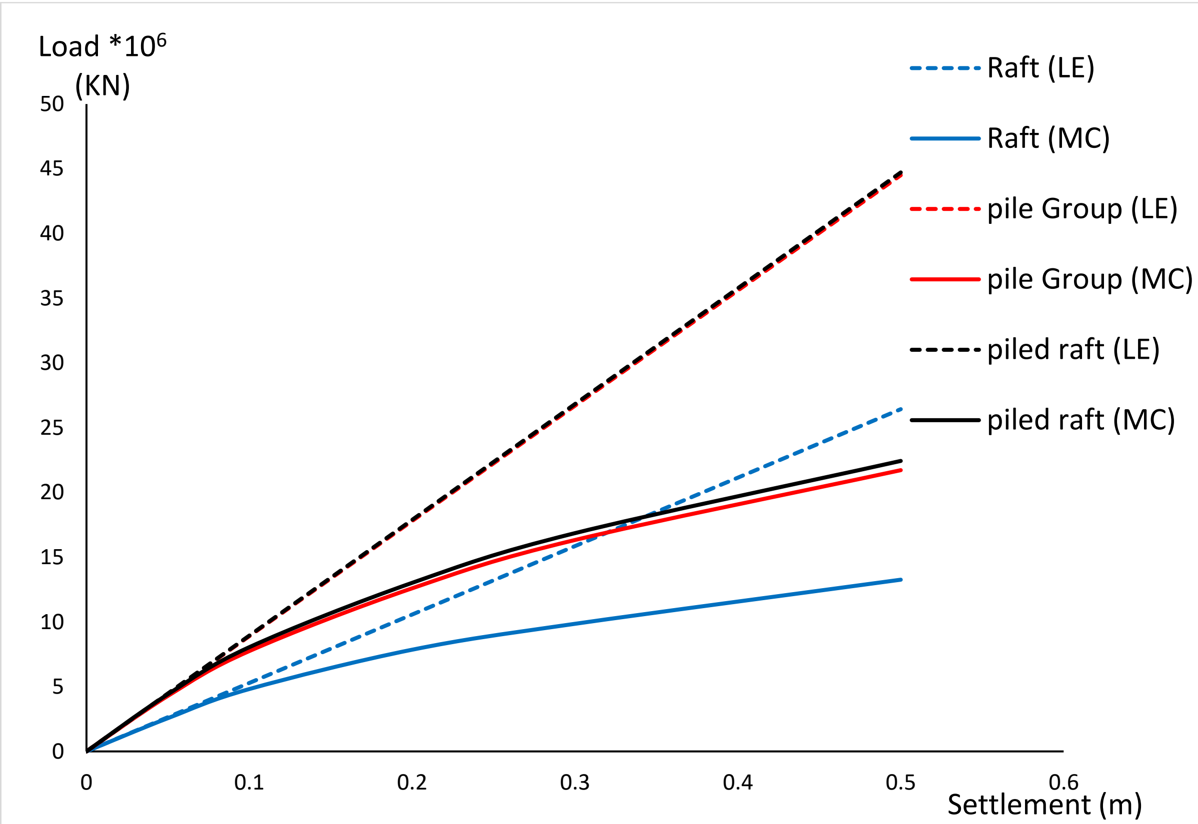

Figure 5. 15 Load settlement case for linear and nonlinear cases.

For linear case, the load settlement curves for pile groups and piled raft were almost identical but for nonlinear case they had slight difference. Also, there were a clear difference between both cases for the three systems.

By using both equations (5.6a) and (5.7) in sections 5.3.1 and 5.3.2 respectively, the ratio of raft load to total load and raft-pile interaction were calculated. Table 5. 9 shows the analysis results for raft-pile interaction and the ratio of raft load to total load.
Based on the analysis results, the nonlinear case gave bigger values for $\mathbf{P_c/P_{tot}}$ than the linear case.

Case / U_z(m)	α_{cp}		P_c/P_{tot}	
	Linear	Nonlinear case	Linear	Nonlinear case
0.0001	0.94	0.87	0.08	0.15
0.05		0.83		0.17
0.1		0.81		0.19
0.2		0.82		0.18
0.299		0.82		0.18
0.5		0.82		0.18

Table 5. 9 The analysis results for raft-pile interaction and the ratio of raft load to total load linear and nonlinear cases.

5.7.3.2 **Applaying the gravity loads for case 2**

The analysis for raft system model was performed to compare the settlement and differential of the piled raft system only. Figure 5. 16 and Figure 5. 17 show the settlement contours for raft and piled raft systems respectively.

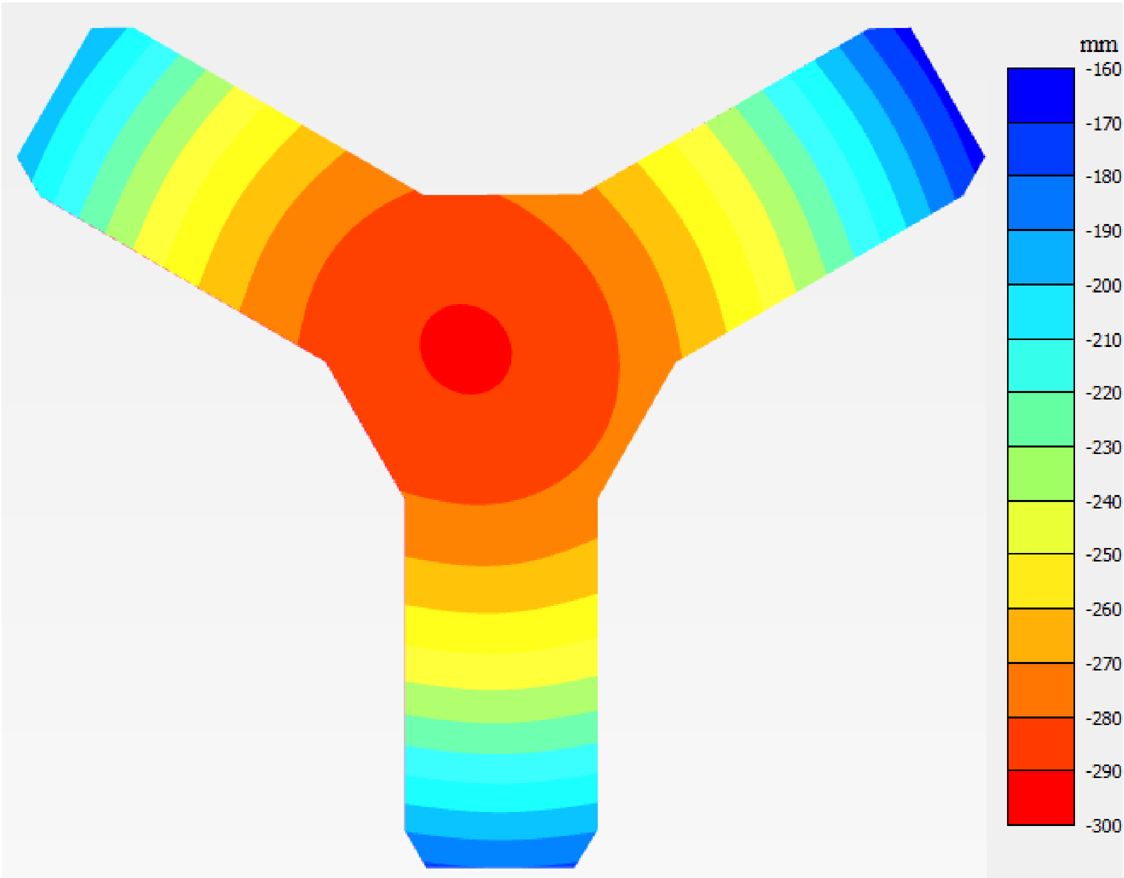

Figure 5. 16 Settlement contours for raft syetem only.

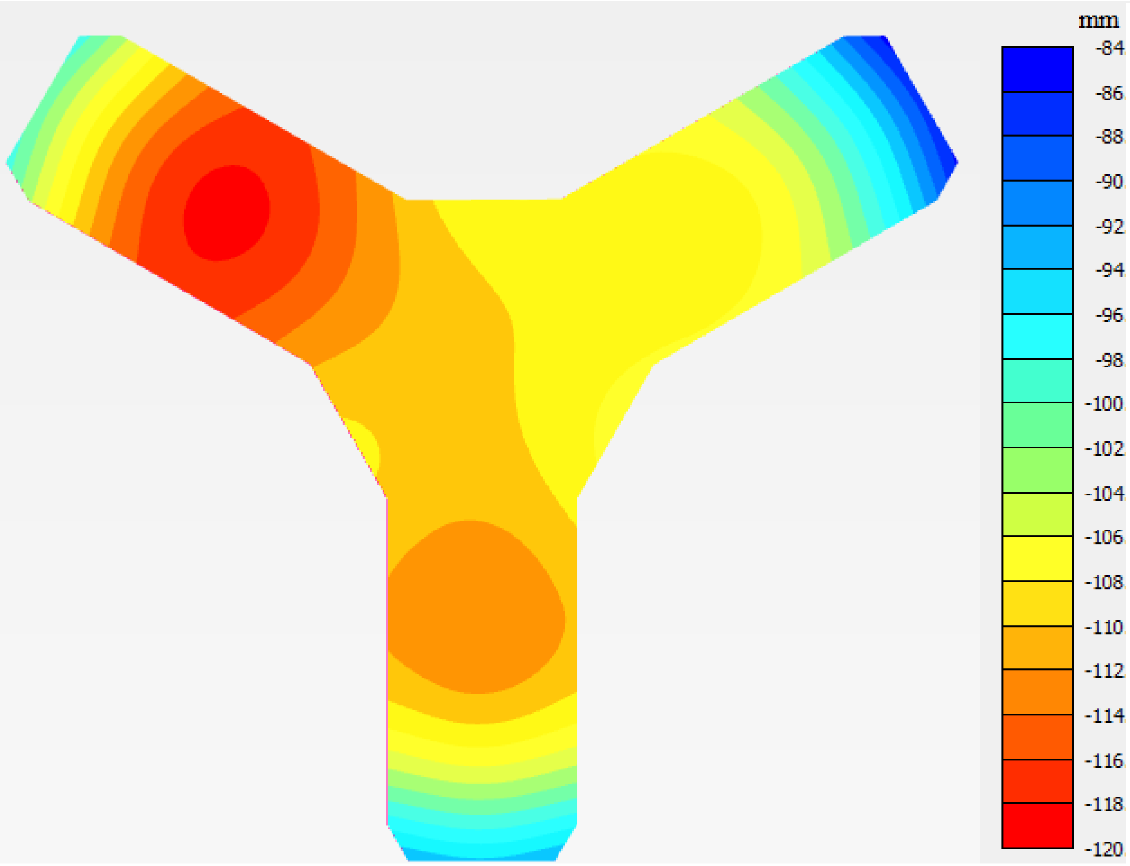

Figure 5. 17 Settlement contours for piled raft syetem.

The analysis showed the following: -

- For raft system only, the maximum settlement equal to 300 mm and the differential settlement equal to 140 mm.
- For piled raft system, the maximum settlement equal to 120 mm and the differential settlement equal to 34 mm.

The comparison of bearing pressure results for raft system only and piled raft system is shown in Figure 5. 18 and Figure 5. 19 respectively. The analysis showed the following: -

- For raft system only, the bearing pressure below the raft varied from 1850 KN/m^2 to 2300 KN/m^2.
- For piled raft system, the bearing pressure below the raft varied from 518 KN/m^2 to 620 KN/m^2.

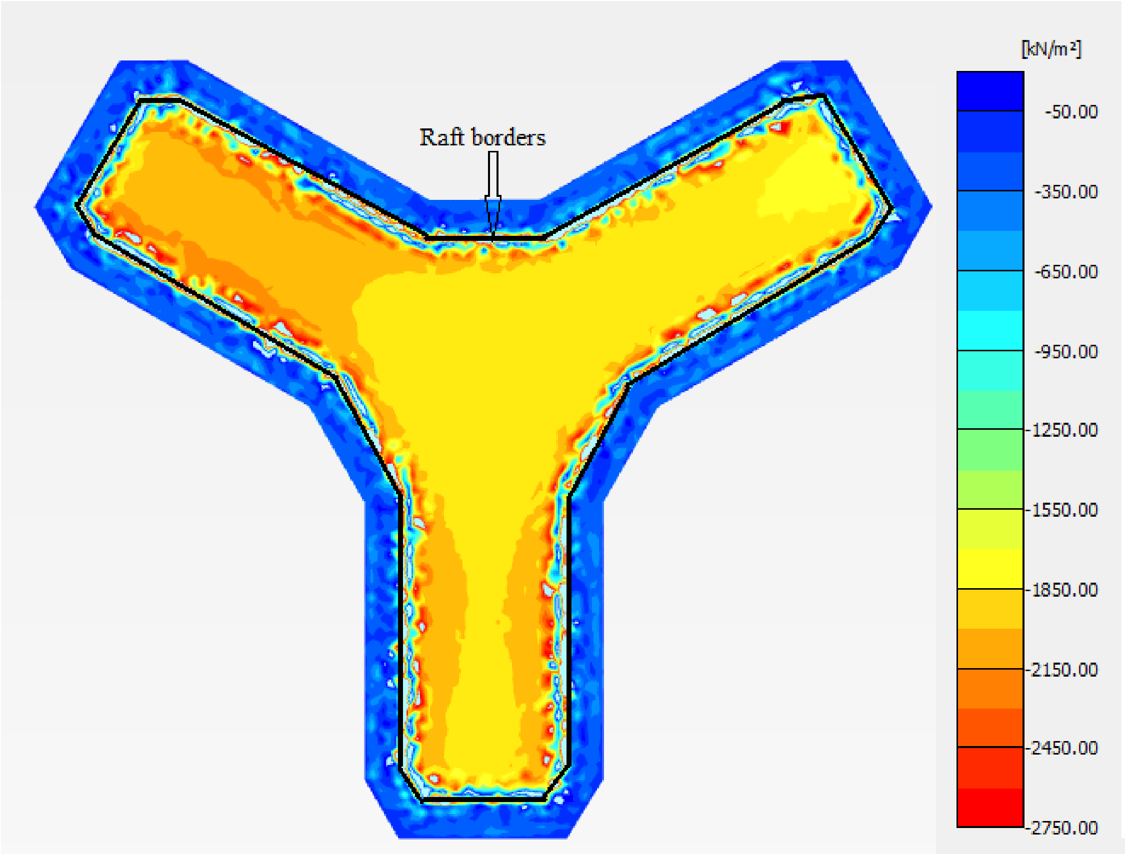

Figure 5. 18 Bearing pressure contours for raft syetem only.

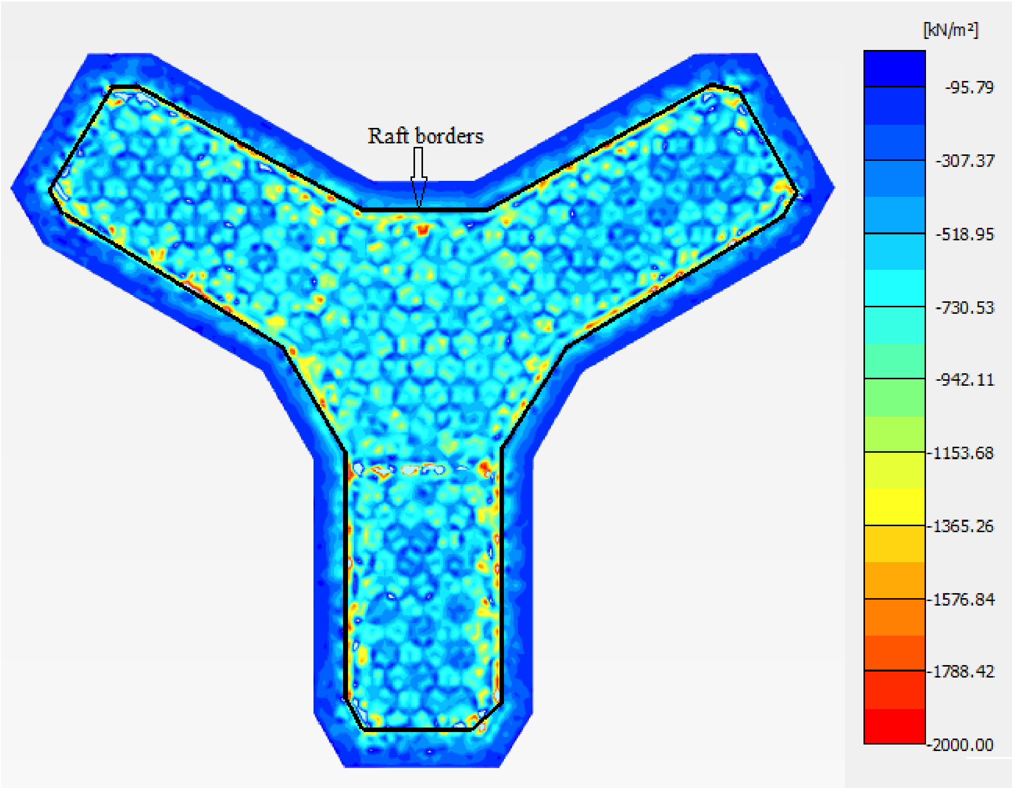

Figure 5. 19 Bearing pressure contours for piled raft syetem.

Finally, the analysis gave the loads distribution for piles within the piled raft system as shown in Figure 5. 20.

The pile loads varied according to the following: -

- For piles with L=45 m and d=1.8 m, the loads varied from 17 MN to 35 MN.
- For piles with L=65 m and d=1.5 m, the loads varied from 20 MN to 25 MN.
- For piles with L=85 m and d=1.5 m, the loads varied from 28 MN to 36 MN.
- For piles with L=105 m and d=1.5 m, the loads varied from 29 MN to 46 MN.

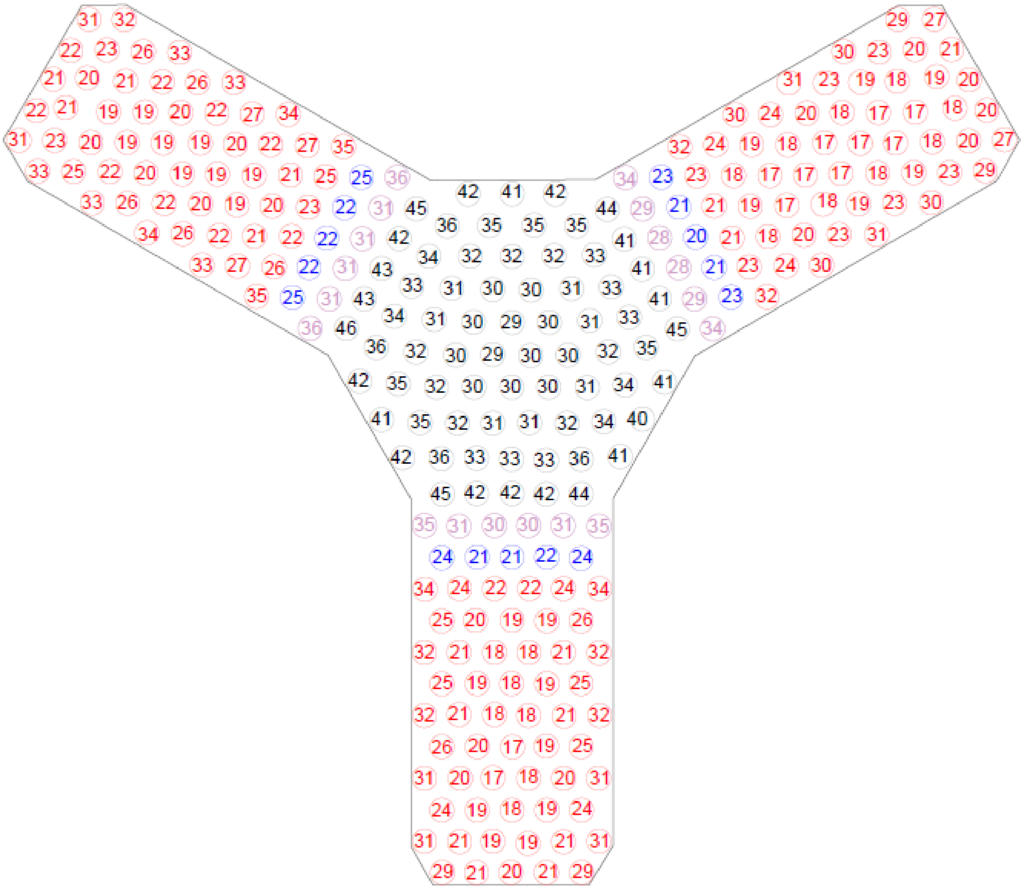

Figure 5. 20 Piles loads distribution within the piled raft system.

Also, the load sharing factor $\mathbf{X_{pr}}$ between piles and raft was estimated from the summation of 270 piles load and divided by the total loads (gravity loads + foundation weight).

$$X_{pr} = \frac{\sum_{i=1}^{270} N_i}{\text{gravity loads + foundation weight}} = \frac{7289}{8600+1345} = 0.73$$

From that, the taken load by the raft equal to 27% from the total load. The average settlement of the piled raft system was 102 mm from Figure 5. 17, and based on Table 5. 9 for the results of $\mathbf{P_c/P_{tot}}$ at settlement equal to 100 mm, the taken load by the raft equal to 19% from the total load. These two results indicated that both equations (5.6a) and (5.7) in sections 5.3.1 and 5.3.2 respectively can be used to estimate $\mathbf{P_c/\ P_{tot}}$ in nonlinear cases and give acceptable results. The results were acceptable comparing with the results of the piled raft system designers by using Midas GTS software package [29].

Chapter 6 Conclusions and further work

6.1 Conclusions

The piled raft system is used to have an economical foundation by making the raft participate to carry the loads, where the piled foundation allows only the piles to carry the loads. Numerical modeling is widely used tool for deep foundations analysis and among that the finite element method which is a very powerful tool and it takes into consideration all different types of complex interactions.

PLAXIS 3D program was used in this thesis as it is directed to analyze finite element geotechnical engineering problems. In this program, the pile is simulated by three methods (Volume element, Embedded beam, and Beam), and this study focused on the first two methods. The Vp model led to large models and as a result gave long calculation time so the Eb model was used to reduce the model complexity and took into account the penetration of the pile for the finite element in any orientation.

The main part of this thesis focused on the validation of Eb model to be used in piled raft foundation system. The strategy depended on the comparison between Vp model and Eb model with the analytical methods for single pile behaviour, the interaction between two piles, pile groups with rigid cap (unconnected with soil), and finally the raft-pile interaction and load sharing between piles and raft for piled raft system.

The general outcomes of the study are listed as follow: -

- The nonlinear analysis for single pile capacity under horizontal and vertical loads shows clear agreement between the Eb model and both Vp model and analytical method and in terms of linear stiffness analysis, the same agreement was gotten.
- The linear elastic analysis for interaction between two piles indicate very good agreement between Vp and Eb models and good agreement with different analytical methods for different cases of **S/d**, **K**, **L/d**, and $\boldsymbol{\nu_s}$.
- For floating pile groups (uniform distributions with different **S/d** and **L/d**) with rigid cap, the linear elastic analysis was done to compare the pile loads distribution and the group efficiency. For the first one, there is a clear agreement between the Vp model and Eb model in the load distributions but for the analytical methods, there is a small difference in case of group 3x3 and 4x4 and this difference increased as the number of piles increased within the group especially for corner and central piles. For the group efficiency, the Eb model gives a slightly higher estimation for the pile group efficiency more than the Vp model for all cases, and for the analytical method, the results varied because the results depended on the $\mathbf{r_m}$ (The distance at which the interaction cut off) and that was cleared in the case of nonuniform piles distribution.
- For linear elastic analysis of a single pile with single raft, the Eb model presents low values for $\boldsymbol{\alpha_{cp}}$ and higher values for $\mathbf{P_c/P_{tot}}$ and especially for L/d=10 and that is due to

lower estimation of stiffnesses but for L/d=25 the results are acceptable compared to the Vp model. The analytical method gives slightly higher values for α_{cp} and lower values for P_c/P_{tot} in comparison with the Vp model.

- The method of the single pile with single raft was extended to floating pile groups (uniform distributions with different **S/d** and **L/d**) to determine α_{cp} and P_c/P_{tot}. Generally, the same behaviour for Eb and Vp models was observed as in single pile with single raft case. Also, the results of the analytical method were varied but still acceptable.

The final part of the thesis discussed the piled raft system of Jeddah Tower with linear and nonlinear cases depending on the Eb model for simulating the different piles. The results were acceptable comparing with the designers results of the piled raft system by using Midas GTS software package.

6.2 Recommendations for further work

The following guidelines are useful for future researches and they are listed as follows: -

- For analytical calculation, the interaction between piles affects the efficiency of pile groups and especially the distance at which the interaction cut off r_m as it has a greater effect. Therefore, the improvement of r_m can be considered in further studies.
- For stiffness estimation and especially for L/d=10, further investigations of the embedded beam model are necessary.
- For numerical analysis, our study focuses on axial load for interaction between piles, pile group, and piled raft system. Therefore, lateral and dynamic loads can be considered in further studies.

References

1. Mosher, R.L. and W.P. Dawkins, *Theoretical Manual for Pile Foundations*. 2000, Washington.: Information Technology Laboratory (U.S.),Engineer Research and Development Center (U.S.).

2. Yang, J., *Influence Zone for End Bearing of Piles in Sand.* Journal of Geotechnical and Geoenvironmental Engineering - J GEOTECH GEOENVIRON ENG, 2006. **132**.

3. Michael Tomlinson and J. Woodward, *Pile Design and Construction Practice*. 5th ed. 2008.

4. Guo, W.D., *Theory and Practice of Pile Foundations*. 1st ed. 2012, London: CRC Press. 576.

5. Mylonakis& Gazetas, G., *Settlement and additional internal forces of grouped piles in layered.* Geotechnique, 1998. **48**: p. 55-72.

6. Viggiani, C., Mandolini, A., & Russo, G. , *Piles and Pile Foundations* 1st ed. 2012, London. 296.

7. Russo, G., *A method to compute the non-linear behaviour of piles under horizontal loading.* Soils and Foundations, 2016. **56**.

8. Gerolymos, N., O. Papakyriakopoulos, and R. Brinkgreve, *Macroelement modeling of piles in cohesive soil subjected to combined lateral and axial loading*. 2014. p. 373-378.

9. Mylonakis, G., *Lateral Vibration and Internal Forces of Grouped Piles in Layered Soil.* Journal of Geotechnical and Geoenvironmental Engineering - J GEOTECH GEOENVIRON ENG, 1999. **125**.

10. N. Gerolymos , M.A., *Phenomenological Constitutive Model for the Structural Behaviour of Reinforced Concrete Sections: Application to the Lateral Response of Piles and Pile-groups*, in *National Congress geotechnical engineering (Greek Scientific Society of Soil Mechanics and Geotechnical Engineering)*. 2019: Athens.

11. A., E., *USC-RC. Software for analyzing behavior of a single reinforced concrete member . Version 1.0.2, USC Civil Engineering Department.* 2001.

12. Poulos, H., *Analysis of the Settlement of Pile Groups.* Géotechnique, 1968. **18**: p. 449-471.

13. Poulos, H. and M. Ns, *Settlement and load distribution analysis of pile groups.* 1971: p. 18-28.

14. Poulos H G, D.E.H., *Pile foundation analysis and design*. Series in geotechnical engineering. 1980, New York : Wiley: John Wiley and Sons.

15. Randolph, M.F.W., C. P., *An analysis of the vertical deformation of pile groups.* Géotechnique, 1979. **29**(4): p. 423-439.

16. Dobry R, G.G., *Simple method for dynamic stiffness and damping of floating pile groups.* Géotechnique, 1988. **38**(4): p. 557-574.

17. Makris N , G.G., *Dynamic pile-soil-pile interaction.Part I: analysis of axial vibration.* Earthquake Engineering & Structural Dynamics 20(2), 1991: p. 115–132.

18. Mylonakis, G. and G. Gazetas, *Vertical Vibration and Additional Distress of Grouped Piles in Layered Soil.* Soils and Foundations, 1998. **38**(1): p. 1-14.

19. Luan, L., et al., *A new dynamic interaction factor for the analysis of pile groups subjected to vertical dynamic loads.* Acta Geotechnica, 2020. **15**(12): p. 3545-3558.

20. Nguyen, D., S.-B. Jo, and D.-S. Kim, *Design method of piled-raft foundations under vertical load considering interaction effects.* Computers and Geotechnics, 2013. **47**: p. 16–27.

21. Modarresi, M., et al., *Experimental and Numerical Study of Pile-to-Pile Interaction Factor in Sandy Soil.* Procedia Engineering, 2016. **161**: p. 1030-1036.

22. McCabe, B. and B. Sheil, *Pile group settlement estimation: suitability of nonlinear interaction factors.* International Journal of Geomechanics, 2014. **15**.

23. Hess, H., et al., *Seismic Response of a Large Pile Group* in *European Conference on Earthquake Engineering* 1998: Paris

24. Burland, J., B. Broms, and V. Mello. *Behaviour of foundations and structures*. in *Conference on Soil Mechanics and Geotechnical Engineering*. 1977. Tokyo, Japan.

25. Clancy, P. and M.F. Randolph, *An approximate analysis procedure for piled raft foundations.* International Journal for Numerical and Analytical Methods in Geomechanics, 1993. **17**(12): p. 849-869.

26. Poulos, H., *Piled raft foundations: Design and applications.* Geotechnique, 2001. **51**(2): p. 95-113.

27. Randolph, M., *Design methods for pile groups and piled rafts*, in *INTERNATIONAL SOCIETY FOR SOIL MECHANICS AND GEOTECHNICAL ENGINEERING*. 1994: New Delhi. p. 61–82.

28. Mylonakis, G. and S. Nikolaou, *Footings under seismic loading: Analysis and design issues with emphasis on bridge foundations.* Soil Dynamics and Earthquake Engineering, 2006. **26**: p. 824-853.

29. Syngros, K. and A. Poeppel, *Soil-Foundation-Superstructure Interaction for the Tallest Tower in the World: The Kingdom Tower*. 2014.

30. Pells, P.J.N., *State of Practice for the Design of Socketed Piles in Rock*. In: Vitharana, Nihal Dhamsiri (Editor); Colman, Randal (Editor). Proceedings 8th Australia New Zealand Conference on Geomechanics: Consolidating Knowledge. Barton, ACT: Australian Geomechanics Society, 1999: 307-327. 1999: In: Vitharana, Nihal Dhamsiri (Editor); Colman, Randal (Editor). Proceedings 8th Australia New Zealand Conference on Geomechanics: Consolidating Knowledge. Barton, ACT: Australian Geomechanics Society, 1999: 307-327.

31. Vrettos, C. *Current design practice for axially loaded piles and piled rafts in Germany*. 2007.